Dissertation

submitted to the

Combined Faculties for the Natural Sciences and for Mathematics

of the Ruperto-Carola University of Heidelberg, Germany

for the degree of

Doctor of Natural Sciences

presented by

Dipl. Biochemiker	Eckehard Freitag
born in:	Halle / Saale
Oral examination:	11th December 2009

Title

Micro-Electrode-Array recordings:
a tool to study calcium signaling pathways involved
in neuronal network plasticity and
late phase long-term potentiation

Referees: Prof. Hilmar Bading
Prof. Christoph Schuster

Be the change

that you wish to see

in the world

Mahatma Gandhi

My parents

and

my sister

ACKNOWLEDGEMENTS

First and foremost, I would like to thank my supervisor Prof. Hilmar Bading for giving me the opportunity to work on this thesis in his laboratory. With his encouragement, advice and continual support riddled with his broad knowledge and unshakeable confidence in my abilities he has been an excellent advisor. He gave me tremendous freedom to choose my own directions, yet was always available with discussions when I needed help. He was keeping me focused on the relevant scientific questions and allowed me to acquire an exceptionally broad spectrum of experimental techniques. It was through his generosity that I was able to attend many conferences in Germany and abroad to expand my view in the field of neuroscience and to meet adventurous and exciting guys of this community.

I also thank my second supervisor Prof. Christoph Schuster for helpful discussions and the support throughout my years as a PhD student.

I cannot fully express my gratitude to C. Peter Bengtson, Daniela Mauceri and Frank Hofmann for being exceptionally generous and supportive during all these years. They, as my daily supervisors, provided my scientific life with refreshing insights, critical questions, thorough eyes but also great enthusiasm. Their efforts and advice have made this a better thesis. However, they not only were a great support in my scientific life, but they also became very good friends.

Many thanks also to Daniela Mauceri, Peter Bengtson, Daniel Bucher and Anna Hagenston for critically reading the manuscript.

For their generous assistance in the research I want to thank Anja Eder, Bettina Buchthal, Oliver Dick, Anna Hagenston, Ruth Jelinek, David Lau, Martina Leibfried, Kirsten Obernier, Ana Oliveira, Jan Weislogel, Ursula Weiss and Simon Wiegert. Life at the bench would have been much harder without them and I want to thank them for their help and contributions to this work. I furthermore owe a particular gratitude to Christin Schmidt for being my ‘executive force’ in summer 2009. She is a brillant and enthusiastic scientist without the help of whom I would not have been able to submit this work so soon.

I owe a great debt of gratitude to Iris Bünzli-Ehret, who provided me with hippocampal tissue of consistent and outstanding quality all these years but especially in 2009. My sincere appreciation to Otto Bräunling, Irmela Meng, Alan Summerfield, Oliver Teubner and Monika Keusch for helping with purchase orders and reimbursements as well as for the efforts to keep the lab running. The ‘Nuthole Movie Night’s’ have always been very enjoyable.

I have experienced stunning and thrilling hours on the bike with my buddies ‘Plasma-Pete’ and ‘Steroid-Simon’; also Carla, Andreas, Aleks and Dan often joined us. Besides biking but astonishingly often subsequently, we share two more fashions: preparing gorgeous and delicious menus for dinner and the love for a good wine. I do not need to mention that all of them are very good friends.

It is pleasant to be a friend of Christian Bormann with whom I have spent most of my holidays in the recent years. It feels exciting that he will become a father of twins, soon. Many thanks also to Daniel Kloß for his scientific support and for being a steady friend. Furthermore I wish to express my gratitude to Marie-Louise and Mr & Mrs Katzenberger for giving me the possibility and the trust to start writing my thesis at their place. The dogs are lovely.

And finally I want to thank my family. Their encouragement and support is always a powerful source of inspiration and energy. Special thoughts are devoted to my parents for their never-ending support, and to my wonderful sister Angelika. Without her, these last few months of finishing my thesis would probably have been a time of much more tension. Furthermore, I wish to thank my lovely grandma for being innumerable times my host. I love to stay at your place – a resort I will never forget.

TABLE OF CONTENTS

LIST OF FIGURES

1 SUMMARY

The molecular mechanisms of many biological signaling pathways are highly conserved in evolution and are, often, regulated by second messengers. One of the most important second messengers is calcium, Ca^{2+}. The huge diversity of calcium-regulated signaling pathways spans from fertilization of the oocyte over the activation of the immune system right up to the activity-regulated transmitter release in neurons. Furthermore, it is known that in cultured neurons, increases in nuclear calcium concentrations are of vital importance for CREB-mediated gene transcription. Those genes control, among other phenomena, neuronal survival and certain forms of learning and memory.

The hippocampal formation is essential for spatial memory and associative learning, and has been extensively characterized in terms of its circuitry and molecular mechanisms which underlie plasticity. The potentiation of Schaffer collateral – CA1 synapses by the activation of NMDAR-mediated postsynaptic signaling cascades is known as long-term potentiation (LTP) and serves as a model for learning and memory in the mammalian central nervous system. The induction of LTP requires postsynaptic calcium influx, the activation of calcium-dependent kinases and relative signaling cascades. These processes are now well-understood but less is known about the mechanisms which make LTP persistent for hours and days. The objective of this study was to establish procedures, by means of Micro-Electrode-Arrays (MEAs), which allow studying especially the signaling pathways involved in the CREB-regulated transcription-dependent late phase of LTP (L-LTP).

In one study I cultured primary hippocampal neurons for two weeks on MEAs and analyzed spontaneous activity of these networks by extracellular recordings. The spontaneous activity pattern strongly influences neuronal network information processing and thus modulation of neuronal network activity, e.g. upon external stimulations, is likely to be a basic feature of processes involved in learning and memory. In this part I could show that the specific inhibition of nuclear calcium signaling (and the associated inhibition of CREB-mediated gene transcription) alters the periodic activity pattern of developing neuronal networks. Moreover, I demonstrated that one target gene of the nuclear calcium signaling pathway, *vegf-d,* is involved in keeping neuronal networks fire. Interestingly, so far VEGF-D has been mainly known as a growth factor important for angiogenesis and lymphatogenesis.

In another study I tried to transfer the results of my work on neuronal networks to acute slice preparations, a system closer to the *in vivo* condition. Acute hippocampal slices enabled detailed studies concerning the initiation of LTP but less is known about the mechanisms that make LTP persist for extended time periods. This is partly due to the difficulty of maintaining stable recordings over several hours from acute slice preparations. MEAs offer stable extracellular field recordings from many points on a brain slice. I could show that on MEAs LTP

induced by high-frequency stimulation lasted four hours and longer, and was NMDA receptor- as well as translation-sensitive. To investigate whether the expression of late phase LTP is nuclear calcium-sensitive and which genes exactly are necessary for the maintenance phase of LTP I established virus-mediated gene transfer into the hippocampus of adult rats to generate genetically modified animals.

In summary, I established two novel methods suitable to investigate especially the signaling pathways important for the maintenance phase of LTP in hippocampal neurons. Both methods can be used to screen for candidate genes involved in L-LTP.

2 ZUSAMMENFASSUNG

Die molekularen Mechanismen vieler biologischer Signalwege sind evolutionär hochkonserviert und werden oft durch zelluläre Botenstoffe, „second messenger“, reguliert. Einer der weitverbreitetsten und bestuntersuchtesten „second messenger“ ist Kalzium, Ca^{2+}. Die enorme Diversität von Kalzium als Botenstoff reicht von der Befruchtung der weiblichen Eizelle über die Aktivierung des Immunsystems bis hin zur aktivitäts-regulierten Signalübertragung zwischen Nervenzellen. Weiterhin ist bekannt, dass der Anstieg der Kalziumkonzentration im Zellkern in kultivierten Nervenzellen von entscheidender Bedeutung für die Expression von Genen ist, die durch den Transkriptionsfaktor CREB reguliert werden. Diese Gene sind u.a. für das Überleben von Nervenzellen als auch für die Ausprägung bestimmter Gedächtnisformen verantwortlich.

Die Hippocampusformation ist essenziell für das räumliche Gedächtnis und das assoziative Lernen. Sie wurde hinsichtlich ihrer Verschaltung sowie der molekularen Mechanismen, die neuronaler Plastizität zugrunde liegen, umfassend charakterisiert. Die Potenzierung von Schaffer Collateralen – CA1 Synapsen durch die spezifische Aktivierung NMDA-Rezeptor-abhängiger Signalwege ist als Langzeitpotenzierung (LTP) bekannt und stellt ein weithin anerkanntes Modellsystem für hippocampusabhängige Lernvorgänge dar. Die Induktion von LTP durch postsynaptischen Kalziumeinstrom, die Aktivierung Kalzium-abhängiger Kinasen und deren Signalkaskaden ist bereits sehr gut untersucht und verstanden; jedoch ist wenig über die Prozesse bekannt, welche LTP für Stunden und Tage persistent machen. Das Ziel dieser Arbeit war es, mit Hilfe von Mikro-Elektroden-Arrays (MEAs) Verfahren zu etablieren, die es erlauben, speziell die in der CREB-regulierte gentranskriptionsabhängige Spätphase von LTP (L-LTP) involvierten Signalwege zu charakterisieren.

In einer ersten Studie habe ich primäre hippocampale Nervenzellen über eine Zeit von zwei Wochen auf MEAs kultiviert und die basale elektrische Aktivität der sich entwickelnden neuronalen Netzwerke durch extrazelluläre Messungen analysiert. Durch zufälliges oder gesteuertes Auftreten spontaner Aktionspotentiale oder Bursts von Aktionspotentialen kommunizieren Nervenzellen in Netzwerken untereinander und prozessieren Informationen. Weiterhin können sie ihre Aktivität als Antwort auf interne und externe Einflüsse modellieren. Dies erfolgt vermutlich über die gleichen Signalwege, welche in hippocampale Lern- und Gedächtnisprozesse involviert sind. In diesem Teil meiner Arbeit habe ich gezeigt, dass durch die spezifische Blockade von Kalziumsignalwegen im Zellkern (und die damit verbundende Inhibierung CREB-regulierter Gentranskription) die typischen elektrischen Aktivitätsmuster von neuronalen Netzwerken während deren Entwicklung geändert werden. Desweiteren konnte ich

zeigen, dass dabei besonders die Expression des Gens *vegf-d* nötig ist; ein Gen, dessen Bedeutung bisher hauptsächlich in der Angiogenese und Lymphatogenese beschrieben wurde.

In einer zweiten Studie versucht ich meine Erkenntnisse aus der Arbeit mit neuronalen Netzwerken auf ein System zu übertragen, das der *in vivo* Situation ähnlicher ist: der Präparation frischer, „akuter“ Gehirnschnitte. Akute Hippocampusschnitte ermöglichten sehr fundierte Studien zur LTP-Induktion, die Untersuchung der transkriptionsabhängigen Spätphase ist bekanntermaßen allerdings recht schwierig, da dafür von diesen Präparaten über viele Stunden stabile Signale aufgezeichnet werden müssen. Dies wird durch LTP-Messungen mit MEAs gewährt. Durch hochfrequente Stimulation induziertes L-LTP war für mehr als vier Stunden stabil und darüber hinaus NMDA-Rezeptor- sowie translationssensitiv. Um in diesen Gehirnschnitten L-LTP hinsichtlich einer möglichen Kernkalzium-Sensitivität und CREB-regulierten Genexpression untersuchen zu können, wurde die stereotaktische Applikation viraler Vektoren in den Hippocampus adulter Ratten etabliert.

In dieser Studie wurden zwei neuartige Verfahren entwickelt, die geeignet sind, um in hippocampalen Nervenzellen speziell die Signalwege zu untersuchen, die bei der Ausprägung des Langzeitgedächtnisses von Bedeutung sein können. Beide Verfahren können in dieser Form für nachfolgende Screeningversuche verwendet werden.

3 INTRODUCTION

I am delighted that I have found a new reaction to demonstrate even to the blind the structure of the interstitial stroma of the cerebral cortex. I let the silver nitrate react with pieces of brain hardened in potassium dichromate. I have already obtained magnificent results and hope to do even better in the future.

Camillo Golgi

The nervous system of vertebrates is divided broadly into two categories: the peripheral nervous system (PNS) and the central nervous system (CNS). It is composed of neurons and glial cells, which form an elaborately interconnected network. The major task of an organism`s nervous system is to communicate information between its surrounding and itself.

The goal of neural sciences is to understand the mind – how we perceive, move, think, behave and remember - and how these abilities are altered by diseases. Although begun by Hippocrates (‘On the Sacred Disease’; by Hippocrates, 400 B.C.E.) more than 2000 years ago neural sciences are still an emerging field in science because of their interdisciplinary nature. Inventions and progress in disciplines such as physics, computational mathematics or molecular genetics have each led to a great leap forward in neural sciences. Innovations like the microscope or the patch-clamp technique, identification of the molecular structure of ion channels or the generation of knock-out mice are some of the important hallmarks in the history of neural sciences.

In the 19th century, microscopes became very useful, enabling neuroanatomists such as Camillo Golgi and Ramón y Cajal to stain and draw individual neurons or neural structures (Figure 1). The second half of the 20th century was shaped and directed by the invention and continuous refinement of physiological and imaging technologies, and also by the emergence of methods in molecular biology. But the need for more novel experimental techniques is still required to resolve the numerous debates which still exist in neural sciences. One such debate concerns the pre- or post-synaptic mechanism of long-term potentiation (LTP) (Lisman, 2009). This ‘Pre/Post LTP debate’ has been pursued for over 20 years and concerns whether LTP is mediated by enhancement of presynaptic release of neurotransmitter or by enhancement of postsynaptic receptor function, or by both (Ahmed et al., 2009; Enoki et al., 2009; reviewed in

Kerchner and Nicoll, 2008). However, the reason why such a seemingly simple question is still unanswered, is due to the constraints of technical advances in analyzing central synapses with increasing precision.

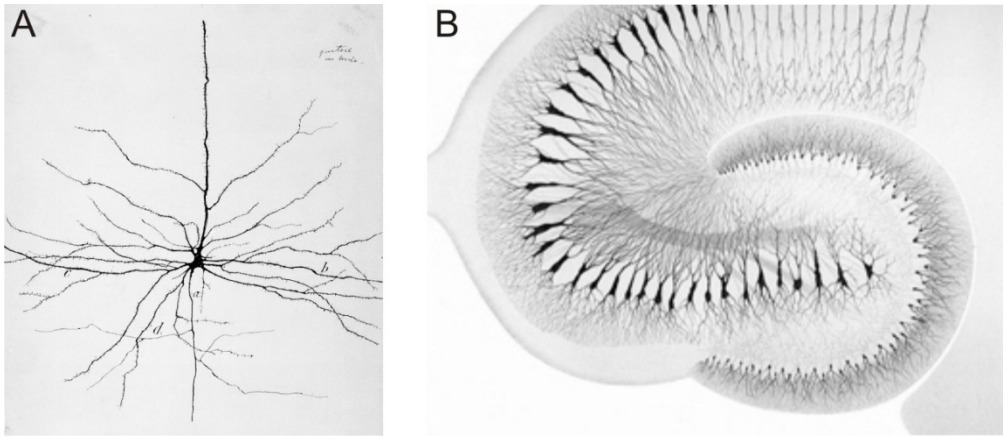

Figure 1 – Schematic image of a neuron and of the hippocampal circuitry.

Schematic drawing of a neuron by Ramón y Cajal (© Herederos de Santiago Ramón y Cajal (1899)) (A) and an image of the hippocampal circuitry consisting of single layers of principle neurons, pyramidal cells, and granule cells by Camillo Golgi (B).

With the explosion of tools to study neural sciences in recent years, one brain region has attracted a disproportionately large attention from neuroscientists – the hippocampus. Today the hippocampus is one of the most widely studied regions of the brain (more than 90.000 PubMed references (www.pubmed.org, August 2009) for the search term `hippocampus`) and it is of interest to a wide spectrum of neuroscientists.

3.1 NUCLEAR CALCIUM SIGNALING

3.1.1 Calcium – an all-rounder in biology

Calcium (Ca^{2+}) plays a pivotal role in the physiology and biochemistry of many cell types and of the organism as a whole. It intercedes in several signal transduction cascades as second messenger, functions in neurotransmitter release from neurons and is a key player in muscle contraction, fertilization, activation of the immune system and in much more. Cells invest considerable energy and employ a variety of complex interacting mechanisms in intracellular calcium homeostasis. Such mechanisms include calcium ATP-ases (or pumps), calcium exchangers, calcium-binding proteins and intracellular calcium stores such as the endoplasmic reticulum and the mitochondria. Additionally, the compartmentalization of eukaryotic cells into membrane-delineated organelles spatially restricts molecules and ions, and allows the

establishment and simultaneous functioning of different biochemical microenvironments. As dysfunctions in adequate calcium levels can lead to severe consequences for health and life, organisms tightly control their calcium homeostasis. Many of its functions are conserved throughout evolution of life and can also be found in simple eukaryotes and even in protists. The question why the calcium ion and not a different monatomic ion has been 'selected' by evolution as an intracellular messenger is discussed elsewhere (Carafoli and Penniston, 1985).

During the evolution of multicellular organisms, the calcium ion has emerged as a crucial intra- and extracellular signaling transmitter. It is nowhere more important than in the mammalian nervous system, being critical for both the relaying and long-term storage of information.

3.1.2 Calcium signaling pathways in neurons

In neurons, calcium is the principal second messenger that controls cellular mechanisms such as proliferation, development, morphology, learning and memory, survival and death. In numerous cases the pivotal requirement for triggering calcium-dependent signaling cascades are physiological levels of synaptic activity.

For example the activation of receptors located on dendritic spines of the postsynaptic membrane can generate intracellular calcium transients which stimulate several signaling cascades. These signals regulate locally the associated synapse, the trafficking of proteins and organelles as well as the spine morphology (reviewed in Bloodgood and Sabatini, 2007). Furthermore, postsynaptic changes of intracellular calcium levels activate also signaling pathways which propagate and thereby transmit information directly into the cell nucleus. These include the extracellular signal-regulated – Mitogen-activated protein (ERK-MAP kinase) and p38 MAP kinase pathways, the calcium/calmodulin-dependent kinase (CaM kinase) pathways, and a signaling pathway activated by calcineurin, a serine/threonine phosphatase (Wiegert et al., 2007; Bading and Greenberg, 1991; Bading et al., 1993; Bading, 2000; Soderling, 1999; Chawla et al., 1998; reviewed in Cruzalegui and Bading, 2000). From its site of signal generation at the plasma membrane or from internal calcium stores calcium itself can spread through the cytosol and even into the nucleus by diffusion or activity induced waves (Bading, 2000; Eder and Bading, 2007; Hardingham et al., 1997; Watanabe et al., 2008; Nakamura et al., 1999; Hagenston et al., 2008; Hong and Ross, 2007).

This synapse-to-nucleus communication is required for transcriptional responses, especially for cAMP response element binding- (CREB) and CREB binding protein- (CBP) mediated gene expression (Chawla et al., 1998; Hardingham et al., 2001). Thus, calcium is the principal second messenger in the nervous system that couples activity of neurons to gene regulation (Bading et al., 1993).

3.1.3 Electrical activity causes a wide range of changes of intracellular calcium levels

Excitability and receptivity to external changes are remarkable characteristics of cells. That is especially true for neurons, where this responsiveness becomes reflected in functional and structural ways. In neurons electrical activity displays the most prominent form of inter-neuronal communication and the synapse represents the predominant port for intercellular communication. The molecular and structural organization of both, the pre- and postsynaptic compartments of synapses, enable neurons to respond differently to particular types of synaptic activity (Engert and Bonhoeffer, 1999; reviewed in Lamprecht and LeDoux, 2004). Additionally, neurons can alter and adjust their responsiveness to electrical activity by structural adaptations in these compartments. Neurons control the strength of their connectivity in an activity-dependent manner by a process termed synaptic plasticity.

Electrical and synaptic activity causes calcium influx into neurons through ligand-gated N-methyl-D-aspartic acid (NMDA) receptors or through voltage-gated calcium channels (VGCC) such as the L-type channels (Bading and Greenberg, 1991; Dolmetsch et al., 2001), thereby activating different signaling pathways in the postsynaptic neuron (see 3.1.2). In an early stage of response upon calcium influx (usually within seconds or minutes, phase I), covalent modifications of existing proteins take place such as the phosphorylation or dephosphorylation of constituents of the ‘postsynaptic density’ (PSD).

These effects are transient, reversible and independent from gene transcription in the cell nucleus. A second stage (phase II) of events is characterized by transcription-independent, local protein synthesis in activated dendrites (Tsokas et al., 2007). Additionally, these temporary changes in synaptic efficacy can be prolonged into more permanent changes by induction of new gene expression and *de novo* protein synthesis (phase III) (Andersen et al., 1971; Bliss and Colingridge, 1993; Nicoll and Malenka, 1999). The role of calcium as a regulator of the different phases of postsynaptic events upon synaptic activity, including nuclear (transcriptional) events, raises the issue of specificity: How can neurons transduce such a large variety of synaptic stimuli into distinct cellular responses through the same second messenger?

There is evidence that neurons encode the electrical activity at the site of calcium entry in a calcium code which modulates the cellular response. This code is characterized by the amplitude, duration, frequency, and spatial limitation or propagation of the calcium signal. The representation of specific firing patterns by precise intracellular calcium signals allows neurons both coordination of local and determination of translational responses (Bading, 2000; Hardingham et al., 2001).

3.1.4 Calcium-induced calcium release

To understand the role of nuclear calcium signaling in neurons it is vital to comprehend the dynamics of its signaling. Both intra- and extracellular sources of calcium can contribute to changes of the intracellular calcium concentration in neurons in a spatially specific manner. Increases in intracellular calcium concentrations caused by calcium influx from the extracellular space are mediated by ligand- and/or voltage-gated ion channels and are further amplified by calcium release from internal stores (Berridge et al., 2000). The dynamics of calcium signaling in neurons include dendritic calcium signals, the propagation of calcium waves from the proximal apical dendrite into the perisomatic region and finally its diffusion through the nuclear pore complex into the cell nucleus. The nuclear pore itself is unlikely to cause a diffusion barrier for calcium (Eder and Bading, 2007) proposing that fast calcium waves (225 $\mu m^2/s$) might facilitate the transfer of information from synapses to the nucleus (Allbritton et al., 1992). A key-player of the calcium-mediated synapse-to-nucleus signaling is implemented by the endoplasmic reticulum (ER).

Calcium signals originated in dendritic spines are mediated to the perisomatic region along the outer membrane of the ER. The cytoplasmic increases in calcium levels induce the further release of calcium from the ER in a regenerative manner, called calcium-induced calcium release (CICR). Thereby the originally synaptic calcium signal is able to propagate as a calcium waves from dendrites to the perisomatic region of the neuron. This task can be easily achieved by the involvement of the ER because its calcium concentration (~ 100 µM) is about three magnitudes higher than that of the cytoplasm at resting conditions (~ 100 nM) and about two magnitude higher at excited conditions (~ 1.0 µM) (Berridge et al., 2000). The ER contributes to increases of intracellular calcium changes upon synaptic activity predominantly by ryanodine receptors (RyRs) and by inositol-1,4,5-triphosphate receptors ($InsP_3Rs$). While RyRs can be directly activated by calcium the activation of $InsP_3Rs$ is more complex. These receptors get activated by calcium only if the receptor agonist $InsP_3$ is present too. The process of CICR enables RyRs and $InsP_3Rs$ to communicate with each other and helps to establish coordinated calcium signals that are often organized into waves propagating through the neuron (Berridge, 1993; Clapham, 1995).

3.1.5 The calcium code and calcium-responsive DNA regulatory elements

The ability of cells to recruit different transcription factors to influence the rate and manner of transcription initiation due to various extracellular stimuli can be regulated by signaling pathways. An external stimulus which is applied to the cell is able to activate intracellular signaling pathways that activate a specific subset of transcription factors. These signaling mechanisms often control regulatory events at the level of transcription factors such as

subcellular localization, DNA binding affinity, or their interactions with the basal transcription machinery (Hunter and Karin, 1992; Whitmarsh and Davis, 2000). In the recent years several DNA elements have been well-characterized as binding sites for transcription factors which are regulated by calcium-activated signaling pathways. Within these the following are the most prominent:

The **cyclic-AMP Response Element (CRE)**, first identified as the promoter of the somatostatin gene, is an 8 bp palindromic sequence (5'-TGACGTCA-3') and is required to confer cAMP inducibility to the respective gene (Comb et al., 1986). The calcium-inducibility of the CRE was first demonstrated in PC12 cells (Sheng et al., 1988, Sheng et al., 1990). Further studies have shown that CRE-dependent gene expression can be activated by NMDA receptor-mediated calcium influx upon bursts of synaptic activity as well as by stimuli that generate long-lasting LTP in area CA1 of the hippocampus (Hardingham et al., 2002; Impey et al., 1996). The transcription factor which can mediate expression via the CRE, the CRE-binding protein (CREB), is a phosphoprotein, getting activated by phosphorylation via either CaM kinase or the ERK1/2 signaling pathways.

The **Serum Response Element (SRE)** comprises the core element 5'-CC$[A/T]_6$GG-3' which is the binding site for the serum response factor, SRF (Treisman, 1987). Target genes of the SRE and its corresponding transcription factor SRF are immediate early genes (IEGs) such as *c-fos*, *c-jun* and *zif268* but also growth factors (BDNF) and proteins of signal transduction cascades (e.g. Homer 1a). The calcium inducibility of SRE in response to activation of L-type VGCC or NMDA receptors is mediated by the ERK1/2 pathway (Bading et al., 1993; Johnson et al., 1997; Hardingham et al., 2001a).

The **Nuclear Factor of Activated T-cells (NFAT) Response Element** is a calcium-response element which gets activated after the nuclear translocation of its activator NFAT. The normally cytoplasmic NFAT is imported through the nuclear pore following its dephosphorylation by the calcium-dependent phosphatase calcineurin (Rao et al., 1997). In the absence of longer-lasting elevated calcium levels, NFAT becomes re-phosphorylated in the cell nucleus by the glycogen synthase kinase 3 (GSK3) and is re-exported into the cytoplasm.

The large number of calcium-responsive DNA regulatory elements raises the question how cells, especially neurons, are able to activate a specific set of 'calcium-responsive-genes' by elevated levels of intracellular calcium. Until a few years ago it was believed that calcium influx into the cell has little scope for specificity, and might activate calcium-responsive genes to a greater or lesser extent, depending on the quantity of influx. However, increasing evidence is emerging that the situation is more sophisticated: Neurons can distinguish between calcium signals of different properties. This includes the site of entry of the signal (Bading et al., 1993; Hardingham et al., 1999; Hardingham et al., 2002; Zhang et al., 2007), its spatial properties

(Hardingham et al., 1997; Hardingham et al., 2001a), its amplitude (Hardingham et al., 1997) and its temporal properties (Hardingham et al., 2001b). Thereby different buffering capacities or calcium clearance mechanisms as well as propagation and prolongation of calcium signals can also lead to different subcellular calcium levels. The various spatial requirements for calcium can be pointed up by the subcellular localizations of calcium-responsive signaling molecules. For example, ERK1/2 requires higher levels of calcium than calcineurin for its activation. Such levels are thought to be reached within a restricted microdomain around the point of calcium entry into the cytoplasm, namely, the NMDA receptor (Hardingham et al., 2001a). Similar evidence for calcium microdomain restricted activation exists for calcium-dependent calcium channels by voltage activated calcium channels, RyRs by neighbouring RyRs (Shuai, Jung, PNAS 2003) or CaM Kinase II anchored close to the PSD. Furthermore, there is evidence suggesting that actively transcribed DNA segments are located near nuclear pore complexes (NPCs) (Taddei et al., 2006; Akhtar and Gasser, 2007). In contrast, CREB-dependent transcription necessarily requires elevated nuclear calcium transients because the calcium sensor calmodulin and CaM kinase IV are predominantely nuclear localized (Hardingham et al., 2001b; Deisseroth et al., 1998; Mermelstein et al., 2001).

These findings support the theory, that differences in spatially restricted calcium transients, induced by different patterns of electrical stimuli can activate various calcium-dependent signaling cascades which initiate or modulate the transcriptional output of the neuron (Emptage et al., 1999a; Emptage et al., 1999b; Magee and Johnston, 1997).

3.1.6 Nuclear calcium signaling and CREB-mediated gene expression

The adaption of single cells and the organism as a whole to the challenges of a permanently changing environment and the demand for new materials and energy, requires the ability to control gene expression in a tightly regulated manner. This can occur at many stages for example at transcription initiation and elongation, RNA processing, mRNA stability, control of translation, posttranslational modifications of folded proteins, subcellular localization of proteins or protein degradation. The initiation of transcription, mostly catalyzed by RNA polymerase II, displays the most critical step in the regulation of gene expression. The basal transcription machinery (consisting of factors like the pre-initiation complex (PIC)), activating transcription factors and sometimes co-activators are required for transcription to take place (Roeder, 1996; Ptashne and Gann, 1997).

The ability of many transcription factors to influence the rate of transcription initiation can be regulated by several signaling pathways. This study will focus on nuclear calcium signaling-dependent and CREB-mediated gene transcription. The nuclear calcium-sensitive activation of CREB-mediated gene expression has shown considerable neurophysiological relevance not only

in mammalian systems, but also in studies on the marine snail, *Aplysia californica* and the fruit fly, *Drosophila melanogaster* (Dash et al., 1990; Tully et al., 1994; Yin et al., 1995). CREB seems to play an important role in the establishment of long-term memory in a variety of organisms, and in diverse of the nervous system including drug addiction, circadian rhythms and neuronal survival (Silva et al., 1998; Blendy and Maldonado, 1998; Gau et al., 2002; Walton and Dragunow, 2000). CREB binds to the CRE as a dimer, mediated by a leucine zipper motif, but the binding itself is not sufficient to regulate CRE-dependent gene expression (Sheng and Greenberg, 1990; Sheng et al., 1990; Yamamoto et al., 1988). CREB-phosphorylation is modulated via kinases (see below) which phosphorylate CREB on serine 133 and this event depends on elevations of intracellular calcium (Note: This must not be necessarily nuclear calcium (see below and Figure 2)). In contrast, the mutation of serine 133 to an alanine abolishes CREB-mediated gene expression (Sheng et al., 1991). As serine 133 serves as a point of control in calcium signaling pathways this led to the assumption that CREB is a calcium-responsive transcription factor.

CREB phosphorylation on serine 133 can be mediated by a number of protein kinases, including Ribosomal protein S6 kinase (RSK2), Mitogen- and stress-activated protein kinase (MSK1), and by the CaM kinases. The multifunctional CaM kinases play a pivotal role in diverse biological processes such as gene expression, LTP, secretion, translational control and cell cycle regulation (reviewed in Schulman, 1993). The regulation and structural organization of CaM kinases II and IV are broadly similar (Schulman, 1993; Ghosh and Greenberg, 1995; Hook and Means, 2001). Despite these similarities and their ability to phosphorylate CREB on serine 133, CaM kinases II and IV have very different effects on CREB-mediated gene expression (Matthews et al., 1994). CaM kinase IV activates CRE-dependent transcription by phosphorylating serine 133, whereas CaM kinase II also phosphorylates CREB at both the serine 133 site as well as its inhibitory site, at serine 142 (Sun et al., 1994) and is thereby not able to directly activate CREB-mediated gene expression. In the recent years numerous studies have shown that CaM kinase IV is largely located in the cell nucleus and it is the primary candidate for the activation of CREB-mediated gene expression by nuclear calcium signals. In neurons, the importance of CaM kinase IV for higher brain functions, such as memory, has been demonstrated disrupting CaM kinase IV signaling either by injection of antisense oligonucleotides, the expression of a recombinant kinase-inactive form of CaM kinase IV (CaMKIVK75E), or in CaM kinase IV-deficient mice. All these studies reported impairments in long-term synaptic plasticity, long-term hippocampal LTP and long-term memory (Bito et al., 1996; Ho et al., 2000; Kang et al., 2001).

The ERK1/2 pathway is also activated by calcium (although the activation step is far upstream) and the ERK1/2 target proteins, such as the CREB kinases RSK2 and MSK1, can also phosphorylate CREB at serine 133 (Blenis, 1993; Xing et al., 1996; Arthur et al., 2004). This pathway is involved in both, the induction and the maintenance phase of LTP, but cannot efficiently activate CREB-mediated gene expression on its own (Impey et al., 1999; Adams and

Sweatt, 2002; Johnson et al., 1997). This characteristic of the ERK1/2 pathway is proven by experiments in which CaM kinase inhibition, e.g. with KN-62, blocks CREB-dependent gene transcription without inhibiting CREB phosphorylation (Chawla et al., 1998; Hardingham et al., 1999). It demonstrates that phosphorylation of CREB on serine 133 is apparently not sufficient to activate CRE-dependent transcription and an additional event for its activation is required (
Figure 2). However, both pathways, the CaM kinase and the ERK1/2 pathway, are needed for a robust CREB-dependent gene expression. CaM kinase IV mediates CREB phosphorylation within a few seconds after calcium influx, whereas the ERK1/2 pathway is needed for a prolonged phosphorylation of CREB after calcium influx has ceased (Hardingham et al., 1999; Hardingham et al., 2001a; Impey and Goodman, 2001; Wu et al., 2001). Due to the uncoupling of CREB phosphorylation and CREB-mediated gene expression a second step for activating the transcription is necessary.

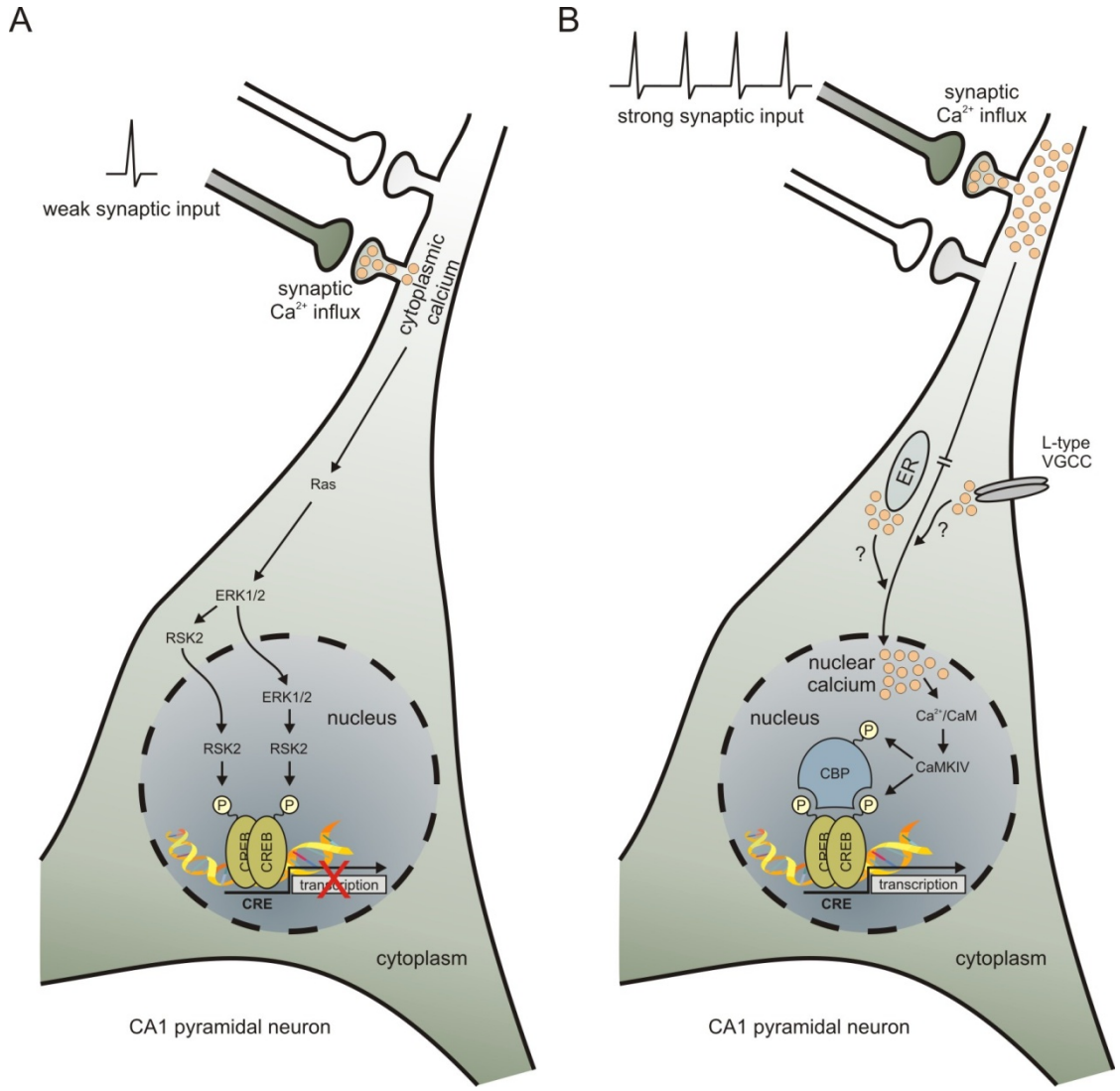

Figure 2 – Synaptically evoked calcium signals trigger two parallel pathways: the ERK1/2 pathway and the CaMKIV pathway.

Weak synaptic stimulation results in locally restricted cytoplasmic calcium transients which activate the Ras-ERK pathway. The mechanisms by which the ERK1/2 signals propagate throughout the neuron into the cell nucleus are poorly understood. Perisomatic activated ERK1/2 can either directly activate transcription factors such as the CREB kinase RSK2 in the cytoplasm or following translocation into the nucleus, activated ERK1/2 can also activate transcription factors. When translocated into the nucleus, RSK2 can activate CREB by phosphorylation at serine 133. However, this phosphorylation event is not sufficient to trigger CRE-mediated gene transcription (A). Apart from activating the Ras-ERK pathway in the cytoplasm (see A), postsynaptic calcium transients evoked by strong synaptic inputs through synaptic NMDA receptors are sufficient to trigger nuclear calcium transients. How the dendritic calcium signal propagates into the nucleus is not fully understood but there is evidence that other calcium sources such as the endoplasmic reticulum and L-type voltage-gated calcium channels contribute to this by amplifying and propagating the calcium wave throughout the neuron. After entering the nucleus, calcium forms a complex with calmodulin that activates CaM kinase IV. CaM kinase IV phosphorylates CREB on serine 133, but also carries out the second critical activation step, the phosphorylation of CBP on serine 301. The combination of both phosphorylation events recruits the transcription machinery necessary for CRE-dependent gene transcription (B).

This second necessary step for activating CREB-dependent transcription is the recruitment and activation of the CREB co-activator CBP. The association of CBP with CREB requires CREB phosphorylation at serine 133 (Chrivia et al., 1993; Parker et al., 1996). However, as described above, this is not sufficient to entirely activate transcription. The trans-activating potential of CBP is positively regulated by its phosphorylation on serine 301 in a CaM kinase IV-dependent manner (Chawla et al., 1998; Hardingham et al., 1999; Impey et al., 2002). CBP functions as a co-activator for several signal-dependent transcription factors such as Elk-1, c-Jun and nuclear hormone receptors (Janknecht and Nordheim, 1996; Arias et al., 1994; Chakravarti et al., 1996). Its ability to robustly activate CRE-mediated transcription results from its ability to recruit components of the basal transcription machinery to the promoter (such as the TATA-binding protein and the RNA polymerase II complex) as well as from its intrinsic histone acetyl transferase activity (Kwok et al., 1994; Swope et al., 1996; Ogryzko et al., 1996). All in all, nuclear calcium transients and CaM kinase IV are the key regulators of CREB-dependent gene transcription by recruiting and activating CBP, while the ERK1/2 signaling pathway ensures a prolonged CREB phosphorylation (thus the association of CREB with CBP).

3.1.7 Interfering with NMDA receptor-mediated nuclear calcium signaling

In neurons, transcriptional changes induced or modulated by electrical activity are crucial for long-lasting adaptive responses such as developmental cell fate, activation of prosurvival programs, neuronal morphology, or memory formation (Bading, 2000; West et al., 2002; Deisseroth et al., 2003; Redmond et al., 2002; Lau and Bading, 2009; Zhang et al., 2009; reviewed in Parrish et al., 2007). Thus, malfunction of nuclear calcium signaling could be an

etiological key factor common in many neuropathological conditions. Thus nuclear calcium impairments could represent a simple and unifying concept to explain disease- and aging-related memory impairments and severe cell loss, as occurs for example in Alzheimer`s disease (Zhang et al., 2009).

Physiological levels of synaptic activity are required for neurons to survive (Hardingham and Bading, 2003). Due to this, processes that interfere with electrical activity and thereby synaptic NMDA receptor function and nuclear calcium signaling can have deleterious effects on neuronal health both *in vitro* and *in vivo*. Enhancing neuronal firing and thereby synaptic NMDA receptor activity is important for neuronal survival, learning and memory, morphology and neuronal development in a nuclear calcium-sensitive manner (Arnold et al., 2005; Papadia et al., 2005; Lee et al., 2005). Blockade of NMDA receptor-mediated calcium influx by the NMDA receptor antagonist MK801 triggers apoptotic neurodegeneration in many brain regions, including the hippocampus (Ikonomidou et al., 1999). Similarly, the selective blockade of nuclear calcium signaling by expressing an the inhibitory peptide Calcium/Calmodulin binding peptide 4 (CaMBP4) prevents in hippocampal neurons the neuroprotective effect of synaptic NMDA receptor activity (Wang et al., 1995). Similarly, expression of a kinase-inactive form of CaM kinase IV (CaMKIVK75E) that functions as a negative interfering mutant, inhibits nuclear calcium/CREB-mediated transcription, by blocking of the activation of CBP (Figure 3) (Chawla et al., 1998; Anderson et al., 1997; Hardingham et al., 1999). Nuclear can control expression of several genes (Zhang et al., 2009). A recent study reports about a whole-genome transcriptional profiling on hippocampal cultures infected with a recombinant adeno-associated virus expressing either CaMBP4 or CaMKIVK75E identifying a core complex of nuclear calcium-/activity-dependent prosurvival genes (Zhang et al., 2009).

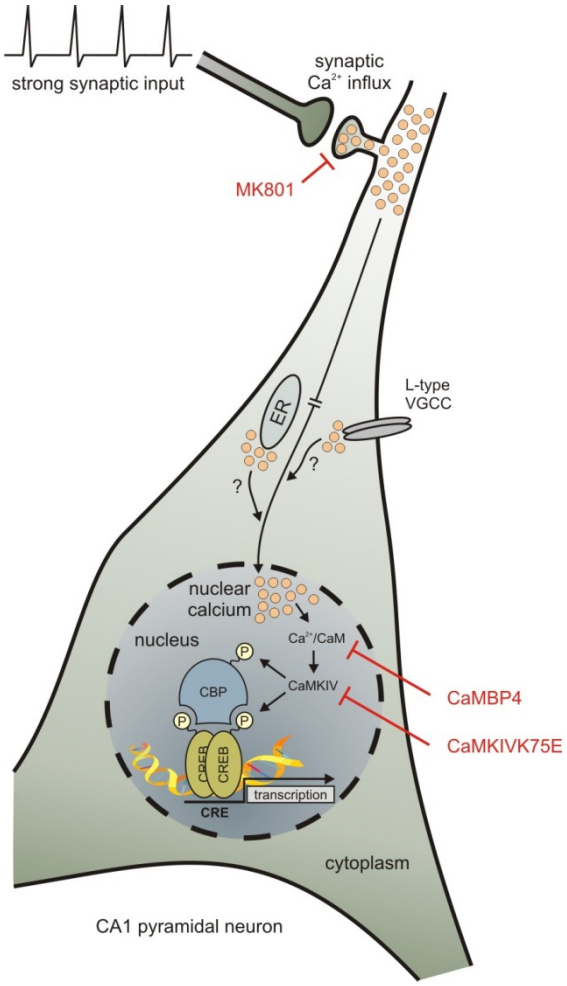

Figure 3 – CREB-dependent gene transcription is blocked by inhibition of NMDA receptor-mediated nuclear calcium signaling.

Synaptic activity induced CREB-dependent gene expression is prevented in the presence of the NMDA receptor-specific open-channel blocker MK801, which inhibits synaptic activity-induced postsynaptic calcium influx via NMDA receptors. The over-expression of proteins that interfere with down-stream targets of nuclear calcium are sufficient to block exclusively the CaM kinase IV-mediated phosphorylation of CBP on serine 301 and leave the ERK1/2 pathway uninfected (not shown). How calcium is released from internal calcium stores and how the calcium influx through L-type channels contributes to nuclear calcium transients is still under debate.

3.1.8 Imaging nuclear calcium signals

The propagation of activity-induced calcium signals to the cell nucleus represents a major route of synapse-to-nucleus communication and is important for learning and memory. Therefore, the visualization and characterization of nuclear calcium signals upon different synaptic stimulations may help to shed light on the complex mechanisms and interactions between neuronal calcium signaling and calcium-dependent gene transcription. This so-called calcium imaging is traditionally done by using synthetic small molecule calcium indicators such as Fluo-3.

When coupled to an acetoxymethyl ester, such indicators can penetrate the plasma membrane before being cleaved by endogenous esterases thus restoring the indicators fluorescence and trapping them intracellulary (Minta and Tsien, 1989). It is possible to target some small molecule indicators (FLaSH, ReASH) to tetra-cystine motifs within recombinant proteins possessing localization sequences and thus restrict their localization to a single subcellular compartment such as the cell nucleus or the endoplasmic reticulum. However, this technique requires both transfection and application of an exogenous dye which complicates and limits the versatility of this technique. A more direct approach involves recombinant genetically encoded calcium indicators, such as the bioluminescent aequorins, or by fluorescent indicators bound to calcium sensitive probes such as CaM or troponin C (Miyawaki et al., 1997; Baird et al., 1999). The recombinant calcium indicator GCaMP2.0 is one of the circularly permutated fluorescent proteins designed by connecting the M13 fragment of the myosin light chain kinase to the N-terminus and by coupling the calmodulin sequence to the C-terminus of a bisected and flipped GFP sequence (Rhoads and Friedberg, 1997; Romoser et al., 1997). Binding of calcium to calmodulin induces a conformational change of GCaMP2.0 due to the calcium/calmodulin-M13 interaction (Figure 4). This conformational change when calcium is bound partly restores the fluorescence of the GFP component (Nagai et al., 2001). Furthermore, a nuclear localization sequence was cloned at the 3'-end of the cDNA of GCaMP2.0 to target GCaMP2.0 to the cell nucleus (Weislogel, PhD Thesis, 2007).

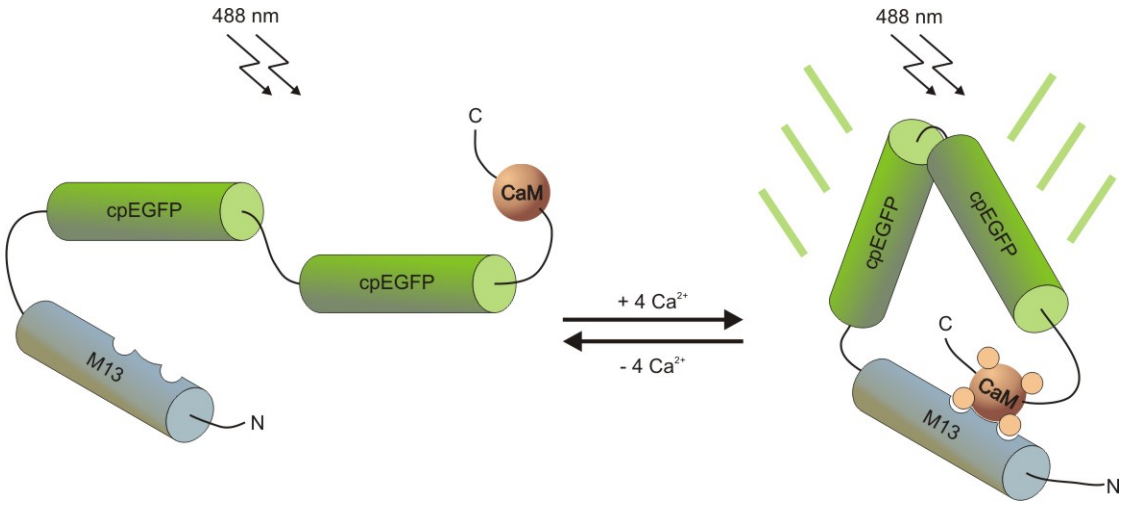

Figure 4 – Schematic representation of the recombinant calcium probe GCaMP2.0 and its calcium-induced conformational change.

GCaMP2.0 consists of three different domains (M13, cpEGFP, and calmodulin (CaM)). The N-terminus of cpEGFP is connected to the C-terminus of M13, a peptide of the myosin light chain kinase. M13 is a target sequence of CaM. The C-terminus of cpEGFP is fused to the N-terminus of calmodulin.

3.2 VEGF-D SIGNALING IN HIPPOCAMPAL NEURONS

3.2.1 The VEGF family of growth factors and their receptors

The evolution of multicellular organisms allowed specialized tissues to perform complex tasks. At least two key steps were crucial for vertebrates to achieve this goal: the development of a nervous system in which highly elaborated and branched nerve cell networks receive, transmit and process electrical signals from the periphery to coordinate tasks, and the formation of a vascular system in which blood-vessel networks branch frequently to ensure that all tissues receive adequate blood supply for providing oxygen and nutrients but also for removing metabolic waste products. Albeit these systems have complete different tasks the molecular processes important for developmental guidance and differentiation during embryogenesis share several similarities.

The formation of blood vessels, also called angiogenesis, occurs during development either by differentiation of endothelial cell precursors (angioblasts) and association of these cells to form primitive vessels, a process called vasculogenesis, or by growth of preexisting vessels, a process called angiogenesis (Risau, 1997). Both are required for the development of the vascular system, and consequently, the growth of vertebrates. Angiogenesis, the sprouting of new capillaries, in the adult is tightly controlled; under normal circumstances it occurs almost exclusively in the female reproductive system (Folkman and Shing, 1992). However, angiogenesis can be activated in the adult in response to tissues damage and is important in certain pathological conditions such as tumorgenesis and diabetic retinopathy (Folkman and Shing, 1992). During both embryogenesis and in the vascularization of tumors tissue-specific changes generate numerous types of functionally distinct vessels (Nicosia, 1998; Risau, 1995). These processes require endothelial cells to respond to a variety of extracellular signals that activate receptors responsible for growth and differentiation.

Major inducers of angiogenesis under normal and pathological conditions are the members of the vascular endothelial growth factor (VEGF) family (Carmeliet et al., 1996; Dvorak et al., 1995; Ferrara et al., 1997; Achen and Stacker, 1998). The prototype of angiogenic factors of the VEGF family, VEGF (also known as VEGF-A and vascular permeability factor) is essential for vascular development during embryogenesis and is crucial for angiogenesis in solid tumors (Carmeliet et al., 1996; Ferrara et al., 1996). Disruption of the vegf gene results in embryonic death (Carmeliet et al., 1996; Ferrara et al., 1996). Besides VEGF-A several new members of this multigene family were recently discovered: placental growth factor (PlGF), VEGF-B, VEGF-C, VEGF-D (also termed FIGF, *c-fos*-induced growth factor), VEGF-E (Orf virus VEGF), and VEGF-F (from snake venom) (Senger et al., 1983; Carmeliet et al., 1996; Maglione et al., 1991; Olofsson et al., 1996; Orlandini et al., 1996; Meyer et al., 1999; Suto et al., 2005). The VEGF-A and PlGF genes are expressed as alternatively spliced mRNAs. All of these factors show a

conserved cysteine-knot motif within the VEGF homology domain (VHD) characteristic of the family. The cysteine-rich domain is important for establishing the tertiary structure of the factors (McDonald and Hendrickson, 1993). The cDNA sequences of the VEGFs encode also for N-terminal hydrophobic secretory sequences that promote active secretion after trafficking and maturation in the Golgi apparatus. While all members of the family form mostly non-covalent bond homodimers, VEGF-B and PlGF can also compose heterodimers with VEGF-A (DiSalvo et al., 1995; Olofsson et al., 1996).

So far, three signaling receptors have been identified: VEGFR-1 (Flt-1) binds VEGF-A, VEGF-B, PlGF-1 and PlGF-2; VEGFR-2 (KDR or Flk-1) binds VEGF-A, -B, -C, -D and -E; and VEGFR-3 (Flt-4) is targeted by VEGF-C and -D (Takahashi and Shibuya, 2005). In addition, co-receptors such as the neuropilins are known (Ferrara et al., 2003; Soker at al., 1998) (Figure 5). VEGFRs are 180-230 kDa integral membrane glycoproteins composed of seven immunoglobulin-like domains in their extracellular parts, a single transmembrane region, and a consensus tyrosine kinase sequence interrupted by a kinase insert domain. They dimerize and undergo autophosphorylation at tyrosine residues upon ligand binding. Their signal transduction involves phosphorylation of further intracellular proteins, e.g. phosphoinositide-3-kinase (PI3-K) or MAPKs (Lee et al., 1996). VEGFRs are all critical for embryonic vascular development as mutant mice deficient in each of these receptors die during embryogenesis due to profound abnormalities in vascular system (Dumont et al., 1998).

In the brain, VEGF-A, VEGFR-1 and -2 are best investigated. VEGF-A is expressed by neurons and astrocytes and exerts pleiotropic effects on neural cells as well as on microglial cells (Jin et al., 2002; Forstreuter et al., 2002; Greenberg and Jin, 2005; reviewed in Brockington et al., 2004). However, recent evidence has shown that VEGF-C and VEGFR-3 are also expressed in the developing *Xenopus* and mouse brains and act on neural progenitors (Le Bras et al., 2006). Furthermore, VEGF-C, -D and VEGFR-3 are expressed in some glioblastomas (Jenny et al., 2006).

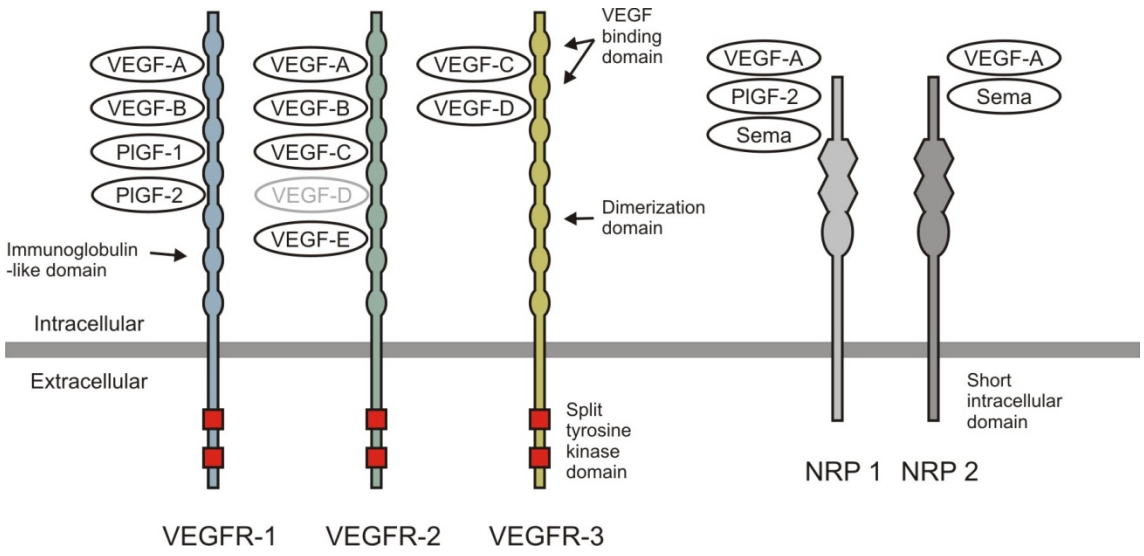

Figure 5 – Vascular endothelial growth factors (VEGFRs) and their ligands.

This schema shows the ligand specificities of VEGFRs and of their co-receptors (NRPs). In the mouse VEGF-D activates only VEGFR-3. The NRP receptors bind only specific splice variants of VEGF-A (not shown). Receptor domains are also illustrated (not shown for the NRPs). VEGFRs are tyrosine kinase receptors composed of seven immunoglobulin-like domains, a single transmembrane domain, and intracellular split tyrosine kinase domain. Figure was obtained from Brockington et al., 2004, and was slightly modified.

3.2.2 VEGF-D: structure, receptor and biological function

Vascular endothelial growth factor-D was initially described in the mouse as *c-fos*-induced growth factor (FIGF) capable of inducing mitogenesis in fibroblasts (Orlandini et al., 1996). In contrast to VEGF-A, less is known about the occurrence and function of VEGF-D and its selective receptors VEGFR-2 and VEGFR-3. However, processed mouse VEGF-D has been reported to target selectively murine VEGFR-3 (Baldwin et al., 2001). While all VEGFRs are broadly expressed on endothelial cells throughout embryonic development, VEGFR-3 in the circulatory system becomes restricted to venous endothelial cells and then to cells of the lymphatic vessels (Kaipainen et al., 1995). Furthermore, recent reports showed expression of VEGFR-3 in brain tissue, in neural progenitors in mouse embryos and in the pyramidal cell layer of the hippocampal CA1 region (Jenny et al., 2006; Le Bras et al., 2006; Shin et al., 2008). VEGF-D is a mitogen for endothelial cells. Aside from their role in the vascular system, VEGF-C and VEGF-D function also as specific regulators of lymphangiogenesis (Joukov et al., 1996; Jentsch et al., 1997, Witmer et al., 2002). In the mouse embryo VEGF-D is expressed in several organs, including teeth, heart, lung, and liver that partially overlaps with VEGF-C (Avantaggiato et al., 1998; Kukk et al., 1996). In cultured fibroblasts, VEGF-D transcription depends on *c-fos*, whereas VEGF-C is induced by serum, IL-1β and TNFα but not by *c-fos* (Orlandini et al., 1996; Enholm et al., 1997). In Kaposi's

sarcoma lesion (KS-IMM) cells VEGF-D stimulates proliferation and chemotaxis and in human umbilical cord vein endothelial cells (HUVECs) it induces growth and morphological changes within a three-dimensional matrix.

From a structural viewpoint, VEGF-D is most closely related to VEGF-C. Indeed, the similarities in overall structure and receptor binding indicate that VEGF-D and VEGF-C form a subfamily within the vascular endothelial growth factors. Besides the N-terminal hydrophobic secretory leader sequences that promote active secretion the primary translation products of these two growth factors consist of the central VHD, and of N- and C- terminal polypeptide extensions that are not present in other VEGF family members (Joukov et al., 1996; Achen et al., 1998). VEGF-D is initially synthesized as a prepropeptide, which is proteolytically processed first cleavage of the C-terminal polypeptide extension and then of the N-terminal extension thereby yielding a mature form consisting only of the VHD (Stacker et al., 1999) (
Figure 6).

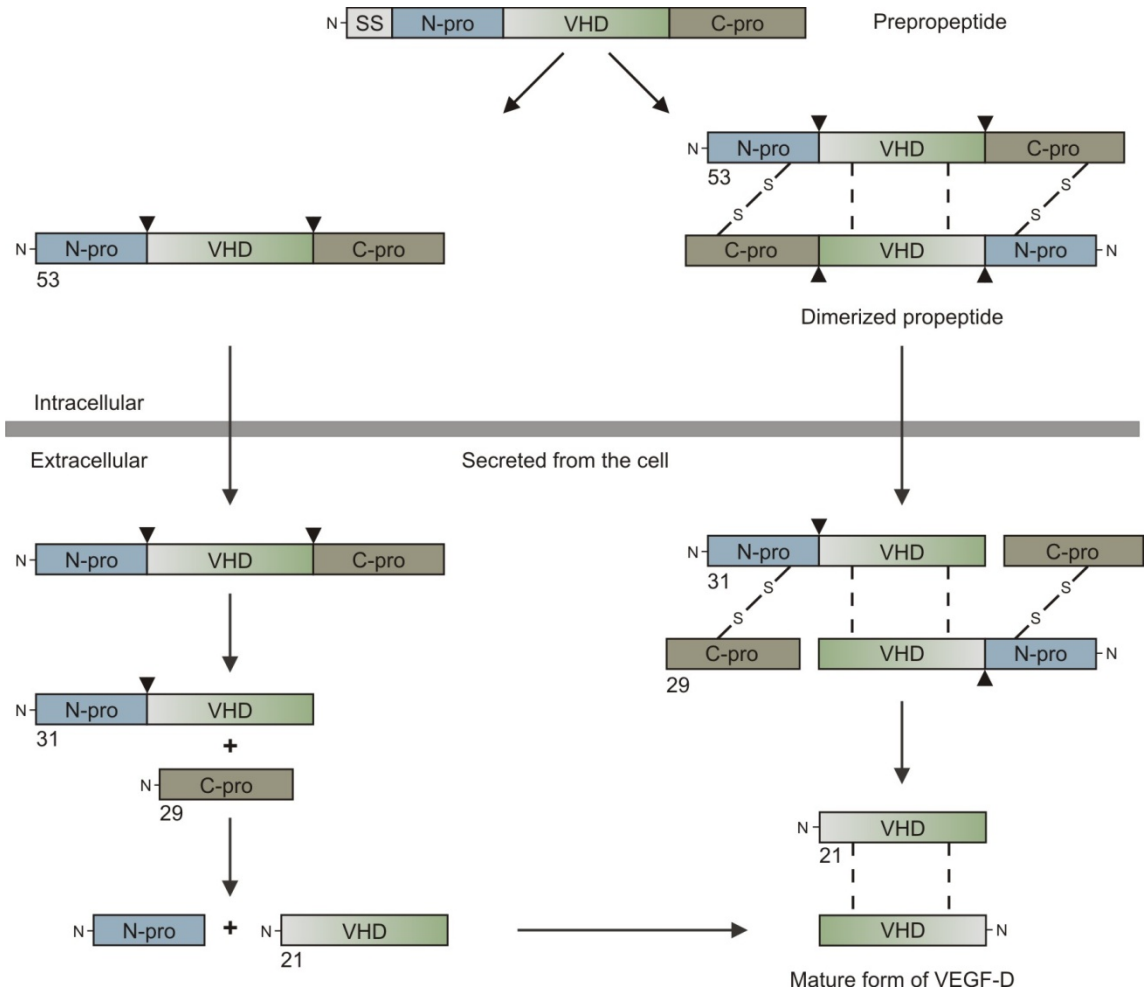

Figure 6 – Schematic representation of VEGF-D processing.

Two forms of unprocessed VEGF-D are secreted from the cell: a monomer (left side) and a disulfide-linked dimer (right side). The dimer is assumed to have an anti-parallel configuration based on the known structure of other family members. Arrows lead from the intracellular forms to the products of stepwise proteolytic processing, which give rise to a mature form that is predominantly a non-covalent dimer of the VHD. However, not all polypeptides become fully processed; therefore, unprocessed and partly processed forms are detected in cell culture supernatants. Dimeric derivatives in which N- and C-terminal cleavage has occurred in only one subunit exist, but, for simplicity, are not shown here. All combinations of subunits with no processing or partial processing can be envisaged. N-pro denotes the N-terminal propeptide; C-pro, the C-terminal propeptide; SS, secretory sequence; VHD, the VEGF homology domain; dashed lines, non-covalent interactions between domains; -S-S-, intersubunit disulfide bonds; N-, the N-termini of polypeptides; arrowheads, the approximate locations of proteolytic cleavage sites; [numbers], approximate molecular weights of corresponding polypeptide. Figure was obtained from Stacker et al., 1999, and was slightly modified.

3.2.3 Nuclear calcium- / VEGF-D signaling shapes dendritic morphology of hippocampal neurons

It is known that in the nucleus, calcium-dependent signaling induces transcription of genes important for neuronal survival and the consolidation of changes in synaptic efficacy (Zhang et al., 2009; Limback-Stokin et al., 2004). Moreover there are also evidences for an implication of transcriptional events in regulating dendritic growth, branching, maintenance and remodeling (Redmond et al., 2002; reviewed in Parrish et al., 2007). At resting conditions, hippocampal neurons in which nuclear calcium signaling is impaired via expression of CaMPB4 or of CaMKIVK75E significant impairments at the levels of dendritic length and dendritic complexity as well as dendritic spine density (unpublished observations). Since nuclear calcium controls the expression of several genes, a whole-genome transcriptional profiling was carried out to find candidate genes that might affect neuronal architecture at resting conditions. Therefore, hippocampal neurons were infected with recombinant adeno-associated viruses expressing CaMBP4 or CaMKIVK75E (Zhang et al., 2009). Among the genes affected by nuclear calcium signaling one has been previously implicated in cellular remodeling: *c-fos*-induced growth factor / vascular endothelial growth factor-D (FIGF/VEGF-D) (Marconcini et al., 1999; Orlandini et al., 1996). In primary hippocampal cultures and in mouse hippocampi VEGF-D expression is developmentally controlled. *In vitro* and *in vivo* VEGF-D expression increases at DIV 10 / P14 and then remains constant at later timepoints (unpublished observations). On the contrary, VEGF-D expression in the cortex is not varying through developmental stages.

In hippocampal neurons transfected with CaMBP4 both over-expression of VEGF-D and direct treatment with mature VEGF-D restored neuronal morphology while control neurons do not show a detectable effect on neuronal morphology. However, in CaMBP4-transfected neurons VEGF-D is not able to rescue dendritic spine density impairment. The key role of VEGF-D in hippocampal morphology is confirmed by experiments in which VEGF-D expression was specifically blocked by RNA interference. Hippocampal neurons deficient in VEGF-D expression show similar reduction in dendritic length and complexity as CaMBP4-transfected neurons, and these effects can be partly rescued by bath application of the mature VEGF-D. Moreover, RNA interference experiments on VEGF-D *in vivo* could confirm that specific down-regulation of VEGF-D expression leads directly to neuronal morphology impairments (Figure 7).

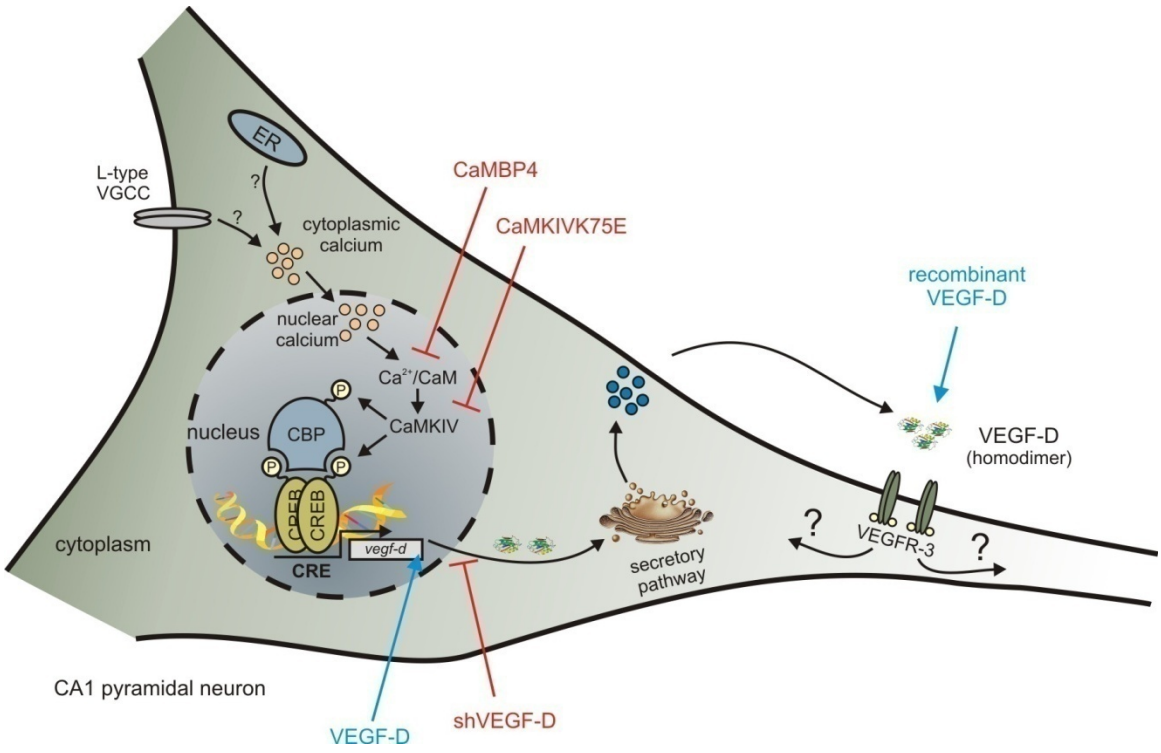

Figure 7 – VEGF-D expression in hippocampal neurons is regulated by nuclear calcium signaling and Golgi apparatus-mediated secretion.

Elevations in nuclear calcium concentration trigger CRE/CREB-dependent gene transcription of VEGF-D via Ca^{2+}/CaM-mediated activation of CaMKIV. Expression of CaMBP4 or CaMKIVK75E blocks nuclear calcium signaling and subsequently transcription of VEGF-D. Due to its N-terminal secretory sequence (not shown but see
Figure 6) VEGF-D enters the Golgi apparatus, gets further processed, packed into secretory vesicles and finally released. Once released homodimeric VEGF-D activates its unique receptor VEGFR-3, a tyrosine kinase receptor. How signaling downstream of VEGFR-3 shapes dendritic length and complexity is still unknown. Additionally to CaMBP4 and CaMKIVK75E, VEGF-D expression is suppressed by RNA interference-mediated knock-down (shVEGF-D) but the impairments on neuronal morphology are rescued by supplementing medium with mature recombinant VEGF-D.

3.2.4 Objectives of this study I

Given nuclear calcium signaling and especially VEGF-D role in shaping the morphology of hippocampal neurons, I investigated whether these signaling pathways have implications on neuronal network activity in primary hippocampal cultures. Since these experiments only required the assessment of spontaneous firing frequency and bursting behavior in the neuronal networks the use of micro-electrode arrays was favored. Plating neurons on MEAs allows non-invasive characterization of the activity state across the entire population of neurons and, moreover, it enables repeated recordings from the same cells over extended periods of time. I used recombinant adeno-associated viruses expressing either CaMBP4 or a short hairpin RNA specific against VEGF-D (shVEGF-D) to interfere with the majority of neurons of the cultured networks.

Developmental changes in network activity were assessed by daily recordings (DIV 7 to DIV 13). Thereby, it was possible to compare how a global decrease in nuclear calcium signaling on one hand and the precise knock-down of a single gene, VEGF-D, on the other hand affect neuronal network activity. Furthermore, recording single cultures for several consecutive days made it possible to temporally define the point of when VEGF-D signaling becomes essential to maintain network activity.

In addition to the characterization of network activity in cultures deficient in VEGF-D expression, I further tried to rescue these effects by bath application of the mature, recombinant VEGF-D. Similar to the rescue of the morphology of transfected neurons, supplementing the medium with mature VEGF-D could partly recover network activity in shVEGF-D infected cultures. The reason why mature VEGF-D was only partly able to rescue the observed effects on network activity could not unambiguously revealed in this study.

3.3 LONG-TERM POTENTIATION – A MODEL FOR LEARNING AND MEMORY

3.3.1 LTP in the hippocampus is NMDA receptor dependent

The hippocampus and its associated medial temporal lobe structures are required for the formation, consolidation, and retrieval of episodic memories (Morris et al., 1982; Eichenbaum, 2000). Sensory information enters the hippocampus via two inputs from entorhinal cortex (EC). The first input comprises the axons of layer II EC neurons that terminate on the dendrites of the dentate granule cells. This input is then processed serially via two additional sets of synapses in the hippocampal subfields, CA3 and CA1 (Cajal, 1968). Together, these three sets of synapses constitute the trisynaptic pathway. The second input comprises the axons of layer III EC neurons that terminate directly on the distal dendrites of CA1 neurons. On the two EC inputs, the trisynaptic pathway has received the most attention to date in experimental and theoretical studies on hippocampal function.

The encoding of new memories in the brain is thought to depend on long-lasting changes in the strength of synaptic connections between neurons (Hebb, 1949; Martin et al., 2000). The ability of central nervous system synapses to change their synaptic strength as a response to changes in synaptic activity is commonly referred to as synaptic plasticity. One form of synaptic plasticity that has received much attention is long-term potentiation (LTP), an activity-dependent long-lasting increase of synaptic strength that occurs in response to brief, repetitive electrical stimulation (Lynch, 2004; Bliss and Lomo, 1973; Andersen et al., 1977). LTP at the hippocampal Schaffer Collateral synapses on CA1 pyramidal cells is the most extensively studied form of functional plasticity and serves as a model for learning and memory in the mammalian central nervous system. The classic properties of LTP comprise input specifity, cooperativity and

associativity as well as rapid induction and persistence (Andersen et al., 1977; Douglas and Goddard, 1975; McNaughton et al., 1978).

Despite the fact that LTP was discovered more than three decades ago, the molecular and cellular mechanisms underlying this phenomenon are still not well understood. Major advances in this effort occurred when it was found that LTP induction depends on the activation of NMDA receptors and the resulting postsynaptic calcium influx through these receptors (Morris et al., 1986; Malenka et al., 1988; MacDermott et al., 1986; Lynch et al., 1983). NMDA receptor-mediated calcium transients activate one or more protein kinases in the postsynaptic neuron such as CaM kinase II, protein kinase A (PKA), protein kinase C (PKC), and others (Miyamoto, 2006). Like memory, LTP can be divided into two distinct phases: an early phase (E-LTP), which lasts only minutes to few hours and involves modification of preexisting proteins, and a late phase (L-LTP), which persists from hours to days and requires gene transcription and protein synthesis (Kandel, 2001).

3.3.2 The synaptic tagging hypothesis

The induction and maintenance of the late phase of long-term potentiation require the activation of a molecular cascade that includes signaling to the nucleus, alterations in gene expression, and the synthesis of new gene products that stabilize LTP in activated synapses (Kandel, 2001). A CA1 pyramidal neuron in the hippocampus typically receives inputs from thousands of synaptic contacts, yet changes in synaptic strength can be input-specific and are spatially restricted (Lynch et al., 1977; Andersen et al., 1977). This is surprising because signal transduction pathways underlying synaptic plasticity involve diffusible second messenger molecules such as cyclic adenosine monophosphate (cAMP) and diffusible proteins, e.g. those translated from newly transcribed mRNAs. Different models have been proposed to explain how new gene products come to reside into activated synapses. In the “mail” hypothesis, the newly synthesized mRNAs and proteins are sent specifically to activated synapses. In the “synaptic tag” model, the new gene products can only be captured and productively used at those synapses that have been tagged by local activity, a phenomenon called “synaptic tagging” (Frey and Morris, 1997). The synaptic tag model has been supported by a number of studies in the rodent hippocampus (Frey and Morris, 1998; Barco et al., 2002; Martin and Kosik, 2002). There is evidence that setting the ‘tag’ during LTP induction is critically regulated by PKA, and that spatial compartmentalization of PKA signaling is achieved via binding to A kinase-anchoring proteins (AKAPs) (Young et al., 2006; Huang et al., 2005). Anchoring PKA to AKAPs is one way that neurons may achieve localized PKA signaling in the face of diffusible cAMP, allowing for input-specific changes in synaptic strength (reviewed in Nguyen and Woo, 2003).

However, there is evidence that in CA1 pyramidal neurons synaptic tagging is compartment restricted across apical and basal dendrites (Alarcon et al., 2006). Additionally to a spatially restricted PKA activity, gene expression of the brain-specific PKMζ mRNA is necessary to maintain the late-phase of LTP at potentiated synapses (Serrano et al., 2005).

3.3.3 Late-phase LTP requires CREB-mediated gene expression

LTP can be divided into at least two distinct temporal phases, i.e., E-LTP and L-LTP. E-LTP is typically induced by a single train of high-frequency stimulation (HFS) at 100 Hz and is dependent on the modification of pre-existing protein. In contrast, L-LTP is typically induced by multiple trains of stimulation at 100 Hz or bursts of stimulation at 100 Hz repeated at 5 Hz (theta burst stimulation (TBS)). Those forms of L-LTP are blocked by both inhibitors of translation and transcription (Frey et al., 1996; Nguyen and Kandel, 1997; Impey et al., 1996; Nayak et al., 1998; Barco et al., 2002; Kelleher et al., 2004; Alarcon et al., 2004). However, there are reports about different forms of chemical- and electrical-induced L-LTP which are transcription-independent (Kang and Schuman, 1996; Huang and Kandel, 2005).

Stimuli that usually generate L-LTP in area CA1 of the hippocampus induce CREB-dependent gene transcription in a PKA-sensitive manner (Impey et al., 1996). Moreover, training on hippocampus-dependent tasks increased phosphorylation of CREB (Taubenfeld et al., 1999). Although some studies argued against the role of CREB in hippocampal L-LTP and memory formation (Balschun et al., 2003) numerous studies in mice, d*rosophila* and *aplysia* have demonstrated that the transcription factor CREB is involved in long-term memory (Impey et al., 1996; Kaang et al., 1993; Yin et al., 1994; reviewed in Kaplan and Abel, 2003). One well-established mechanism for CREB-dependent gene transcription is that upon being phosphorylated on serine 133, CREB undergoes conformational change and recruits CBP. CBP further needs to get activated by CaM kinase IV at serine 301 to initiate CRE-mediated gene transcription (Lonze and Ginty, 2002). Studies from CBP mutant mice showed that CBP is critical for the late-phase of hippocampal LTP and some forms of long-term memory (Alarcon et al., 2004). The importance of CREB-mediated gene transcription to transduce E-LTP into a persistent and more stable L-LTP is further demonstrated by a study in which VP16-CREB transgenic mice reveal facilitated expression of L-LTP (Barco et al., 2005). In mice expressing VP16-CREB, a constitutively active form of CREB, a single high-frequency stimulus is capable to induce long-lasting LTP. In these animals the mRNA transcript(s) encoding the protein(s) necessary for L-LTP might already be present in the basal condition. The cell-wide distribution of these protein(s) can prime synapses in a way that even a relatively weak stimulus will give rise to a long-lasting form of LTP. Transcriptional activity triggered by induction of L-LTP involves activation of the rapid expression (within 30 minutes) of the mRNA of several immediate-early genes such as *zif268*,

cytosceletal-associated protein *arc* and brain-derived neurotrophic factor (BDNF) (Dudek and Fields, 2002; Steward and Worley, 2001; Lu, 2003). However, gene expression studies using transgenic mice with a CRE-β-galactosidase reporter construct have revealed detectable expression two hours after the induction of L-LTP, reaching a maximum level after 4-6 hours (Impey et al., 1996). Furthermore, a range of CRE-dependent gene products have also been identified in VP16-CREB mice by using oligonucleotide arrays (Barco et al, 2005).

3.3.4 Objectives of this study II

Long term potentiation (LTP) at schaffer collaterals – CA1 synapses in the hippocampus is NMDA receptor-dependent and, once initiated, persistent for hours to days and serves therefore as a model for learning and memory (Bliss and Collingridge, 1993). Much interest is focused on the initiation of LTP but less is known about the mechanisms which make LTP persist for such extended time periods. This is partly due to the difficulty of maintaining stable recordings over several hours from acute slice preparations. Recordings with substrate integrated electrodes should be more stable as they are less invasive than glass pipettes or tungsten electrodes positioned with a manipulator, sample the activity from a large number of cells over a large number of sites, recordings are more robust to the death of some cells and are less insensitive to factors such as vibration.

In this study the capability of MEAs was investigated to study the late-phase of LTP at schaffer collateral – CA1 synapses in acute slice preparations of the rat hippocampus. It was addressed whether repetitive high-frequency stimulation (4x 100 Hz) applied via substrate-integrated electrodes is able to induce LTP and whether it is characterized by a maintaining phase that last for more than 4 hours. Furthermore, the dependency on NMDA receptor activation and translation of pre-existing mRNAs could be easily investigated by using the respective pharmacological inhibitors. In addition stereotaxic injections were combined with virus-mediated gene transfer to establish a technique suitable to study the maintenance phase of LTP, a process that requires CREB-dependent gene transcription (Cetin et al., 2006; Impey et al., 1996). The genetically encoded nuclear calcium indicator GCaMP2.0-NLS was used as exemplary probe to investigate whether recombinant proteins expressed by virus-mediated gene transfer can be used for functional experiments.

I showed here that MEA recordings are a suitable technique to study LTP in acute slice preparations. Especially the late-phase of LTP is more easily accessed than with traditional electrodes attached to manipulators. Besides addressing basic properties of LTP such as its dependence of NMDA receptor activation, the techniques of virus storage, handling and stereotaxic injection as well as slice preparation for MEA recordings, were refined into a robust protocol. Hence, in the future it is possible to proceed with more sophisticated questions about

LTP such as the importance of nuclear calcium signaling in CREB-mediated gene transcription and the contribution of selective genes to the maintaining phase of L-LTP by RNA interference.

3.4 MICRO-ELECTRODE-ARRAY RECORDINGS IN NEURONAL NETWORKS

3.4.1 Micro-Electrode-Arrays (MEAs)

Since its introduction more than 30 years ago, the MEA technology and the related culture methods for electrophysiological cell and tissue assays have been vastly improved (Thomas et al., 1972; Stett et al., 2003; reviewed in Potter, 2001). In contrast to traditional electrophysiological *in vitro* techniques such as the patch-clamp technique, in which recording periods are limited to a few hours at most, the combination of substrate-integrated microelectrode arrays and cell culture techniques can overcome this limitation. In principle, MEAs consist of several extracellular electrodes in a planar substrate suitable for cell and tissue culture. Design and microstructure of a common MEA is depicted in Figure 8. Moreover, signals can be detected from all electrodes simultaneously (Hammerle et al., 1994) and, additionally, single or multiple electrodes can be used for non-invasive electrical stimulations (Jimbo et al., 2003; Stett et al., 2000; Wagenaar et al., 2005). Thus, extracellular recordings via MEAs facilitate repeated recordings from the same group of cells over extended periods of time. Stable long-term measurements can be achieved since cells and tissue can be plated and cultured directly on the MEA electrodes. Given the fact that MEAs usually consist of 60 electrodes, MEAs are especially suitable to address questions about the burst nature of network firing, the development of spontaneous activity and synaptic plasticity across an entire network rather than at any single point (Wagenaar et al., 2006; Brewer et al., 2009; Arnold et al., 2005). More detailed information about the use of MEAs and recent progress in this field of neural sciences can be found elsewhere (Stett et al., 2003; Hofmann and Bading, 2006).

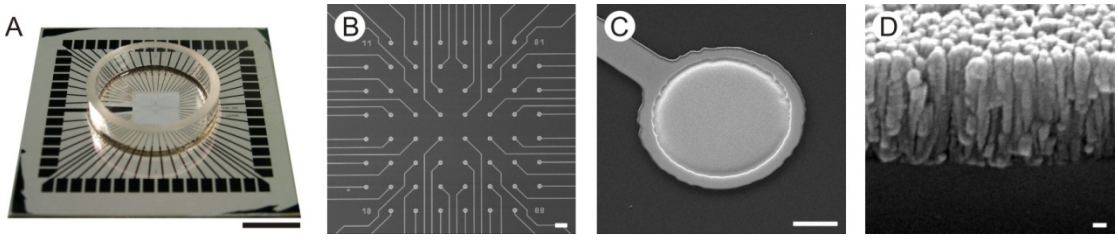

Figure 8 – Design and microstructure of a MEA as revealed by scanning electron microscopy.

Micro-Electrode-Array (A). The recording field is located in the centre of a circular well which can be filled with medium. The array is composed of 60 electrodes connected to strip conductors (B). A single Ti_3N_4 electrode is shown. It is well formed and freely accessible (C). The nanostructure of the electrode consists of densely packed columns, resulting in a dramatic increase in surface area (D). Scale bars: A: 1 cm, B: 100 mm, C: 10 mm, D: 0.1 mm. Pictures B – D were taken from Egert et al., 1998.

3.4.2 Spontaneous activity in cultured hippocampal network

Among a huge variety of applications, the most favored feature of MEAs is their adaptability to culture and to record from cells and tissue slices in a non-invasive manner over extended periods of time. Electrical stimulation via single electrodes and induction of synchronized burst pattern, e.g. by glutamate or bicuculline, are often used to study synaptic plasticity in cultures neurons (Brewer et al., 2009; Wagenaar et al., 2005; Wagenaar et al., 2006; Arnold et al., 2005; Antonova et al., 2001). However, questions concerning the development of the network can be addressed by recording spontaneous activity only. Spontaneous activity shows alternating periods of seemingly uncorrelated firing at some electrodes and of short synchronized firing at many electrodes, usually referred to as network bursts (Gross et al., 1995; van Pelt et al., 2004). Spontaneous network activity itself can be characterized by the means of network spike or firing frequency, the number of electrodes showing activity and the cumulative firing probability. These parameters do not assess different phases of spike patterns of one electrode but simply state the recorded activity of the electrodes of a MEA. In contrast, to analyze phases of synchronized firing (also referred to as bursting behavior) key parameters such as burst duration, interburst interval, burst frequency, spike frequency in bursts, spikes within bursts, percent of spikes in bursts, and inter-spike-interval in bursts are investigated to characterize burst patterns and to compare different bursting behaviors.

3.4.3 LTP in acute slice preparations

While MEAs have become a widely used tool in extracellular physiology, relatively few studies used their potential to investigate LTP in the hippocampus by field potential recordings (Stett et al., 2003; Arnold et al., 2005; Heuschkel et al., 2002). It is the fact that in the hippocampus neurons are organized in a laminar layer (and thereby creating a so called “open field” arrangement) which makes extracellular recordings suitable to study LTP by measuring field potentials. Using MEAs electrical stimulation and recording can be done in parallel and acute slices can be probed on up to 60 points in a slice. Most importantly, MEAs facilitate the investigation of the late phase of LTP which is difficult to assess using single electrode electrophysiological methods. In LTP recordings the slope of the synaptic response is measured before and after the period of high-frequency stimulation. Additionally, the relation between synaptic input and action potential output can be accessed by plotting the slope of the extracellular excitatory field EPSP versus the extracellular population spike amplitude.

4 MATERIALS AND METHODS

The chief function of the body is to carry the brain around.

Thomas A. Edison

4.1 PLASMIDS AND CLONING

4.1.1 Plasmids

The following plasmids were used: shVEGF-D_mCherry, shScr_mCherry, and empty-vector_mCherry (kindly provided by Dr. D. Mauceri, Neurobiology, Im Neuenheimer Feld 364, University of Heidelberg, 69120 Heidelberg, Germany); GCaMP2.0-NLS, eYFP-NLS and mCherry (kindly provided by Dr. J.-M. Weislogel, Neurobiology, Im Neuenheimer Feld 364, University of Heidelberg, 69120 Heidelberg, Germany); CaMBP4 (Wang, et al., 1995); mCherry-NLS, and CaMBP4-mCherry. The vectors used for the generation of recombinant Adeno-associated virus (rAAV) constructs were described previously (Klugmann et al., 2005) and provided by Matthias Klugmann and Matthew During.

4.1.2 Cloning

To generate mCherry-NLS, the mCherry construct was amplified using PCR (Pyrostart, Fast™ PCR Mix(2x), Fermentas, St. Leon-Rot, Germany). The existing AgeI restriction site was used at the 5´ end upstream of the start-codon. At the 3´ end the existing stop-codon of mCherry was eliminated and a NheI site was introduced in-frame to the NLS-coding sequence of the rAAV-GCaMP2.0-NLS vector. The following primers were used in order to generate the new restriction sites: sense direction: 5´-CCGAGATCTACCGGTATGGTGAGCAAG-3´; antisense direction: 5´-CCGGCTAGCGGATCCACCCTTGTACAGCTC-3´. The insert was ligated into the rAAV-GCaMP2.0-NLS vector between the AgeI and NheI restriction sites (Quick Ligation™ Kit, New England Biolabs, Frankfurt, Germany).

To generate CaMBP4-mCherry, the CaMBP4 construct was amplified using PCR. The existing BamHI restriction site was used at the 5´ end upstream of the start-codon. At the 3´ end the existing STOP-codon of CaMBP4 was eliminated and a BspEI site was introduced in a way that both coding sequences, CaMBP4 and mCherry, are in-frame to each other. Furthermore, the

3´ primer contained a coding sequence for two glycine residues serving as a linker between the CaMBP4 and mCherry sequences. The following primers were used in order to generate the new restriction sites: sense direction: 5´-CCGGGATCCACCGGTATGGGACCCCTCGGG-3´; antisense direction: 5´-CCGTCCGGAACCACCCTTGTCATCGTC-3´. The insert was ligated into the rAAV-mCherry vector between the BamHI and the AgeI restriction sites.

Cloned vectors were sequenced by GATC-Biotec (GATC-Biotech GmbH, Konstanz, Germany) and the proper expression was validated by DNA transfection and immunocytochemistry before starting with rAAV construction.

4.1.3 Short hairpin RNAs for gene silencing

The mouse VEGF-D-targeting shRNA sequence was generated using the mouse VEGF-D pre-pro-mRNA (NM 010216) and a software supplied by Dharmacon RNAi Technologies (Thermo Scientifics, Chicago, USA). In this study the following sequences were used: 5´-GGGCTTCAGGAGCGAACAT-3´ as shRNA to knock-down VEGF-D and 5´-GTGCCAAGA CGGGTAGTCA-3´ as a control shRNA that does not target any mRNA of the mouse genome (from here on referred to as shScr). The vector `empty vector_mCherry` (from here on referred to as empty vector mC) does not contain any shRNA downstream of the U6 promotor.

4.2 RECOMBINANT ADENO-ASSOCIATED VIRUS CONSTRUCTION

For infection of neurons *in vitro* and *in vivo*, recombinant and replication-deficient viruses of the mosaic serotypes rAAV1/2 were produced by co-transfection of human kidney cell line 293 (ATCC, Manassas, Virginia) by calcium phosphate precipitation. HEK293 cells were grown in high-glucose-containing (4.5 g/l) Dulbecco`s Modified Eagle Medium (DMEM; Life Technologies/Invitrogen, Carlsbad, CA) supplemented with 10 % fetal bovine serum (FBS; Life Technologies/Invitrogen, Carlsbad, CA), 1 % non-essential amino acids (Life Technologies/ Invitrogen, Carlsbad, CA), 1 % sodium pyruvate (Life Technologies/Invitrogen, Carlsbad, CA) and 0.5 % penicillin/streptomycin (PenStrep; Sigma-Aldrich, Munich, Germany) at 37°C in a humidified atmosphere containing 5 % CO_2. 2-3 hours before transfection each 14-cm-diameter plate of HEK293 cells (60 to 70 % confluent) was exchanged with 25 ml of fresh Iscove`s Modified Dulbecco Medium (IMDM; Life Technologies/Invitrogen, Carlsbad, CA) containing 5 % fetal bovine serum without antibiotics. Packaging of chimeric serotypes rAAV1/2 transducing vectors was carried out with 25 µg of a mini-adenovirus helper plasmid pFΔ6, 6.25 µg of AAV2 helper plasmid pRV1, 6.25 µg of AAV1 helper 4 plasmid pH21 and 12.5 µg of the rAAV plasmid containing the respective GOI for each 15-cm tissue culture dish. 18-22 hours after transfection, the medium was replaced by fresh DMEM containing 10 % FBS and antibiotics. Cells were washed once with pre-warmed PBS and harvested with a tissue-scratcher in PBS 60-65 hours

after transfection. After centrifugation for 5 min at 800 × g, cells were resuspended in 150 mM NaCl and 20 mM Tris (pH 8.0). Then cells were lysed with 0.5 % sodium deoxycholate monohydrate (Sigma-Aldrich, Munich, Germany) and 50 U/ml Benzonase® Nuclease (Sigma-Aldrich, Munich, Germany) for 1 hour at 37°C. Afterwards, cell debris was spun down at 4°C at 3000 × g for 15 min and supernatant was frozen at -20°C over-night. The following day, samples were thawed at RT and viruses were purified as previously described (Klugmann et al., 2005). Briefly, purification of viruses was performed with HiTrap™ Heparin HP Columns (GE Healthcare, Munich, Germany) and viruses were then concentrated with Amicon® Ultra-4 Centrifugal Filter Units (Millipore, Schwalbach, Germany). Integrity of viral particles was routinely checked by SDS-PAGE (10 % resolving gel). Genomic titers (genome copies/ml) of final viral stocks were determined by using the sequence detection system model 7300 Real Time PCR System (Applied Biosystems, Foster City, California, USA) with primers designed to the woodchuck hepatitis virus posttranslational regulatory element (WPRE) as described previously (Klugmann et al., 2005).

The rAAV protein expression cassette contained a 1.3 kbp fragment of the mouse CaMKII promoter (kindly provided by A. Cetin and P. Seeburg, Max Planck Institute for Medical Research, 69120 Heidelberg, Germany), the woodchuck hepatitis virus posttranslational regulatory element (WPRE) and a bovine growth hormone polyA signal. For expression of short hairpin RNAs (shRNAs) a rAAV vector was used that contained the U6 promotor for shRNA expression and a CaMKII promoter driving mCherry expression as a reporter gene.

4.3 CELL CULTURE

4.3.1 Preparation of coverslips

12 mm glass coverslips (Carl Roth GmbH & Co. KG, Karlsruhe, Germany) were washed with 70 % ethanol for 30 minutes and subsequently with absolute ethanol, in which they were swayed from time to time. After an ultrasonic bath for 5 minutes at RT, coverslips were washed again with absolute ethanol. To evaporate the ethanol the glass bottle containing the coverslips was put into a dryer for 2 hours and swayed from time to time to avoid from sticking together. Afterwards, the coverslips were transferred into a new glass bottle and sterilized at 140°C for 4 to 5 hours.

4.3.2 Preparation of Micro-Electrode-Arrays

Due to high acquisition costs, Micro-Electrode-Arrays (MEAs) (Multi Channel Systems, Reutlingen, Germany) were reused for at least six cultures and were kept in distilled water for storage between cultures. Two days before plating, MEAs were swayed in 1 % (w/v) Tergazyme solution (Alconox, NY, USA) (new MEAs in PBS) on a rocker for 16 to 20 hours at RT. At the next

day MEAs were rinsed four times 30 min each in distilled water on the rocker. Afterwards, they were dried with a soft wipe (e.g. from Kimtech. Koblenz, Germany) and hydrophilised for 2 min at $2x10^{-4}$ bar in a vacuum deposition system (type: Med 010, Balzer AG, Germany). For sterilization, MEAs were cleaned thoroughly with 70 % ethanol (derived from absolute ethanol) by a cotton swap and were dried until coating. During cleaning and treatments the inside of the dish was not touched at any time.

4.3.3 Coating of coverslips and Micro-Electrode-Arrays

1 ml of coating solution ((poly-D-lysine (2 µg/cm²) + laminin (1 µg/cm²) (both Becton Dickinson Labware, Heidelberg, Germany) in water) was added to each MEA-dish and 2 ml of coating solution to each 35-mm dish (Nunclon Surface, Denmark) containing four coverslips. Coating was done twice with a first coat for 60 minutes, a 30 min period of drying and a second coat over-night. MEAs and dishes were washed twice with water for 30 minutes and dried well (~ 1 hour). 15 minutes before plating, MEAs and dishes were wet with NB-A growth medium. Coating was done under sterile conditions and preferentially 24 hours before dissection.

4.3.4 Dissection of hippocampi and dissociation of neurons

Opti-MEM/glucose and NB-A growth medium were pre-warmed and pH-equilibrated in a tissue culture incubator (37°C, 5 % CO_2). 4 ml KyMg solution and 55 ml NaOH (0.2 N) were added to 36 ml dissection medium (DM) and stored at RT. Two 60-mm dishes each with 9 ml of DM/KyMg were prepared to collect the left and right hemispheres, respectively. Furthermore, two 60-mm dishes each with 7 ml of DM/KyMg were prepared, one for the dissection and one to collect the dissected hippocampi (HC). New-born mice (C57BL/6, Charles River Laboratories, Sulzfeld, Germany) were used for the dissection of their HC. The freshly killed mice were fixed on a silicon board with needles and the skull was opened using micro forceps and scissors (Fine Science Tools, Heidelberg, Germany). Both hemispheres were removed with three precise cuts (one between cortex and olfactory bulb, one between both hemispheres, and one between cortex and cerebellum). Left and right hemispheres were transferred in the 60-mm dishes containing 9 ml DM/KyMg. The HC were dissected from the hemispheres with micro forceps and scissors under a stereomicroscope at 16x magnification (Stemi SV 6, Carl Zeiss MicroImaging GmbH, Göttingen, Germany). The single HC extracted from left and right hemispheres were kept in one of the 60-mm dishes containing 7 ml DM/KyMg.

Inhibitor and enzyme solutions were thawed, warmed up and stored in water bath at 37°C during the various steps of dissociation. HC were transferred into a sterile round bottom tube containing a stirrer and were incubated in 3 ml enzyme solution for twice for 20 minutes in the water bath (37°C, slow stirring). Additionally, the tube was swirled carefully by hand every 5 minutes. HC were washed three times with 2 ml DM/KyMg each, while inverting the tube constantly for 1 minute.

Three times 2 ml of inhibitor solution was added to the HC and they were left for 5 minutes at RT after each addition. Then, HC were washed three times in 2 ml GM each, while the tube was consistently inverted for 1 minute. GM was left at RT and cells were dissociated in three turns in GM (twice for 50 times and once for 20 times) by pipetting the HC in 2 ml GM up and down and avoiding air bubbles. After each dissection step, 2 ml GM was added and cells were left to rest for 5 minutes. Then, most of the homogeneous cell suspension (3.0 to 3.5 ml) was transferred to a 15 ml Falcon tube. The remaining fraction was dissociated by pressing the pipette to the bottom of the tube and by pipetting up and down for 20 times and this fraction was then also transferred to the 15 ml Falcon tube too. The cell suspension was diluted with pre-warmed OptiMEM/glucose to obtain the desired cell densities (0.78 HC per 2 ml for 35-mm dishes and 0.45 HC per 1 ml for MEA-dishes). The cells were seeded into 35 mm dishes (2 ml per dish) containing four coverslips or into MEA-dishes (1 ml per dish). Two and a half hours after plating the medium was replaced by fresh, pre-warmed and pH-equilibrated GM.

4.3.5 Culturing primary hippocampal neurons

Primary hippocampal neurons from new-born C57BL/6 mice were dissociated and plated on poly-D-lysine/laminin-coated 12 mm coverslips (four coverslips in each 35-mm plastic dish) or in MEA-dishes as described in 4.3.4 or by Bading and Greenberg (1991) except that GM was supplemented with B27 (Invitrogen, Karlsruhe, Germany). The cells were grown for 6 days in NB-A growth medium. After three days in culture (day *in vitro* 3, div03) 2.4 µM cytosine β-D-arabinofuranoside (AraC) was added to each dish in order to prevent proliferation of non-neuronal cells. On day *in vitro* 6 (div06) NB-A was replaced by pre-warmed and pH-equilibrated TM (1 ml per MEA-dish; coverslips were transferred to 24-well plates, 1 ml TM per well).

4.3.6 Media and buffers for primary hippocampal neurons

Dissociation medium (DM)

Na_2SO_4 (1 M)	20.45 ml
K_2SO_4 (0.25 M)	30.0 ml
$MgCl_2$ (1.9 M)	0.77 ml
$CaCl_2$ (1 M)	0.063 ml
Hepes (1 M)	0.25 ml
Phenol Red	0.5 ml
Glucose (2.5 M)	2.0 ml
H_2O	to 250.0 ml

sterile filtered through 0.22 µm Millipore filter

Ky/Mg solution (KyMg)

Kynurenic acid	158.56 mg
H_2O	10.0 ml
Phenol Red	0.4 ml
NaOH (1 M)	5x 200 µl
	thorough vortexing until kynurenic acid is in solution
Hepes (1 M)	0.4 ml
	vortexing
$MgCl_2$ (2 M)	4.0 ml
H_2O	to 80.0 ml

sterile filtered through 0.22 µm Millipore filter and stored in 5 ml aliquots at -80°C

Salt Glucose Glycin solution (SGG)

NaCl (5 M)	11.4 ml
$NaHCO_3$ (7.5 % solution)	14.6 ml
$MgCl_2$ (1.9 M)	0.264 ml
$CaCl_2$ (1 M)	1.0 ml
KCl (3 M)	0.882 ml
Hepes (1 M)	5.0 ml
Glucose (2.5 M)	6.0 ml
Glycin (1 M)	0.5 ml
Na-pyruvate (0.1 M)	2.5 ml
Phenol Red	1.0 ml
H_2O	to 500.0 ml

sterile filtered through 0.22 µm Millipore filter

Transfection medium (TM)

SGG	88.0 ml
MEM (without glutamine)	10.0 ml
Insulin-Transferrin-Selenium	1.5 ml
PenStrep	0.5 ml

sterile filtered through 0.22 µm Millipore filter

NB-A / Growth medium (GM)

Neurobasal A-medium	96.5 ml
B27	2.0 ml
1 % Ratserum	1.0 ml
L-glutamine (200 mM)	0.25 ml
PenStrep	0.5 ml

sterile filtered through 0.22 µm Millipore filter

Enzyme solution

5.0 ml KyMg solution was added to 45.0 ml of DM
50.0 ml of DM/KyMg was added to a bottle containing 22.5 mg L-cysteine
pH was adjusted with 0.2 M NaOH (until Phenol Red turns slightly to purple)
500 units of papain latex were added
wait until papain latex is in solution (takes 15 min)
sterile filtered, aliquoted and stored at -20°C

Inhibitor solution

10.0 ml KyMg solution was added to 90.0 ml of DM
96.0 ml of DM/KyMg was added to a bottle containing 1.0 g of trypsin inhibitor
pH was adjusted with 0.2 NaOH
500 units of papain latex was added
wait until trypsin inhibitor is in solution (takes 10 min)
sterile filtered, aliquoted and stored at -20°C

4.4 CHEMICALS AND SOLUTIONS

4.4.1 Solutions

Phosphate-buffered saline (PBS)

NaCl	8.0 g
KCl	0.2 g
Na_2HPO_4	1.44 g
KH_2PO_4	0.24 g

pH adjustment to 7.4 with HCl
H_2O was added to a final volume of 1 liter

Blocking solution for immunocytochemistry (BS)

BSA (20 % w/v)	500 µl
NGS	500 µl
Triton-X100	25 µl
PBS	3.975 ml

Solution for incubation of antibodies for immunocytochemistry (AS)

BSA (20 % w/v)	500 µl
NGS	50 µl
Triton-X100	15 µl
PBS	4.435 ml

add antibody of choice

Moviol 4-88 mounting medium

Glycerol	6.0 g
Moviol 4-88	2.4 g
H_2O	6.0 ml
Tris (0.2 M, pH 8.5)	12.0 ml

4.4.2 Chemicals

Cytosine β-D-arabinofuranoside (AraC)	Sigma-Aldrich, Munich, Germany
Bicuculline methiodide	Sigma-Aldrich, Munich, Germany
Bisbenzimide Hoechst 33258	Serva GmbH, Heidelberg, Germany
Recombinant mouse VEGF-D	R&D Systems, Minneapolis, USA
Anisomycin	Sigma-Aldrich, Munich, Germany
APV	Biotrend Chemicals, Zürich, Switzerland
MK801	Biotrend Chemicals, Zürich, Switzerland

4.5 DNA TRANSFECTION AND DNA INFECTION

4.5.1 DNA Transfection

DNA transfection of hippocampal neurons was done 9 to 11 days after plating using Lipofectamin 2000 (Invitrogen) at a concentration of 5 µl/ml and a total DNA concentration of

1.6 µg/ml. Coverslips were transferred into 4-well plates. The Lipofectamin/DNA mixture was left on the cells for 2 to 3 hours before it was replaced with TM. Cells were left for additional 30 to 40 hours before experiments were performed.

4.5.2 DNA Infection

After virus preparation coverslips were infected on day 4 after plating with increasing volumes of virus solution (0.5 – 1.0 – 2.0 – 4.0 µl) to evaluate infection rates. For all used viruses, 0.5 to 1.0 µl virus solution was suitable to achieve infection rates of about 60 to 70 % of living neurons which was equivalent to 2-5 × 10^9 particles/ml).

4.6 IMMUNOCYTOCHEMISTRY

4.6.1 Immunocytochemistry

Cells were fixed with paraformaldehyde (4 %) / sucrose (4 %) solution (PFA). After fixation, cells were washed two times for 10 minutes each with PBS and permeabilised with Triton X-100 (0.5 %) in PBS (containing 10 mM glycine to quench residual PFA). Cells were washed three times for 10 minutes each with PBS and were incubated with BS for 1 hour to block non-specific binding sites. After washing cells once with PBS AS, containing primary antibodies was added and left for over-night at 4°C. The following day cells were washed five times for 10 minutes each with PBS before AS containing secondary antibodies was added for 1 hour at RT. Then cells were washed again five times for 10 minutes each with PBS and for nuclear staining cells were incubated for 5 min with HOECHST solution (1:5000 in PBS of a 1 % stock solution). After washing three times for 5 minutes each in PBS and once 5 minutes in distilled water, cells were mounted with Moviol 4-88.

4.6.2 Table of antibodies

Table 1 – Primary and secondary antibodies used in the present study.

Primary antibody	Species	Dilution	Company
Flag (flag M2)	mouse	1:1000	Sigma
HA (HA.11)	mouse	1:2000	Covance
Myc (c-Myc)	mouse	1:1000	Santa Cruz

Secondary antibody	Species	Dilution	Company
mouse-IgG (Alexa-488 conjugated)	goat	1:1500	Molecular Probes
mouse-IgG (Alexa-594 conjugated)	goat	1:1500	Molecular Probes

4.7 ACUTE SLICE PREPARATIONS

At P36-P41 rats were anesthetized by inhalation of isofluran and killed by decapitation. The brain was rapidly removed and submerged in ice-cold slicing solution. A vibratome (CU65 Cooling Unit & HM650V Vibratome, Microm, Walldorf, Germany) was used to cut 300 µm thick slices at an angle of approximately 30° above the horizontal level in slicing solution maintained at 0.3°C. Hippocampi were dissected from the slice and transferred to a holding chamber containing aCSF. Slices were maintained at 32°C for the first 30 minutes and then returned to room temperature for additional 30 to 45 minutes.

Some slices were put on cell culture filter inserts (PET, 0.4 µm pore size, BD Biosciences, Belgium), turned upside down, and kept overnight in an incubator at 28°C (gassed with 5 % CO_2) before recording. Analogous to the method for organotypic slice cultures described by Stoppini (1991), the slices were sucked dry and placed on the interface between air und aCSF,. The day of preparation is referred to as day *in vitro* 0, the following day is termed DIV 1.

4.8 STEREOTAXIC INJECTIONS

4.8.1 Anesthesia

Sleep mix

Domitor® (1.0 mg/ml)	1.5 ml
Dormicum® (5.0 mg/ml)	4.0 ml
Fentanyl® (0.785 mg/ml)	1.0 ml
H_2O	6.5 ml

sterile filtered and stored at 4°C

Wake-up mix

Antisedan® (5.0 mg/ml)	0.6 ml
Anexate® (0.1 mg/ml)	8.0 ml
Naloxon® (0.4 mg/ml)	1.2 ml

sterile filtered and stored at 4°C

4.8.2 Stereotaxic injections

rAAVs were delivered by stereotaxic injection into the ventral hippocampus of 22 day-old female Sprague-Dawley rats (Cetin et al., 2006). Rats were anaesthetized intraperitoneal with sleep mix (3 µl / gram body weight) and fixed with ear bars and a head holder in the stereotaxic frame (small animal stereotaxic instrument, Kopf Instruments, Tujunga, California). In each

hemisphere a total volume of 2 µl (two times 1 µl each) containing 1×10^9 genomic virus particles were injected at a flow rate of 200 nl/min over a period of 15 minutes at the following coordinates relative to Bregma: anteroposterior: - 4.3 mm; mediolateral: ± 4.1 mm; dorsoventral: – 4.0 and - 3.6 mm from the skull surface (Figure 9). After surgery rats were sewn up and antagonized with wake-up mix (5 µl / gram body weight), applied subcutaneously. Animals had free access to food and water and were housed under diurnal lighting conditions for another 15 to 19 days. Procedures were done in accordance with ethical guidelines for the care and use of laboratory animals (Local Animal Care Committee, Karlsruhe, Germany) and to the respective European Community Council Directive 86/609/EEC.

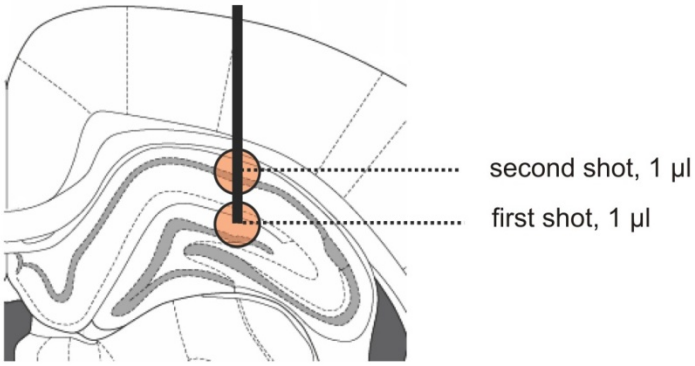

Figure 9 – Stereotaxic injection by double line shot.

Schematic drawing of virus injection by line shot in the rat hippocampus. 1 µl of virus solution was separately injected at two different dorso-ventral levels (adapted from Y. Aso, Master Thesis, 2007, Heidelberg).

4.9 ELECTROPHYSIOLOGY

4.9.1 Solutions

	Slicing solution	aCSF
Sucrose	150.0 mM	---
NaCl	40.0 mM	125.0 mM
KCl	4.0 mM	3.5 mM
$MgCl_2$	7.0 mM	1.3 mM
NaH_2PO_4	1.25 mM	1.2 mM
$CaCl_2$	0.5 mM	2.4 mM
Glucose	25.0 mM	25.0 mM
$NaHCO_3$	26.0 mM	26.0 mM

Slicing solution and aCSF were purged with carbogen (95 % O_2 and 5 % CO_2).

4.9.2 Recording hippocampal cultures on Micro-Electrode-Arrays

Hippocampal neurons were plated at a density of about 400 cells (neurons and glia) per mm² onto MEA dishes containing a grid of 60 planar electrodes (Multi Channel Systems, Reutlingen, Germany). The distance between the electrodes was 200 µm and the electrode diameter was 30 µm. To avoid hyperosmolality (Potter and DeMarse, 2001) MEA dishes were sealed with a thin membrane of fluorinated ethylene-propylene (FEP Teflon® film, ALA Scientific Instruments, New-York, USA) two and a half hours after plating neurons. Recordings were acquired with an MEA-60 amplifier board (10 Hz – 35 kHz, gain 1200, sampling frequency 20 kHz, Multi Channel Systems) at 35.5°C (Temperature Controller TC02, Multi Channel Systems). After a culturing period of 7 to 13 days network activity was daily recorded for 5 minutes (or until a train of activity has ended for at least 2 seconds). On DIV 13 cultures were recorded twice, before and after stimulation with bicuculline, respectively (Figure 10). On DIV 7, cultures showing an average network activity of less than 0.5 Hz were excluded from recordings. After each recording, cultures were put back into the incubator. On DIV 9 and DIV 12, half of the medium was replaced with fresh pre-warmed and equilibrated TM under sterile conditions after recording. To avoid contaminations, cultures were kept sterile by the use of sealed culture chambers until application of bicuculline. Spikes were detected with the integrated spike detector of the MC Rack software (Multi Channel Systems) and further analyzed with Neuroexplorer (NEX Technologies, v2.680, www.neuroexplorer.com). The following values were used to analyze bursting behavior: “maximal interval to start burst”: 0.05 s, “maximal interval to end burst”: 2 s, “maximal interval between bursts”: 2.01 s, “minimum duration of bursts”: 0.15 s, and “minimum number of spikes in bursts”: 15.

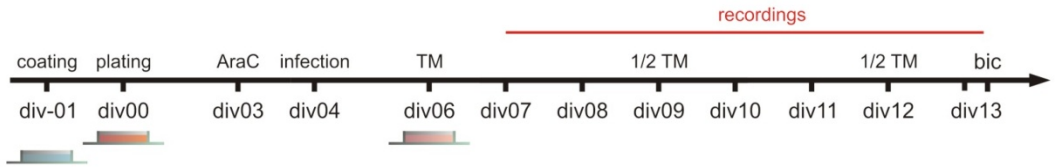

Figure 10 – Timescale of culturing hippocampal networks on MEAs.

MEA dishes were coated with poly-D-lysine/laminin (see 4.3.3) over-night and washed thoroughly before preparation. Hippocampal neurons were plated at a density of about 400 cells / mm². At day *in vitro* (div) 3, proliferation of non-neuronal cells was stopped by adding AraC (4.3.5) and at div 4 cultures were infected by the respective virus (4.5.2). Growth medium was replaced by serum-free transfection medium at div 6. From div 7 on daily recordings were performed for 5 minutes to record network activity (4.9.2). At div 13 bicuculline (bic, 50 µM) stimulation was done to activate network bursting.

4.9.3 Acute slice recordings on Micro-Electrode-Arrays

Slices were transferred to a MEA containing a grid of 60 planar electrodes (Multi Channel Systems) and constantly perfused with purged aCSF at a flow-rate of 3 ml per minute. The distance between the electrodes was 200 µm and the electrode diameter was 30 µm. Temperature in the recording chamber on the MEA was kept constant at 30°C (Temperature Controller TC02 set to 35°C, Perfusion Cannula PH01 set to 32°C, both Multi Channel Systems). Recordings were acquired with two MEA-1060 BC amplifier boards (10 Hz – 35 kHz, gain 1200, sampling frequency 20 kHz, Multi Channel Systems) connected via a MEA Switch 2-to-1 (MEAS2/1, Multi Channel Systems) to the MC-Card (64-channel data acquisition system, Multi Channel Systems). The advantage of using a double-system at the one hand is that two slices can be recorded in parallel and on the other hand that one slice can be ran under control conditions (or a slice of an uninfected hemisphere) and the second can be perfused by the respective drug (or a slice of the infected hemisphere). This method allows the interpretation of effects independently from tissue quality. Slices were put under a platinum ring covered with a mesh of thin nylon stripes to improve slice-to-electrode contact and to avoid movements. The accompanying software 'MC_Rack' was used to record spontaneous and evoked activity. Field potentials were recorded simultaneously on all electrodes selected for each slice, usually covering the whole CA1 region and parts of CA3 and the dentate gyrus (DG). Monopolar biphasic voltage pulses (positive/negative, 100 µs per phase) were used for electrical stimulation of Schaffer collateral/commissural and perforant pathway fibers through MEA electrodes using a STG 1002 or STG 4004 stimulus generator (both Multi Channel Systems) (Figure 11). Two electrodes in the *stratum radiatum* were chosen as stimulation electrodes to evoke field excitatory postsynaptic potentials (fEPSPs) in two independent pathways, termed S1 and S2. The S1 pathway was used to apply the tetanic stimulation to evoke LTP, whereas the S2 pathway functioned as an internal control. At the beginning and at the end of each recording, an input-output curve (IO curve) was obtained. Voltage pulses from 0.5 to 3V were applied, increasing with 0.25V steps and two pulses for each step. The stimulation strength resulting in about 30 to 40% of the maximum response was chosen for the test pulse and for the tetanic stimulation, which was usually between 0.75V and 1.5V. S1 and S2 pathways were stimulated alternating at a frequency of 0.083Hz (one stimulus per 5 minutes at each pathway).

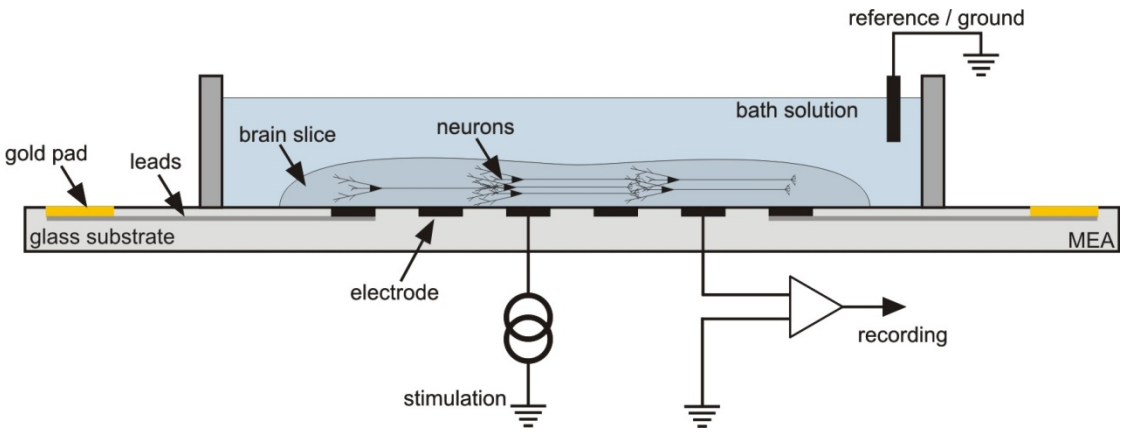

Figure 11 – Schematic drawing of a hippocampal slice positioned in a MEA chamber.

Hippocampal slices were positioned in MEA dishes composed of substrate-integrated TiN_3 electrodes, platinum leads, and gold pads for signal transduction. Each electrode can be used either as stimulating or recording electrode. Slices were brought down and hold by a platinum ring covered with thin nylon strings (not shown). Sizes of MEA, electrodes and of the slice are not scaled to each other.

Before evoking LTP in the S1 pathway, stable baselines were recorded on both pathways for 30 to 50 minutes. Long lasting LTP (L-LTP) was induced by the application of four high-frequency trains of stimuli, 5 minutes apart, each comprising a single 1 s - 100 Hz tetanus. Early LTP (E-LTP) was induced by a single 1 s - 100 Hz tetanus. Slices of preparations where either the baseline of S1 or S2, or the EPSP slope of S2 after LTP induction of the control slice had a drift of more than 20% were excluded from further analysis. EPSPs were monitored for at least 4 hours following the application of the tetanus. During the whole recording period, background spontaneous activity was monitored on all electrodes. Spontaneous events were detected by the spike detector tool of MC_Rack. Application of drugs to interfere with the induction of LTP was done at the same flow-rate as stated above. Perfusion was started at least 20 min before the first tetanus and lasted as long as described in ‘Results’ (see corresponding Figure).

4.10 LIVE-IMAGING

Acute slices of rats expressing the genetically-encoded, nuclear-localized calcium indicator GCaMP2.0-NLS were used for slice recordings on MEAs combined with calcium imaging. Genetically modified rats were generated as described in 4.8 and were used at an age of P36 to P37. Electrophysiology was done as described in 4.9.3 except that thin (180 µm thick) Indium-tin-oxide MEAs (ITO MEA, interelectrode distance: 200 µm, electrode diameter: 30 µm) were used, which are suitable for live-imaging. Calcium imaging was done on an inverted microscope (IX70, Olympus Hamburg, Germany) with a 20x oil objective (N Plan, NA 0.4, Leica, Wetzlar, Germany). GCaMP2.0 fluorescence was excited with 470-490 nm light from a

monochromator (Polychrome IV, TILL Photonics, Gräfelfing, Germany), detected with a CCD camera (Imago QE, TILL Photonics, Gräfelfing, Germany) and analysed with TILLvisION imaging software (v4.0, TILL Photonics, Gräfelfing, Germany).

GCaMP2.0 showed rapid exponential decay in fluorescence at the start of imaging but recovered fluorescence after several seconds in the dark, indicating that the decrease in fluorescence results from photoisomerization (reversible bleaching) but not from bleaching. For this reason all experiments were performed at a constant imaging rate (2 Hz) and stimulations were applied after baseline intensities were stable. Data is presented as: $\Delta F/F_0 = (F - F_0)/F_0$ where F represents the average background subtracted emission fluorescence intensity in a region of interest (ROI) and F_0 represents the baseline F measured prior to each stimulation. At the end of all recordings aCSF depolarizing solution containing 45 mM K^+ and 4 mM Ca^{2+} was applied to the slice to elicit a near maximal calcium response.

4.11 DATA ANALYSIS

All data quoted in the results and plotted in graphs and histograms represent means ± standard error of the mean (SEM). One-way analysis of variance (ANOVA) with Tukey`s posthoc test or a student`s T-test were used for all statistical analyses. All fluorescence data were background substracted.

For faster and simplified analysis of cell death a plugin of ImageJ was used. Dead cells have much smaller and round nuclei (compact DNA, pyknotic appearance) than nuclei of healthy cells. The plugin was programmed to scan all pixels within a HOECHST-stained picture and analyze the light intensity of each pixel. It counted objects which were bigger than 20 pixels and whose light intensities were above an adjustable threshold. So, all cells could be counted by applying a threshold which detected all visible cells. Afterwards a higher threshold covering only the dead cells was set and cells were counted.

Offline analysis of the EPSP slopes was performed using the MC-Rack software (Multi Channel Systems). The same program was used to analyze the slope and the population spike amplitude from electrodes in the CA1 pyramidal cell layer. The baseline value for the slope of the EPSPs was averaged for each electrode to the mean rate during the 30 minutes baseline recording. For each stimulation strength applied during recording of the IO curve the three signals from one electrode were averaged. From this averaged trace of an electrode in the CA1 pyramidal cell layer, the slope of the EPSP and the amplitude of the population spike were extracted and plotted against each other. All data were normalized to the values obtained at 3 V stimulation strength before LTP induction.

5 RESULTS

The large brain, like large government,
may not be able to do simple things in a simple way.

Donald Hebb

5.1 CHARACTERIZATION OF NEURONAL NETWORK ACTIVITY OF HIPPOCAMPAL CULTURES BY MICRO-ELECTRODE-ARRAY RECORDINGS

5.1.1 Reuse of Micro-Electrode-Arrays slightly changes their condition over time

Contrary to usual cell culture dishes and glass coverslips, MEAs were reused for six to seven cultures due to cost restrictions (about € 300 per MEA). Each cycle of culturing a neuronal network on MEAs for extended time periods implies their exposure to different chemicals, biological substances as well as physical and chemical cleaning procedures (see 4.3.2 to 4.3.4). Over time these treatments can slightly harm the surface of MEAs, especially the integrity of electrodes and the quality of the insulation layer. Since analyzing network activity quantitatively, depends greatly on signal-to-noise ratios and the rate of signal detection, it was of great importance to ensure that changes in MEA integrity are negligible within subsequent cultures. Therefore spontaneous network activity of hippocampal cultures grown on MEAs was recorded at DIV 7 and analyzed depending on their time in use. Recordings acquired from the 1st up to the 7th culture of different MEAs were pooled and the ‘number of electrodes showing activity’ and the ‘average network activity’ were analyzed. To reduce the influence of false-positive-events (events that wrongfully passed the signal-to-noise-filter) only those electrodes were included into analysis that had shown an activity of at least 0.05 Hz. Additionally, recorded data of electrodes that show less activity cannot be normalized. As shown in Figure 12, number of culture periods (for MEAs a parameter equivalent to the time in use) slightly effected both, ‘number of electrodes showing activity’ and ‘average network activity’. The ‘number of electrodes showing activity’ is hardly impaired in the first five culture uses (1st culture: 38.7 ± 2.1; 5th culture: 35.2 ± 2.8) and showed a slight decrease in the sixth period (Figure 12 A). In contrast, network activity was highest with the first culture (1.42 Hz ± 0.14) whereas activity recorded from cultures plated on reused MEAs was reduced but remained more or less stable and was only slightly reduced with reuse (2nd culture:

1.09 Hz ± 0.09; 7th culture: 0.88 Hz ± 0.12) (Figure 12 B). Since reusing MEAs for up to seven culture periods had no severe effects on intrinsic culture properties (like 'number of electrodes showing activity' and 'average network activity') data acquired from different cultures has been pooled in this work regardless of the age of the MEAs.

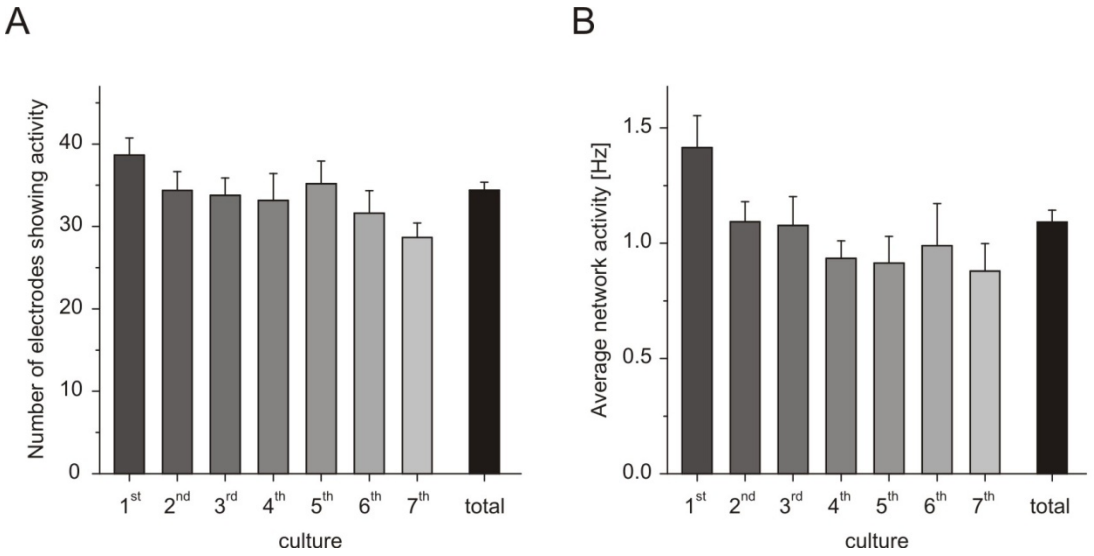

Figure 12 – Reuse MEAs for multiple cycles slightly decreases rate of signal detection.

Mean values of 'number of electrodes showing activity' (A) and 'average network activity' (B) are depicted against the number of reuse cycles per MEA (n = 9). Especially the average network activity reveals in better rates of signal detection in the first cycle than in subsequent cycles.

5.1.2 Hippocampal network formation is not affected by reusing Micro-Electrode-Arrays multiple times

The effects on 'number of electrodes showing activity' and 'average network activity' by reusing MEAs were probably not due to changes in culturing conditions since no differences in total cell number and dendritic network density was visible (Figure 13). Representative pictures of hippocampal cultures plated on a new MEA, on a three or on a seven times reused MEA on DIV 13 are shown in Figure 13 (A–C). The fact that formation and quality of hippocampal networks are not affected by plating cells on reused MEA dishes permits the multiple reuses of MEAs to study spontaneous network activity in a quantitative manner.

To study and characterize developing neuronal networks with MEAs it was necessary to consider whether data such as spike activity and changes in spike patterns should be analyzed as absolute or relative values. To answer this question, between-culture differences which are represented as the error bars in Figure 12 (A+B), were considered also, apart from consequences arising from possible effects due to the quality of MEAs. Hence, intrinsic properties especially of recordings from cultures plated on new MEAs should be quite similar. However, network activity recorded at DIV 7 varied even between cultures from new MEAs by a factor of

higher than 5 (0.46 Hz to 2.74 Hz; n = 20) (Figure 13, D+E). Interestingly, recordings from cultures plated on reused MEAs showed more similar network activities although this was not significant (0.39 Hz to 2.54 Hz; n = 20) (Figure 13 E). This implies that for questions addressing issues about network development key values such as firing frequency and bursting behavior should be calculated in relative values rather than in absolute numbers to get findings significant with smaller sample sizes. Nevertheless this has to be separately decided for every parameter of interest. Since this work is based on a rather large number of experiments and sample sizes same parameters are depicted as absolute numbers while others will be in relative values.

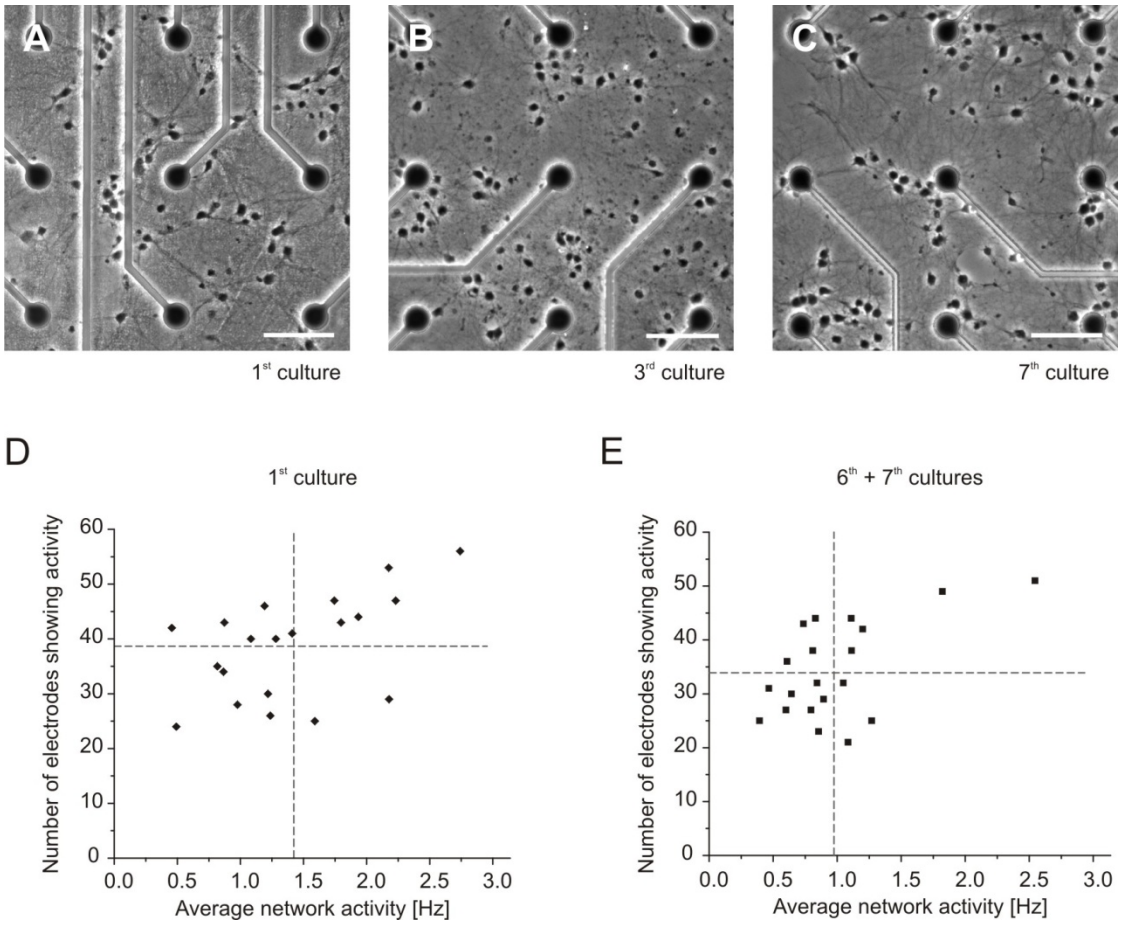

Figure 13 – Quality of cell cultures is not affected by reusing MEAs multiple times but rate of detected spikes is slightly reduced.

Representative pictures of primary hippocampal cultures plated on MEAs of different 'ages' taken with a 10x objective on DIV 13. Intrinsic properties of cultures such as cell density and dendritic arborization look after the first culture period (A) visually similar to cultures plated on MEAs after their 3rd (B) and 7th (C) use, respectively. Number of electrodes showing activity of individual recordings is plotted against the mean value of the spike frequency of the respective recording (D+E). Data of recordings of the 6th and 7th cultures are pooled. Interestingly, recorded activities of cultures plated on MEAs reused many times show less variation than recordings of cultures plated on new MEAs. Dashed lines represent the mean value of all recordings plotted (D+E). Scale bar: 100 µm.

5.2 BASAL NUCLEAR CALCIUM SIGNALING AFFECTS NEURONAL NETWORK ACTIVITY IN PRIMARY HIPPOCAMPAL CULTURES

5.2.1 CaMBP4 is nuclear localized and does not induce neuronal cell death

To block nuclear calcium signaling, cultured mouse hippocampal neurons were infected with viruses expressing CaMBP4, a protein that binds the calcium/calmodulin complex thereby preventing activation of CaM kinase IV within the nucleus. Due to an internal nuclear localization sequence (NLS) in its coding sequence CaMBP4 is exclusively localized in the cell nucleus and cannot interfere with cytoplasmic calmodulin-regulated signaling pathway (Wang et al., 1995) (Figure 14 A+D). To simplify visualization of infected cells CaMBP4 was cloned at the N-terminus of the red fluorescent protein mCherry (from here on referred to as 'CaMBP4-mC') (Shu et al., 2006). Furthermore it was shown that functionality of CaMBP4 is not impaired by the conjunction to mCherry (Lau et al., 2009). Neurons were infected as controls with a virus expressing a nuclear localized mCherry ('mC-NLS') or were left uninfected. It was shown by immunocytochemistry that both CaMBP4-mC and mC-NLS are properly expressed and nuclear localized (Figure 14 A). To prove nuclear localization nuclei were counterstained with Hoechst. Efficiency of viral infections were calculated by counting double stained nuclei and were about 70 % (CaMBP4-mC: 69.0 % ± 0.6; mC-NLS: 74.6 % ± 5.4; n = 2) (Figure 14, B). Neuronal cell death was determined to rule out that interfering with basal nuclear calcium signaling affects neuronal survival. Neither inhibition of nuclear calcium signaling via CaMBP4 nor over-expression of the recombinant nuclear localized protein mC-NLS influences cell viability in hippocampal cultures until DIV 13. Cell death in CaMBP4-infected cultures was slightly increased compared to mCherry-NLS-infected- and uninfected control cultures (uninf.contr.) but this difference was not significant (CaMBP4-mC: 18.4 % ± 0.9; mC-NLS: 14.6 % ± 2.6; uninf.contr.: 14.6 % ± 2.5; n = 2) (Figure 14 C).

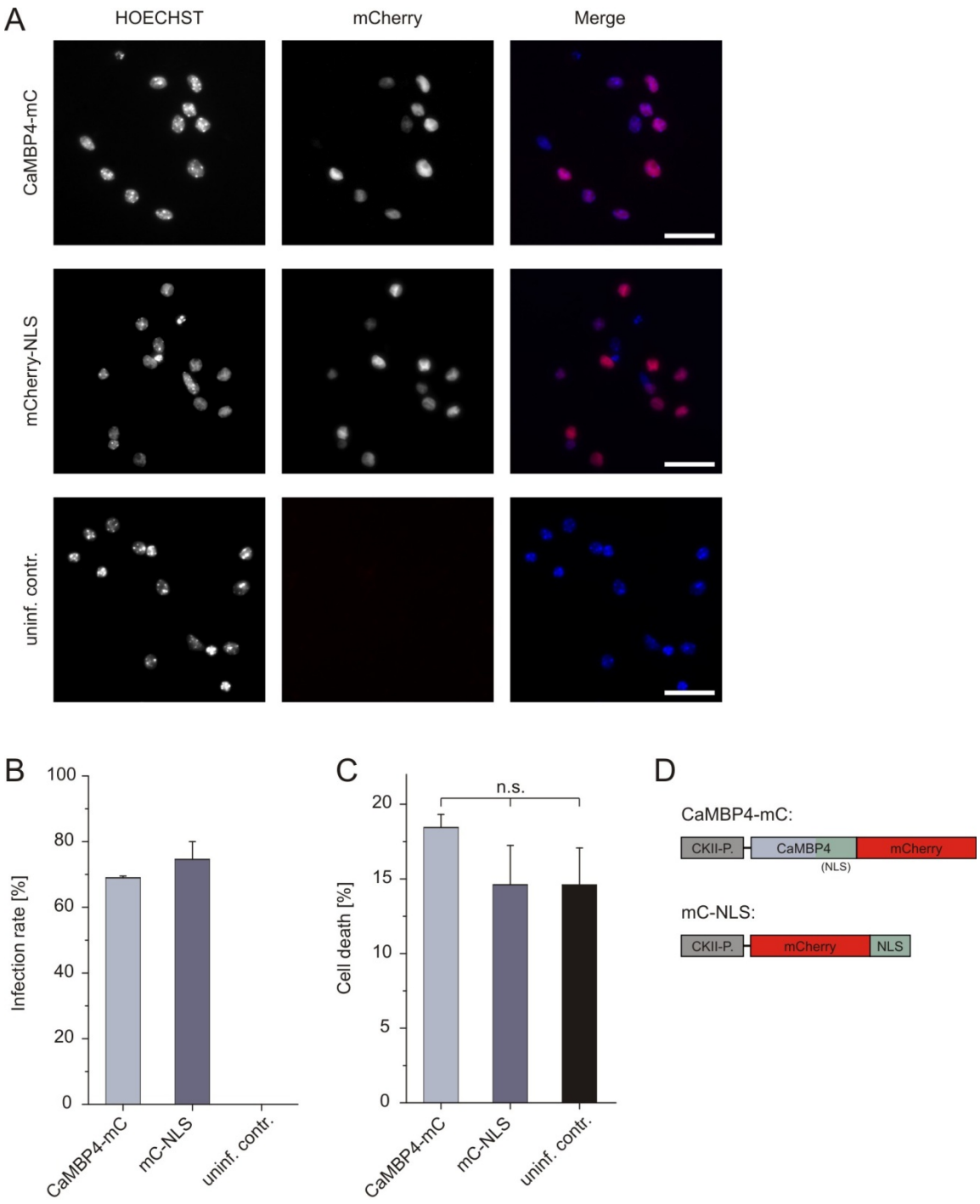

Figure 14 – Analysis of rAAV-mediated expression of CaMBP4-mC and mC-NLS.

Primary hippocampal cultures were infected with the indicated constructs at DIV 4 and were fixed at DIV 13. Nuclei are stained with Hoechst (left column), whereas mCherry signal is used to detect virus expression and to calculate infection rates. Merge pictures are shown on the right (A). Infection rates are determined by calculating rate of mCherry-expressing cells (B). Cell death is calculated using a plugin with ImageJ by counting apoptotic cell bodies of the corresponding images of the HOECHST channel (left column in (A)) (C). The composition of the two different constructs is depicted in the schematic cartoons (D). Scale bar: 50 µm. n.s. – not significant; CKII-P. – CaM Kinase II promoter; NLS – nuclear localization sequence.

5.2.2 Neuronal network activity persists in cultures expressing CaMBP4 until DIV 7

It was shown that over-expression of CaMBP4 or CaMKIVK75E affects neuronal morphology (e.g. reduced dendritic complexity) and also dendritic spines (unpublished observations). Therefore, it was investigated whether basal nuclear calcium signaling has an effect on the formation and number of functional connections within neuronal cultures, too. To study the development of action potential firing rates and activity patterns of neuronal networks over time primary hippocampal neurons were plated on MEAs. *Ex vivo* developing networks, from almost all brain regions including the hippocampus (van den Pol et al., 1996), show spontaneous activity within the first few days after plating (Baughman et al., 1991; Wagenaar et al., 2006). After one week in culture hippocampal neurons show activity typically composed of sporadic action potentials and synchronized clustered activity (Nakanishi and Kukita, 1998) mediated by functional NMDA-type and AMPA-type glutamate receptors (Bading et al., 1995; Hardingham et al., 2001a). Synchronized activity in hippocampal networks is particularly prominent in cultures derived from mice rather than from rats (unpublished observations).

Cultures were recorded first seven days after plating as dissociated neurons need time to rebuild an elaborate dendritic network of functional synaptic connections as well as to reduce disturbances on culture development by recording in the early phase of development too often. As cultures where infected on DIV 4 it was first analyzed if neuronal networks expressing CaMBP4-mC have already different electrical properties at DIV 7. Therefore, spontaneous network activity was recorded for 5 minutes and plugins of the NEX software were used to evaluate the dimension of key parameters and benchmarks of multi-site network recordings. Because data of extracellular recordings obtained from MEAs do not necessarily give similar results for dishes even from the same preparation (Figure 13 E) data from recordings of several MEAs and preparations were pooled. Four important parameters were analyzed to assess the network properties on an electrophysiological level: absolute spike frequency (which resembles network activity), number of electrodes showing activity, cumulative firing probability and bursting behavior (Figure 15 and Figure 16). To prevent data distortion due to the possible detection of false-positive events a threshold was set. Only those electrodes were included into analysis whose recorded activity exceeded 0.01 Hz.

This part of the study, reporting about the developmental importance of nuclear calcium signaling for electrical network properties of hippocampal cultures, includes data of the following groups (number of MEAs / number of independent preparations): CaMBP4-mC: 8/4; mC-NLS: 10/6; uninf.contr.: 17/12. At DIV 7 cultures infected with CaMBP4-mC showed a spike frequency similar to the control groups mC-NLS and uninf.contr. (1.13 Hz ± 0.23 for CaMBP4-mC, 1.16 Hz ± 0.15 for mC-NLS, and 1.02 Hz ± 0.10 for uninf.contr.) (Figure 15 A). Statistical distribution was similar for all groups (Figure 15 B). Number of electrodes showing activity did also not show a significant difference within groups (34.0 ± 4.1 for CaMBP4, 38.4 ± 4.1 for mC-

NLS, and 33.9 ± 3.4 for uninf.contr.) (Figure 15 C). Statistical distribution was similar for all groups (Figure 15 D). Plotting of 'number of active electrodes showing activity' against 'absolute spike frequency' was also similar for all groups which supports the finding that spontaneous network activity in cultures infected with CaMBP4-mC was not affected until DIV 7 (Figure 15 E). In all cultures distribution of activity within the electrodes showing activity was similar whereby the small left-shift of the uninf.contr. group is explained by the slightly decreased mean value of the spike frequency (Figure 15 F). Additionally, bursting behavior was analyzed at DIV 7. All groups showed similar bursting behavior in all seven analyzed parameters (see 3.4.2). Burst frequency, burst duration, spike frequency in bursts and duration of interburst intervals are the four most prominent indicators of bursting behavior in cultures and are thus depicted for representiveness (Figure 16).

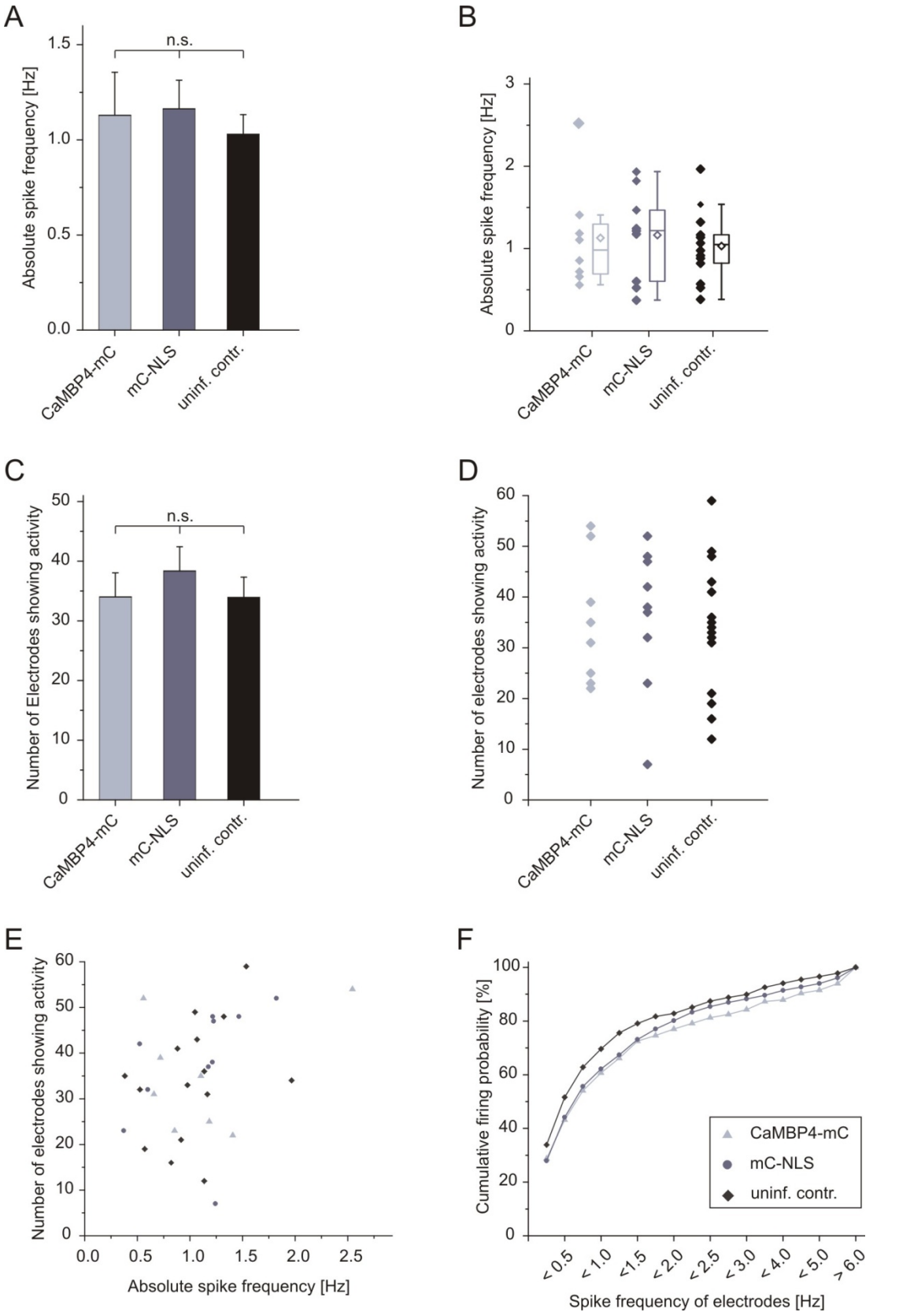
A
n.s.
Absolute spike frequency [Hz]
1.5
1.0
0.5
0.0
CaMBP4-mC
mC-NLS
uninf. contr.
B
Absolute spike frequency [Hz]
3
2
1
0
CaMBP4-mC
mC-NLS
uninf. contr.
C
n.s.
Number of Electrodes showing activity
50
40
30
20
10
0
CaMBP4-mC
mC-NLS
uninf. contr.
D
Number of electrodes showing activity
60
50
40
30
20
10
0
CaMBP4-mC
mC-NLS
uninf. contr.
E
Number of electrodes showing activity
60
50
40
30
20
10
0
0.0
0.5
1.0
1.5
2.0
2.5
Absolute spike frequency [Hz]
F
Cumulative firing probability [%]
100
80
60
40
20
0
CaMBP4-mC
mC-NLS
uninf. contr.
< 0.5
< 1.0
< 1.5
< 2.0
< 2.5
< 3.0
< 4.0
< 5.0
> 6.0
Spike frequency of electrodes [Hz]

Figure 15 – Hippocampal cultures infected with CaMBP4-mC: Assessment of spontaneous network activity of recordings on DIV 7.

Mean values of network activity of the three indicated different groups recorded three days after infection (A). Mean values of activity of individual recordings from all groups are plotted as single data points. Additionally, the respective box plot analyses (representing quartiles, median and mean) are shown (B). Mean values of the 'number of electrodes showing activity' of the three different groups recorded three days after infection (C). Mean values of the 'number of electrodes showing activity' of individual recordings are plotted as single data points (D). Calculation of individual values for each recording was confined on electrodes with an activity of more than 0.01 Hz (A+C). Number of electrodes showing activity of every individual recording is plotted against the respective mean value of the spike frequency (E). For each group, electrodes above threshold (0.01 Hz) of all recordings are pooled and firing probability is plotted in bins (F). n.s. – not significant.

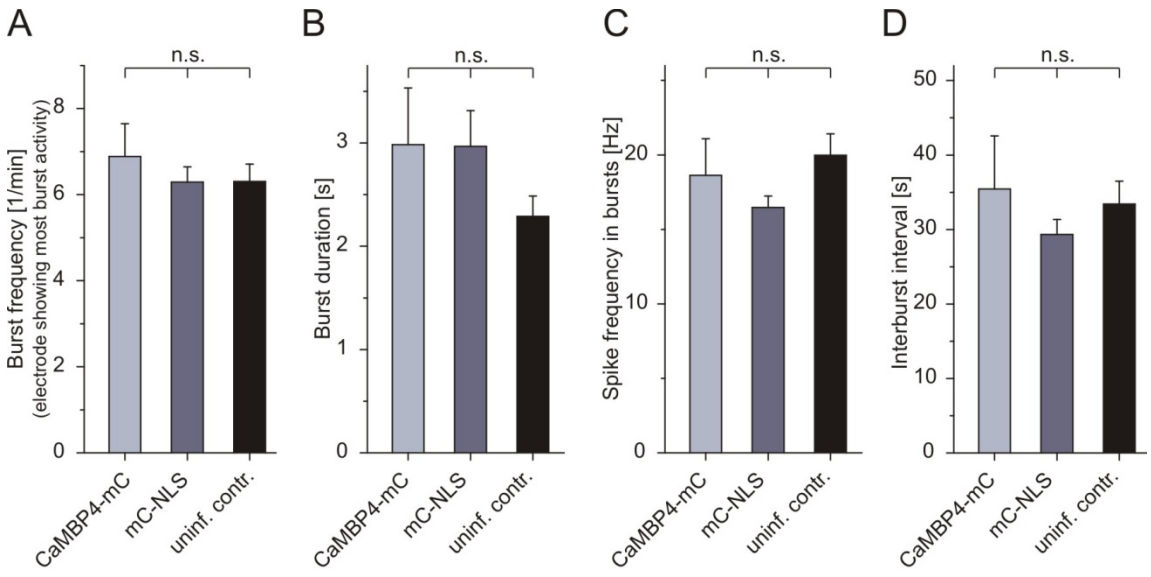

Figure 16 – Hippocampal cultures infected with CaMBP4-mC: Assessment of bursting behavior of recordings on DIV 7.

Mean values of burst duration (A), burst frequency (B), interburst intervals (C), and spike frequency in bursts (D) of recordings of hippocampal cultures are depicted as exemplary parameters to characterize bursting behavior three days after infection. Burst duration is slightly prolonged in virus-treated cultures although this is not significant. Moreover, this tendency is not due to interfering with nuclear calcium signaling (B). All other parameters evaluating bursting behavior do not show significant differences either (data not shown). n.s. – not significant.

5.2.3 Overexpression of CaMBP4 does not change spontaneous firing frequency

Network activity of CaMBP4-infected cultures and of control groups was daily recorded over one week (DIV 7 to DIV 13) to study developmental changes of network behavior. As presented and justified in 5.1.2 recorded activity was proportioned within cultures, whereby data recorded on DIV 7 served as reference values. Again spike frequency, number of electrodes showing activity and cumulative firing probability were analyzed to characterize developmental

changes in firing frequency. In hippocampal cultures expression of CaMBP4-mC did not induce a consistent, detectable change in spontaneous network activity compared to control groups in the second week of cultivation (Figure 17 A). At DIV 13 cultures were exposed to the $GABA_A$ receptor antagonist bicuculline (bic) to activate excitatory neurons in a synchronous network-wide manner. Removal of GABAergic inhibition leads to action potential bursting by a strong depolarizing shift in membrane potential (Arnold et al., 2005). Bic induces rhythmic depolarizations and bursts were mediated throughout the network. Interestingly, total spike activity remained unchanged under 50 µM bic (Figure 17 A). As with spontaneous activity, number of electrodes showing activity in cultures expressing CaMBP4-mC did not change during development compared to control groups. However, the number of electrodes showing activity decreased between DIV 9 and DIV 11 by about 20 % as happened also in control groups (Figure 17 B). Cumulative firing probability was calculated for recordings from DIV 10 and DIV 13. On both time-points spike frequency distribution of electrodes showing activity were similar to control groups. Cumulative firing probability of DIV 7 is shown in Figure 15 F. Moreover, for all groups cumulative firing probability hardly changed between DIV 7 and DIV 13 or under bicuculline treatment (data not shown).

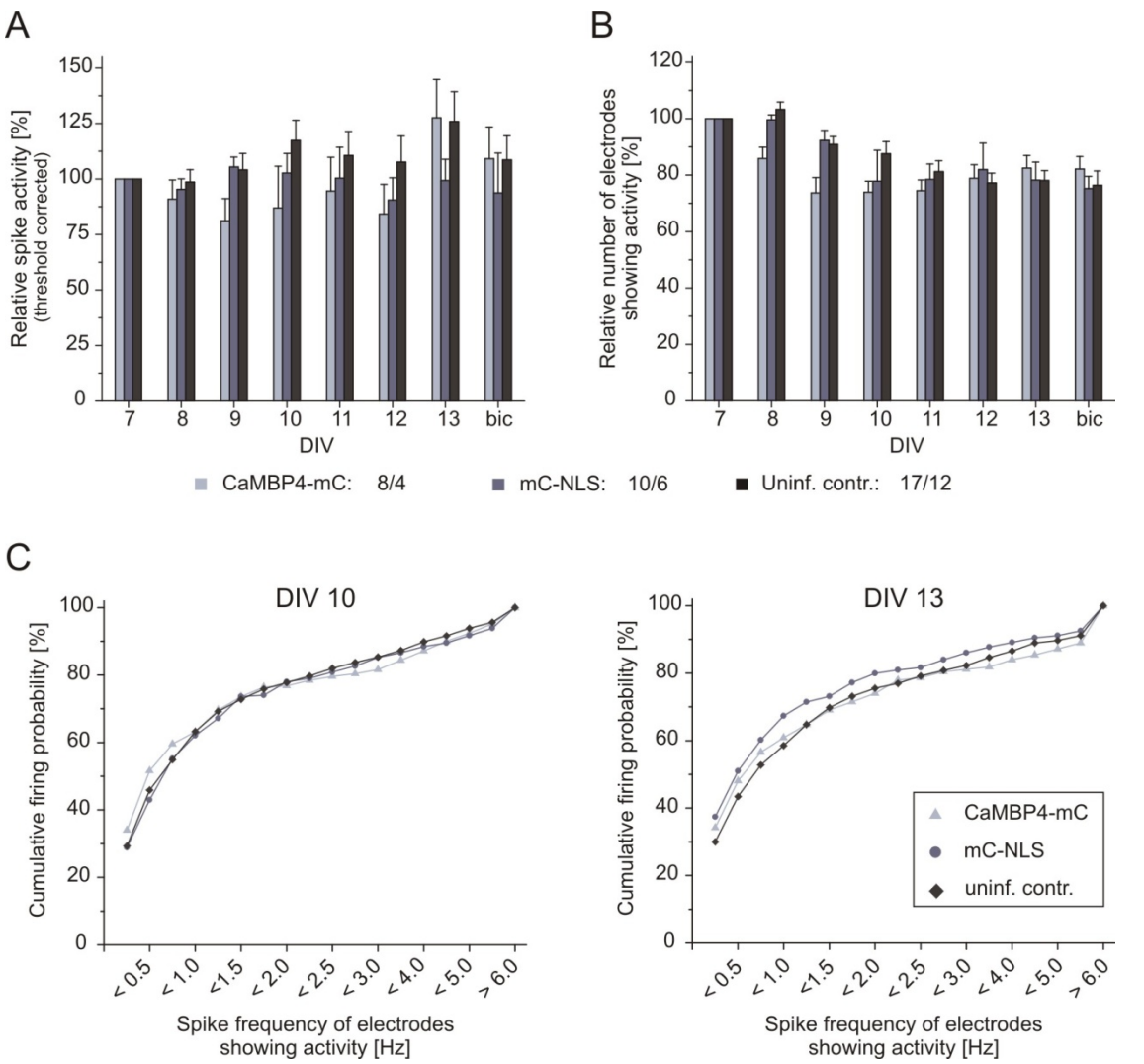

Figure 17 – Expression of CaMBP4-mC does not change spontaneous activity until DIV 13.

Developmental changes of spontaneous network activity in cultured hippocampal networks expressing CaMBP4-mC are assessed by daily recordings. Relative values of spontaneous firing frequency (A) and relative values of the number of electrodes showing activity (B) are depicted for each group on every day. For each group, electrodes of all recordings showing an activity above threshold (0.01 Hz) are pooled and firing probability is plotted in bins. Exemplary traces for DIV 10 and DIV 13 are shown (C). For cumulative firing probability on DIV 7, see Figure 15. Network activity of cultures was recorded twice on DIV 13: before and two hours after bicuculline treatment (50 µM). Numbers in the legend reveal corresponding sample sizes (number of MEAs / number of independent cultures).

5.2.4 Overexpression of CaMBP4 prolongs burst duration

Next, bursting behavior was analyzed during the second week of culturing (Figure 18). Hippocampal cultures infected with CaMBP4-mC revealed similar burst frequency and spike frequency in bursts as control groups (Figure 18 B, C). However, burst duration changed during the second week of culturing. With DIV 10 the usually regular recurrent bursting became

disrupted by episodes of longer bursts (sometimes burst duration lasted up to 60 s) while the main portion of bursts did not change their duration (CaMBP4-mC: DIV 7: 3.0 s ± 0.5, DIV 13: 9.4 s ± 1.45) (Figure 18 E). This phenomenon was stable until the end of experiments. Bicuculline stimulation partly diminished this effect (Figure 18 A). However, burst duration was increasing a little also in control groups during DIV 7 and DIV 13 (mC-NLS: DIV 7: 3.0 s ± 0.5, DIV 13: 5.5 s ± 0.7; uninf.contr.: DIV 7: 2.4 s ± 0.2, DIV 13: 4.1 s ± 0.4). Recordings of spontaneous activity of cultured hippocampal networks suggest that inhibition of nuclear calcium signaling by expression of CaMBP4-mC did not affect the level of absolute firing frequency (Figure 17) but bursting behavior was different compared to control groups. However, only one of the depicted key parameters was significantly different (Figure 18).

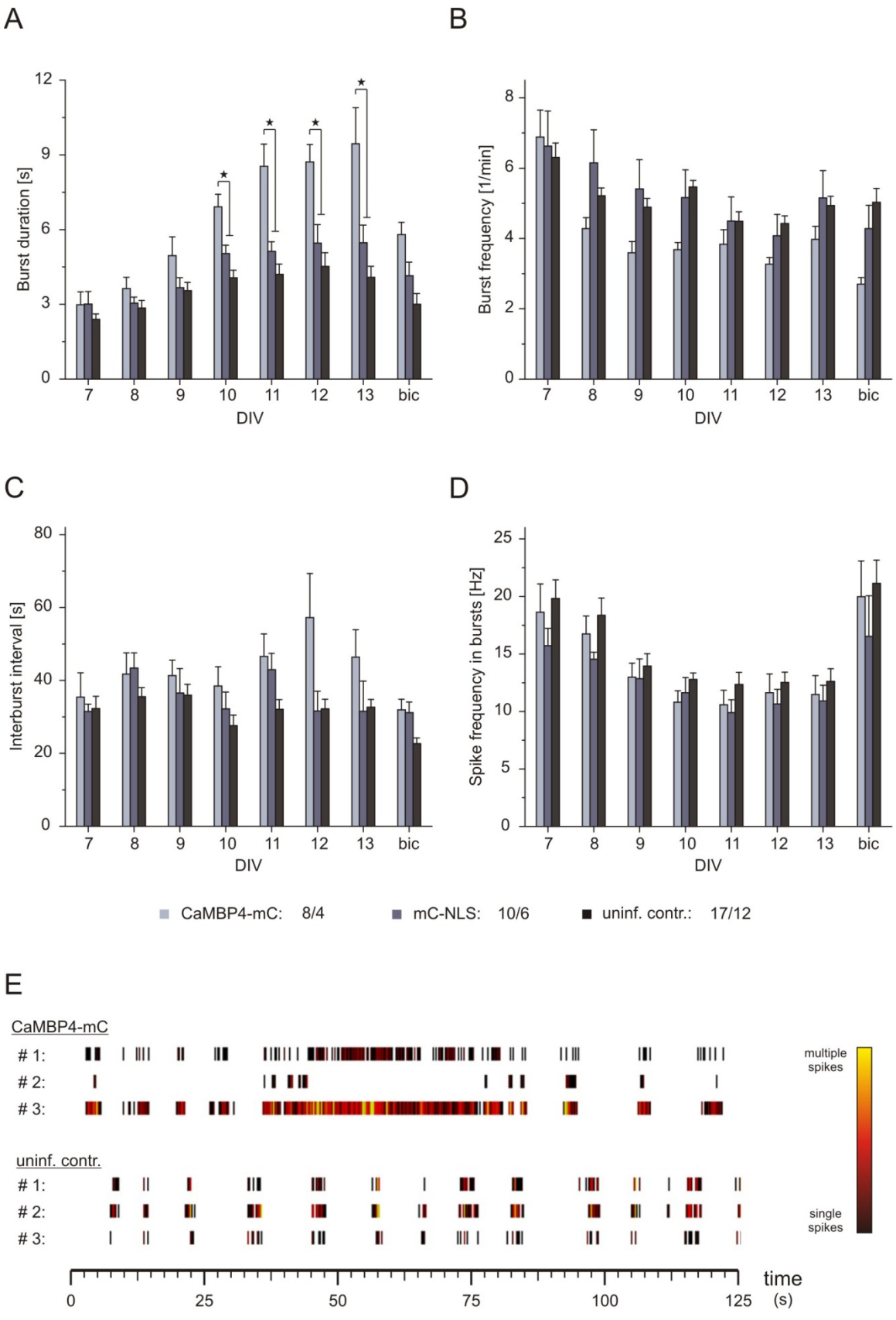
A
B
C
D
E
Burst duration [s]
Burst frequency [1/min]
Interburst interval [s]
Spike frequency in bursts [Hz]
DIV
7
8
9
10
11
12
13
bic
CaMBP4-mC: 8/4
mC-NLS: 10/6
uninf. contr.: 17/12
CaMBP4-mC
1:
2:
3:
uninf. contr.
multiple spikes
single spikes
time
(s)
0
25
50
75
100
125

Figure 18 – Burst duration is prolonged in cultures expressing CaMBP4-mC upon DIV 9.

Developmental changes of bursting behavior in cultured hippocampal networks expressing CaMBP4-mC are assessed by daily recordings. Represented are the mean values of four key parameters of bursting behavior in the second week of culturing: burst duration (A), burst frequency (B), interburst interval (C) and spike frequency in bursts (D). Representative traces of three electrodes of recordings on DIV 13 are shown for a CaMBP4-mC infected and a control culture. Each vertical line represents the detection of a spike on the respective electrode. To visualize spike density lines are color-coded (E). Network activity of cultures was recorded twice on DIV 13: before and two hours after bicuculline treatment (50 µM). Numbers in the legend reveal corresponding sample sizes (number of MEAs / number of independent cultures). * $p<0.05$

5.3 INHIBITION OF VEGF-D SIGNALING IN HIPPOCAMPAL CULTURES

5.3.1 Functional down-regulation of VEGF-D expression

It was shown that in hippocampal cultures inhibition of nuclear calcium signaling by over-expression of CaMBP4 or CaMKIVK75E suppresses transcription of VEGF-D but not of its most closely relative VEGF-C, to about 75 % (unpublished observations). Since the results presented in point 5.2 indicate that basal nuclear calcium signaling is sufficiently involved in the regulation and development of neural network activity, target genes of this signaling pathway such as *vegf-d* were investigated further (Zhang et la., 2009). It is known that the VEGF-D mRNA level in dissociated hippocampal cultures is 3 to 4-fold upregulated between DIV 7 and DIV 10 (unpublished observations). This time window of increased VEGF-D expression mirrors the period in which neuronal network activity becomes vulnerable to impairments in nuclear calcium signaling (Figure 18 A). A possible role of VEGF-D in the maintenance of neuronal network activity is furthermore supported by the fact that VEGF-D-signaling as well as over-expression of CaMBP4 are involved in shaping dendritic trees. In addition, VEGF-D over-expression rescues the effects of CaMBP4 on dendritic morphology (unpublished observations). Therefore, MEA recordings were performed to investigate the role of VEGF-D in the development of neuronal network activity.

One way to specifically probe a protein of interest is through the silencing of its mRNA. This can be achieved by the RNAi strategy in which a sequence of RNA that makes a tight hairpin turn is used to silence gene expression via RNA interference. Using a small hairpin RNA with a sequence that exclusively targets the *vegf-d* mRNA recruits the RNA-induced silencing complex (RISC), a cellular machinery that specifically cleaves the *vegf-d* mRNAs thereby preventing VEGF-D expression. To investigate the effects of VEGF-D on neuronal network activity hippocampal cultures were infected with the following constructs: a vector containing a short hairpin RNA designed to target the mouse *vegf-d* mRNA (shVEGF-D) and as controls a vector containing a scramble shRNA (shScr) and a vector without any shRNA (empty vector-mC), respectively (Figure 19 D). All construct harbor an expression cassette for mCherry under the

control of the neuronal-specific CaMKII promoter to visualize infected cells. First, viruses were validated regarding their infection rate and their potential to induce neuronal cell death (Figure 19). For all three viruses mCherry was cytoplasmic localized and showed similar infection rates (shVEGF-D: 73.2 % ± 1.8; shScr: 69.6 % ± 1.7; empty vector-mC: 67.7 % ± 2.7; n=2) (Figure 19, A+B). To asses neuronal cell death nuclei were counterstained with HOECHST. Non of the viruses induced any increase in cell death compared to an uninfected control group (shVEGF-D: 14.5 % ± 1.3; shScr: 17.0 % ± 1.3; empty vector-mC: 16.2 % ± 2.5; uninf.contr.: 16.1 % ± 2.5; n=3) (Figure 19 A+C). The functional down-regulation of *vegf-d* mRNA to about 10 % of the endogenous level by expression of shVEGF-D was demonstrated by Q-PCR experiments. Additionally it was verified that shVEGF-D does not down-regulate *vegf-c* mRNA as well as that *vegf-d* mRNA levels is not affected by both the expression of shScr and empty vector-mC, respectively (unpublished observations).

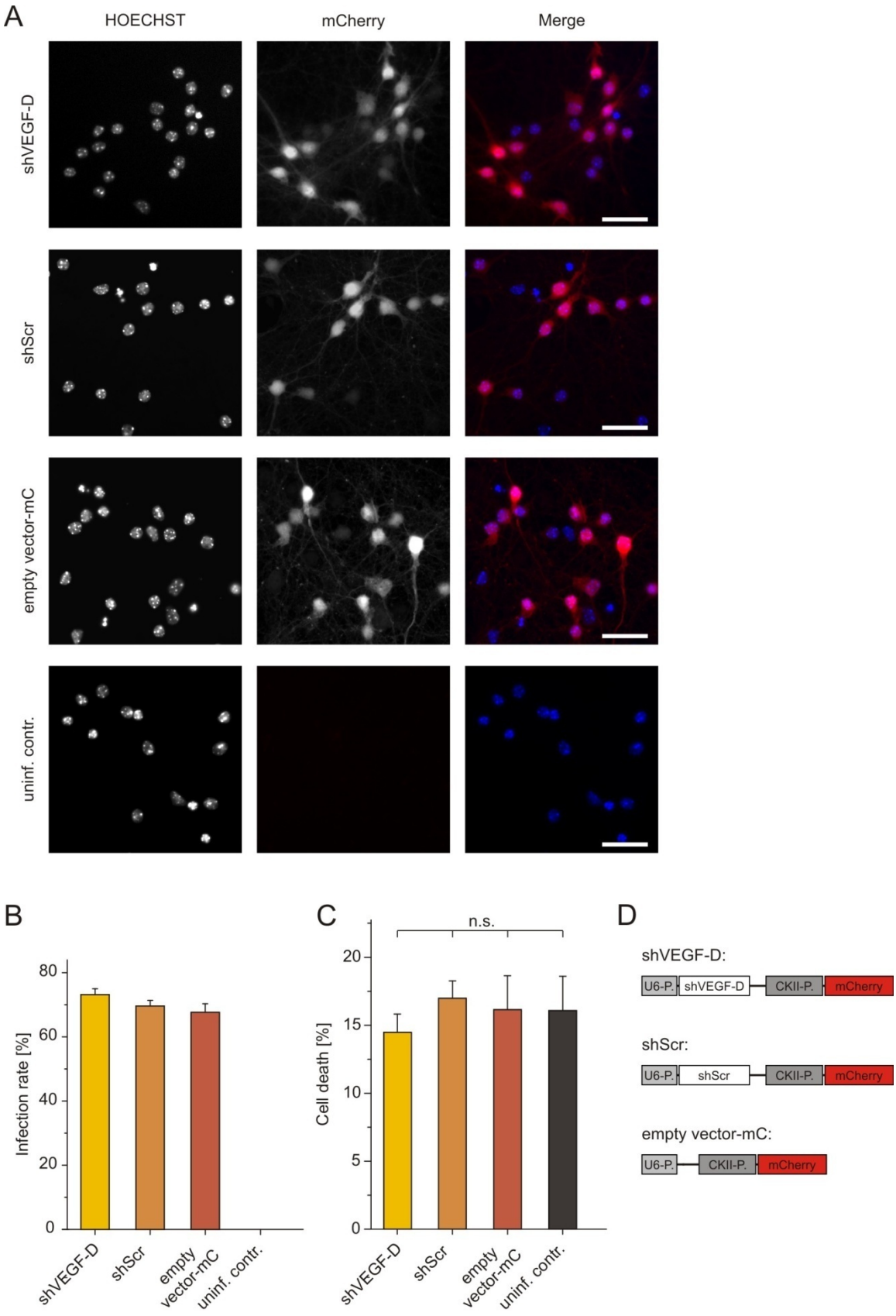
A
HOECHST
mCherry
Merge
shVEGF-D
shScr
empty vector-mC
uninf. contr.
B
Infection rate [%]
0
20
40
60
80
shVEGF-D
shScr
empty vector-mC
uninf. contr.
C
n.s.
Cell death [%]
0
5
10
15
20
shVEGF-D
shScr
empty vector-mC
uninf. contr.
D
shVEGF-D:
U6-P.
shVEGF-D
CKII-P.
mCherry
shScr:
U6-P.
shScr
CKII-P.
mCherry
empty vector-mC:
U6-P.
CKII-P.
mCherry

Figure 19 – Analysis of rAAV-mediated infection and viability of different shRNA constructs.

The left column of images shows the HOECHST staining indicating all neurons present in the field of view. mCherry signal in the second column reveals neurons infected with the respective construct. The third column shows merged images of the two pictures on the left-hand side (A). Infection rates of the respective constructs are determined by counting double-labeled cell bodies since mCherry is predominantly perisomatic localized (B). Cell death rate is calculated using a plugin with ImageJ by counting apoptotic cell bodies of the corresponding images of the HOECHST channel (left column in (A)) (C). The composition of the different constructs is depicted in schematic cartoons (D). Scale bar: 50 µm.
n.s. – not significant; U6-P. – U6 promoter; CKII-P. – CaM kinase II promoter.

5.3.2 Neuronal network activity persists in VEGF-D-deficient cultures until DIV 7

Since the *vegf-d* mRNA level in dissociated hippocampal cultures is upregulated between DIV 7 and DIV 10, shVEGF-D-infected cultures were recorded first on DIV 7 to establish a stable baseline. MEA recordings from DIV 7 were analyzed separately to assure that expression of shVEGF-D or viral infection itself has no effect on neuronal network activity until DIV 7. Comparable to 5.2.2, spontaneous network activity was recorded for 5 minutes and plugins of NEX software were used to evaluate the dimension of key parameters and benchmarks of multi-site network recordings. Again, absolute spike frequency, number of electrodes showing activity, cumulative firing probability and bursting behavior were computed and analyzed (Figure 20 and Figure 21). The threshold to prevent data distortion due to the possible detection of false-positive events was set at 0.01 Hz.

This part of the study, reporting about the developmental implications of VEGF-D-signaling on neuronal network activity in hippocampal cultures, includes data of the following groups (number of MEAs / number of independent preparations): shVEGF-D: 17/12; shScr: 12/8; empty vector-mC: 13/9; uninf.contr.: 17/12. On DIV 7 cultures infected with shVEGF-D showed an ‘absolute spike frequency’ similar to the control groups (0.95 Hz ± 0.12 for shVEGF-D, 1.13 Hz ± 0.13 for shScr, 1.07 Hz ± 0.14 for empty vector-mC, and 1.02 Hz ± 0.10 for uninf.contr.) (Figure 20 A). Statistical distribution was similar for all groups also (Figure 20 B). Mean values of the ‘Number of electrodes showing activity’ did also not show a significant difference between groups (33.0 ± 2.6 for shVEGF-D, 35.5 ± 3.1 for shScr, 34.6 ± 2.9 for empty vector-mC, and 33.9 ± 3.4 for uninf.contr.) (Figure 20 C). Statistical distribution was similar for all groups (Figure 20 D). Plotting of ‘number of active electrodes showing activity’ against ‘absolute spike frequency’ is also similar for all groups which supports the finding that spontaneous network activity in cultures infected with shVEGF-D was not impaired until DIV 7 (Figure 20 E). In all groups distribution of activity within the electrodes showing activity is similar whereby the small left-shift of the groups shVEGF-D and uninf.contr. is explained by the slightly decreased mean values of the network activity (Figure 20 F).

Additionally, bursting behavior of the four different groups was analyzed to characterize synchronized firing activity three days after infection. The same key parameters as in 5.2.2 were chosen to simplify comparability. Each of the four depicted parameters as well as any other analyzed parameter (data not shown) did not show any significant difference between the groups (Figure 21). The fact that some mean values such as interburst interval (Figure 21 C) show quite a bit of a difference is due to technical issues rather than having a biological reason; an issue that is discussed later (see 6.1.1).

Summarizing these results, no significant differences in any of the analyzed parameters of both spontaneous and synchronized activity were found in the mean values of the recordings from DIV 7. For this reason it is unlikely that VEGF-D signaling is of importance for spontaneous network activity in the first week of *in vitro* development however it cannot be ruled out biased on these experiments that the onset of the viral infection-mediated silencing of VEGF-D is too slow to see effects already three days after infection.

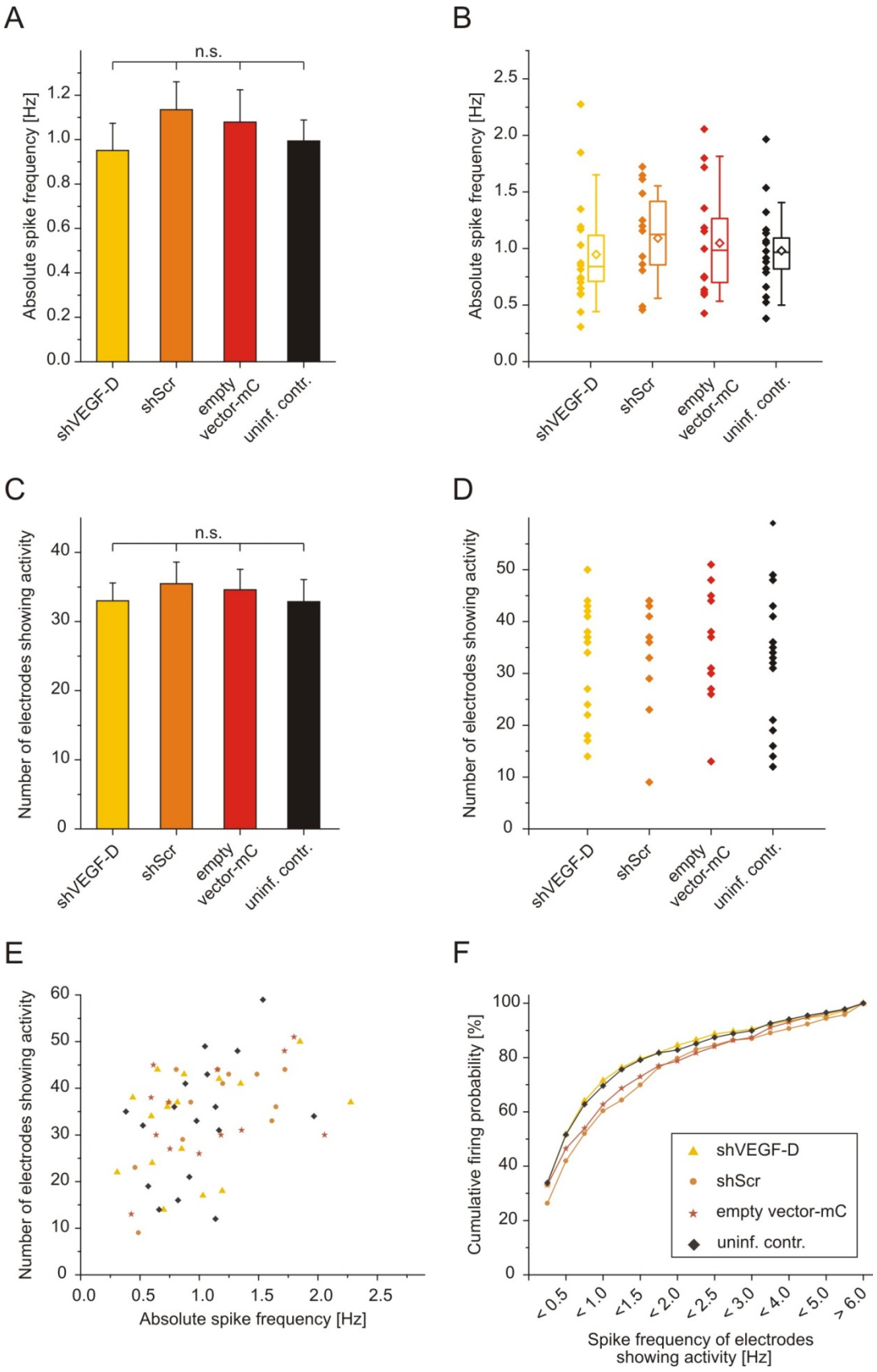
A
n.s.
Absolute spike frequency [Hz]
0.0
0.2
0.4
0.6
0.8
1.0
1.2
shVEGF-D
shScr
empty vector-mC
uninf. contr.
B
Absolute spike frequency [Hz]
0.0
0.5
1.0
1.5
2.0
2.5
shVEGF-D
shScr
empty vector-mC
uninf. contr.
C
n.s.
Number of electrodes showing activity
0
10
20
30
40
shVEGF-D
shScr
empty vector-mC
uninf. contr.
D
Number of electrodes showing activity
0
10
20
30
40
50
shVEGF-D
shScr
empty vector-mC
uninf. contr.
E
Number of electrodes showing activity
0
10
20
30
40
50
60
0.0
0.5
1.0
1.5
2.0
2.5
Absolute spike frequency [Hz]
F
Cumulative firing probability [%]
0
20
40
60
80
100
shVEGF-D
shScr
empty vector-mC
uninf. contr.
< 0.5
< 1.0
< 1.5
< 2.0
< 2.5
< 3.0
< 4.0
< 5.0
> 6.0
Spike frequency of electrodes showing activity [Hz]

Figure 20 – Hippocampal cultures infected with shVEGF-D: Assessment of spontaneous network activity of recordings on DIV 7.

Mean values of network activity of the four indicated different groups recorded three days after infection (A). Mean activity of individual recordings from all groups are plotted as single data points. Additionally, the respective box plot analyses (representing quartiles, median and mean) are shown (B). Mean values of the 'number of electrodes showing activity' of the four different groups recorded three days after infection (C). Mean values of the 'number of electrodes showing activity' of individual recordings are plotted as single data points (D). Calculation of individual values for each recording was confined on electrodes with an activity of higher than 0.01 Hz (A+C). Number of electrodes showing activity of every individual recording is plotted against the respective mean value of the spike frequency (E). For each group, electrodes above threshold (0.01 Hz) of all recordings are pooled and firing probability is plotted in bins (F). n.s. – not significant.

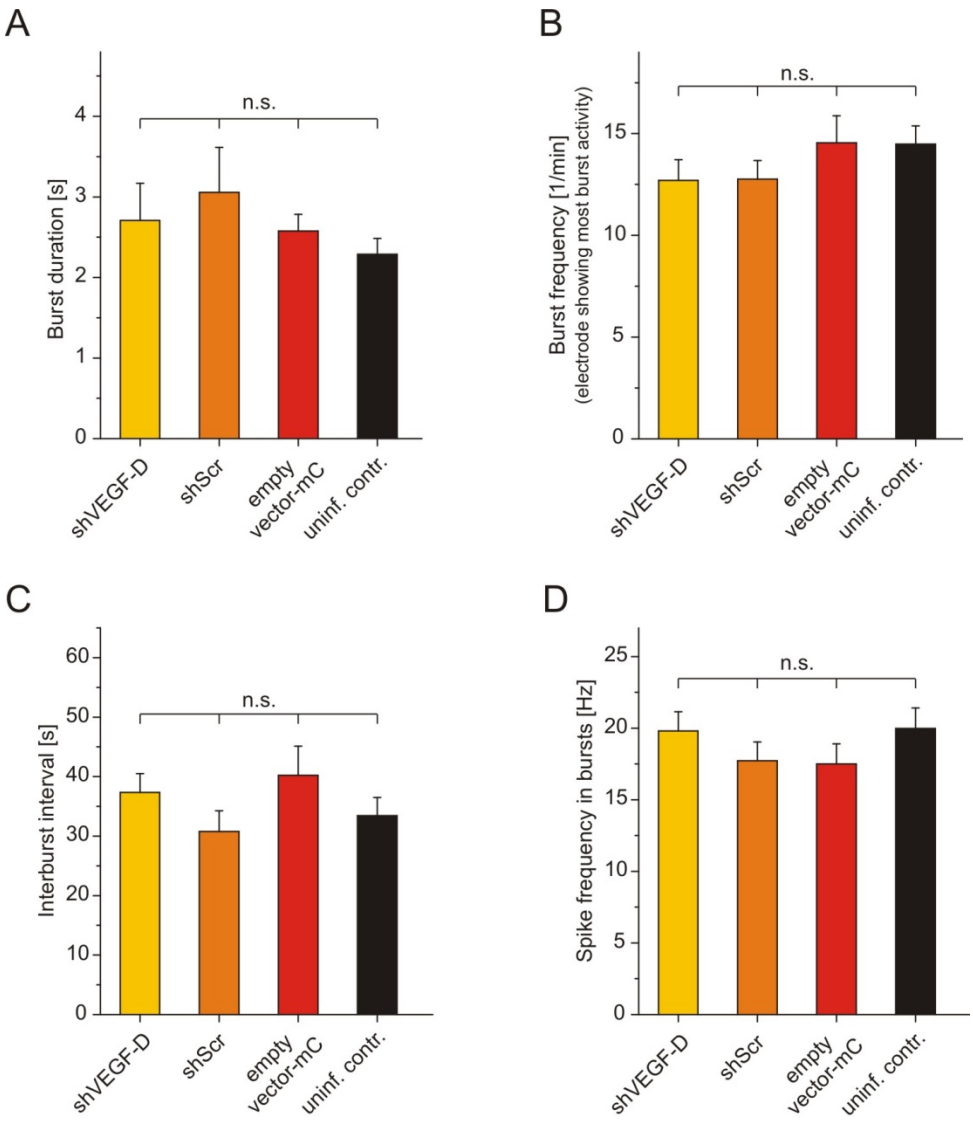

Figure 21 – Hippocampal cultures infected with shVEGF-D: Assessment of bursting behavior of recordings on DIV 7.

Mean values of burst duration (A), burst frequency (B), interburst intervals (C), and spike frequency in bursts (D) of recordings of hippocampal cultures are depicted as exemplary parameters to characterize bursting behavior three days after infection. All other parameters evaluating bursting behavior do not show significant differences either (data not shown). n.s. – not significant.

5.3.3 Knock-down of VEGF-D specifically down-regulates neuronal network activity

Given the fact that basal nuclear calcium signaling is involved in neuronal network development and transcription of *vegfd-d* is reduced to 75 % in cultures expressing CaMBP4 raised the question if VEGF-D has a key role in those developmental changes. To test this hypothesis, daily recordings of network activity were performed during the second week of culturing. Spontaneous activity and number of electrodes showing activity were analyzed and put in relative numbers to the recording from DIV 7 of the respective culture. While spike activity remained steady for all groups until DIV 13, a down-regulation of spontaneous activity was recorded in shVEGF-D-infected cultures starting with DIV 10. The run-down in activity was amplified until the end of the experiments (except for the recordings under bic treatment) to a remaining network activity on DIV 13 of 9.1 % ± 3.0 of the recordings on DIV 7. Spontaneous activity of control groups were stable until DIV 13 (shScr: 86.6 % ± 14.0; empty vector-mC: 86.4 % ± 11.1; uninf. contr.: 125.9 % ± 13.5). Since silencing of VEGF-D expression did not show increased cell death (Figure 19 A+C) this down-regulation in spontaneous network activity is not likely due to neuronal mortality. Cell death was also not different from control groups after 3 weeks in culture (DIV 20) (data not shown). Additionally, bath application of Bic was performed on DIV 13. Bic treatment could partly rescue the effect on network activity while control groups did not show an increase in activity (Figure 22 A). The impairments of VEGF-D signaling on neuronal network activity had a precise onset with DIV 10 and activity steadily decreased until DIV 13 what mirrors the expression profile of endogenous *vegf-d*.

Next, number of electrodes showing activity was analyzed and put in relative numbers compared to the corresponding recording from DIV 7. Again, shVEGF-D-infected cultures showed impairments but with a slower onset and a less strong decrease. Slight differences were detected first on DIV 11 with a run-down to 28.0 % ± 5.9 on DIV 13 compared to DIV 7. Although number of electrodes showing activity of control groups slightly decreased also, no differences could be detected between these groups (shScr: 72.5 % ± 4.4; empty vector-mC: 74.4 % ± 4.5; uninf. contr.: 78.1 % ± 3.6). Treatment of shVEGF-D-infected cultures with bicuculline showed a complete rescue of the run-down (while control groups stayed stable) supporting the idea the connectivity of hippocampal network deficient in VEGF-D signaling was still functional (Figure 22 B). To further characterize the remaining activity of the network cumulative firing probability

was probed on DIV 10, DIV 13 and under bicuculline, and compared to the recording from DIV 7. Firing probability of control groups stayed stable over the second week of culturing while shVEGF-D-infected cultures showed a clear left shift on DIV 10 which was even more pronounced on DIV 13. This means that in shVEGF-D-infected cultures the activity recorded on single electrodes was uniformly decreased, indicating that the firing activity of the whole network is down-regulated (Figure 22 C). The left shift of the trace of shVEGF-D on DIV 13 is partly right shifted after bicuculline application. This shift is in accordance with the rate of rescue detected in spike frequency (Figure 22 A). Thus, the developmental manifestation of spontaneous firing activity in cultured hippocampal neurons severely depends on the expression of VEGF-D upon DIV 9. Moreover, in cultures infected with shVEGF-D the run-down in action potential firing is reflected in the *vegf-d* mRNA level. Given the fact that VEGF-D is a target gene of the nuclear calcium signaling pathway the effects of CaMBP4 on hippocampal network activity might be devolved by VEGF-D (Figure 18 A).

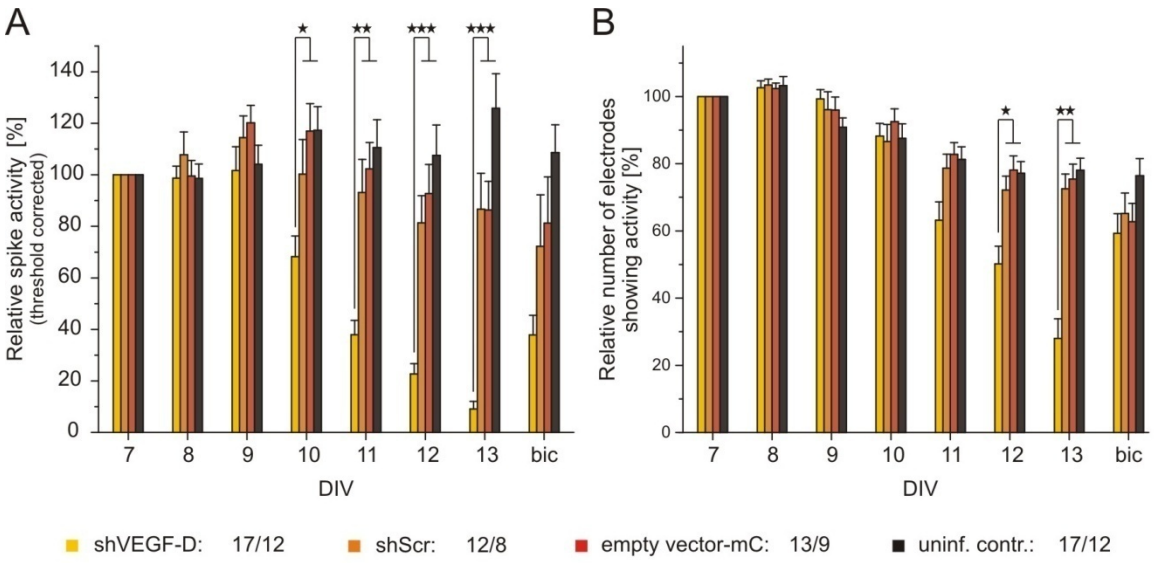
A
Relative spike activity [%] (threshold corrected)
DIV
B
Relative number of electrodes showing activity [%]
DIV
shVEGF-D: 17/12
shScr: 12/8
empty vector-mC: 13/9
uninf. contr.: 17/12

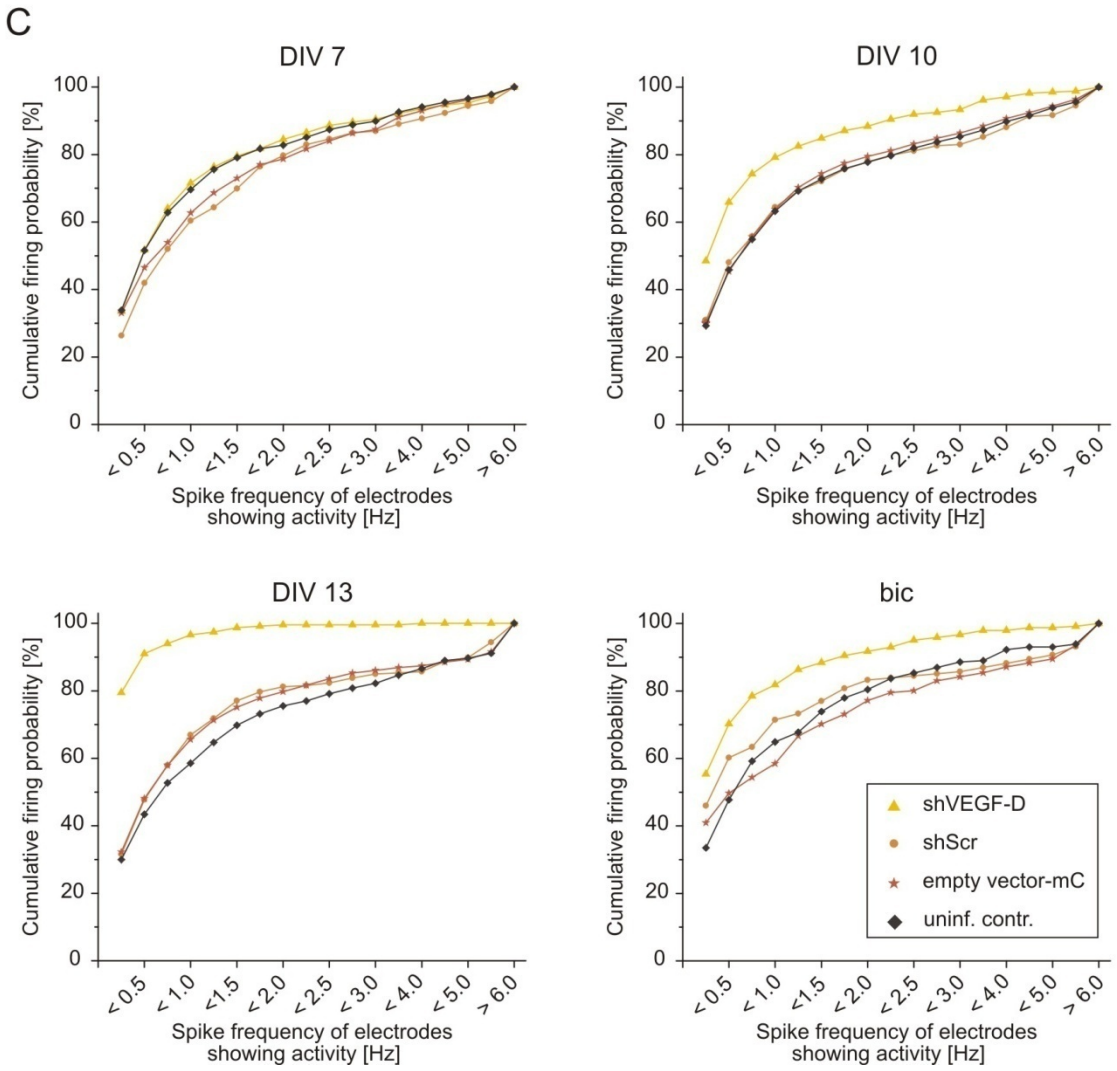
C
DIV 7
DIV 10
DIV 13
bic
Cumulative firing probability [%]
Spike frequency of electrodes showing activity [Hz]
shVEGF-D
shScr
empty vector-mC
uninf. contr.

Figure 22 – Knock-down of VEGF-D down-regulates spontaneous activity upon DIV 10.

Developmental changes of spontaneous network activity in cultured hippocampal networks deficient in VEGF-D signaling are assessed by daily recordings. For every day relative values of spontaneous firing frequency (A) and relative values of the number of electrodes showing activity (B) are depicted for each group. For all groups, electrodes of all recordings showing an activity above threshold (0.01 Hz) are pooled and firing probability is plotted in bins. Exemplary traces for DIV 7, DIV 10, DIV 13 and bic are shown in (C). Network activity of cultures was recorded twice on DIV 13: before and two hours after bicuculline treatment (50 µM). Numbers in the legend reveal corresponding sample sizes (number of MEAs / number of independent cultures). * $p<0.05$; ** $p<0.01$; *** $p<0.001$.

5.3.4 Bursting behavior is massively disrupted in VEGF-D-deficient cultures

Bursting behavior of cultures infected with shVEGF-D was analyzed to confirm the effects on spontaneous firing activity. In addition it was tested whether an effect of silencing VEGF-D signaling on bursting pattern is similar to the onset of the changes in spontaneous firing activity and whether it resembles the developmental changes in bursting behavior of cultures infected with CaMBP4. Therefore, the same four key parameters of burst behavior as selected above were assessed to evaluate developmental changes in the burst pattern of shVEGF-D infected cultures during the second week of culturing. Interestingly, changes in bursting behavior of hippocampal cultures infected with shVEGF-D were more pronounced than in cultures infected with CaMBP4-mC (Figure 18 A) as demonstrated also for spontaneous firing activity (Figure 22). In cultures infected with shVEGF-D the mean value of burst duration became similar to CaMBP4-mC infected cultures, larger from DIV 10 to DIV 13 due to the appearance of extended bursts (DIV 12: shVEGF-D: 10.0 s ± 1.3; shScr: 4.4 s ± 0.5; empty vector-mC: 6.1 s ± 0.6; uninf. contr.: 4.5 s ± 0.6) (Figure 23 A). However, the remaining regular burst pattern reported from cultures infected with CaMBP4 almost completely disappeared in shVEGF-D infected cultures over time. Thus burst frequency is massively down-regulated in VEGF-D deficient cultures, too. This is demonstrated also by extended interburst intervals in shVEGF-D cultures (DIV 12: shVEGF-D: 123.8 s ± 19.6; shScr: 41.9 s ± 4.5; empty vector-mC: 45.5 s ± 3.1; uninf. contr.: 32.6 s ± 2.4) (Figure 23 C). However, spike frequency in bursts was not altered (Figure 23 D). The drop in the mean values of burst duration and interburst interval between DIV 12 and DIV 13 for cultures infected with shVEGF-D was due to the fact that 5-minutes-recording were probably not long enough anymore to perfectly mirror the bursting behavior of a shVEGF-D infected culture. Furthermore, occasionally some of the extended bursts are detected as two shorter ones that explain the drop in the interburst intervals. This implies that mean values of burst duration and interburst intervals obtained from recordings on DIV 13 have to be analyzed very critically (for a detailed discussion see 6.1.3). Representative traces of recordings from DIV 13 obtained from a hippocampal culture infected with shVEGF-D and a control culture are shown in Figure 23 E, to illustrate the effects of silencing VEGF-D expression on bursting behavior.

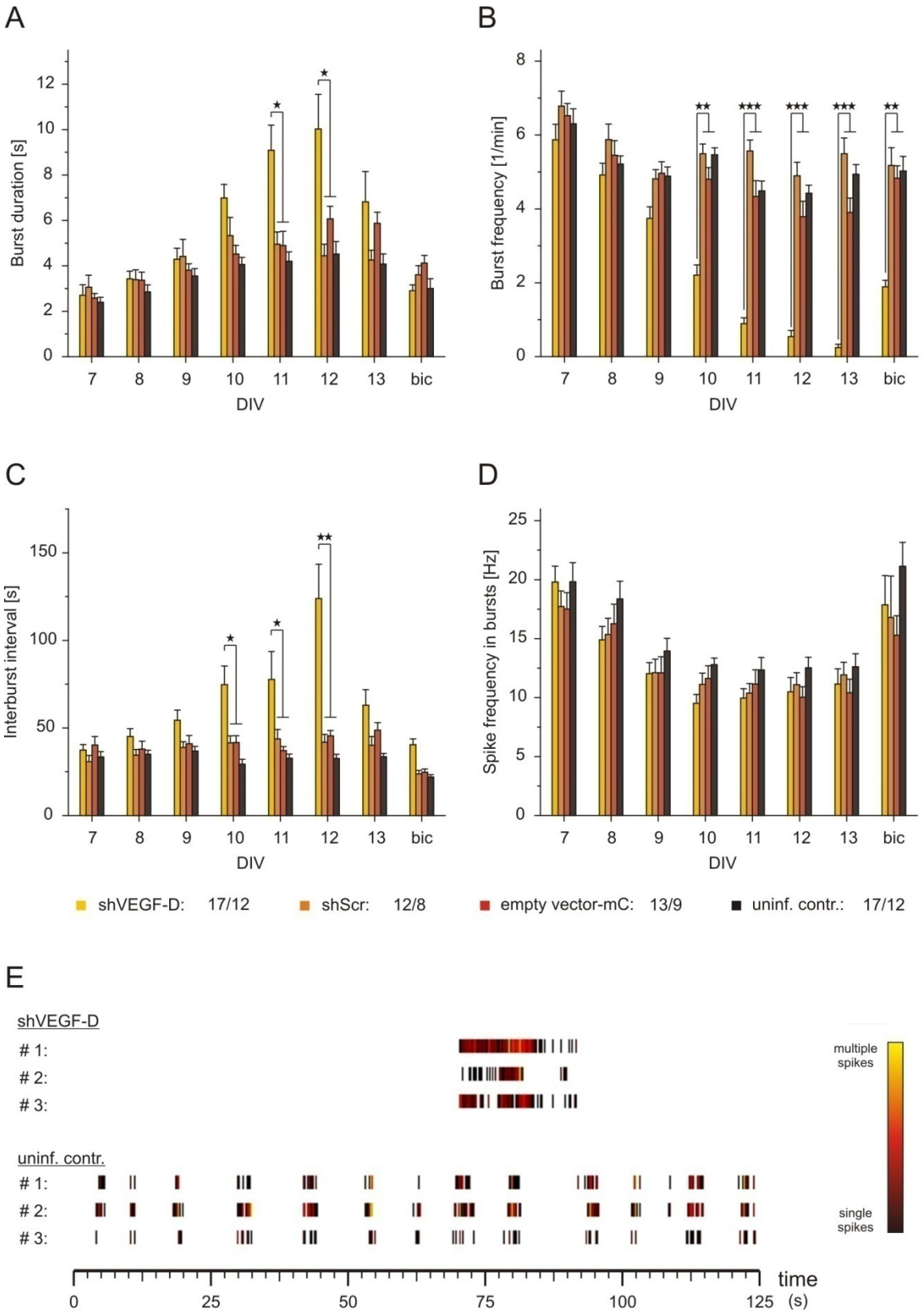
A
Burst duration [s]
DIV
B
Burst frequency [1/min]
DIV
C
Interburst interval [s]
DIV
D
Spike frequency in bursts [Hz]
DIV
shVEGF-D: 17/12
shScr: 12/8
empty vector-mC: 13/9
uninf. contr.: 17/12
E
shVEGF-D
1:
2:
3:
uninf. contr.
1:
2:
3:
multiple spikes
single spikes
time
(s)

Figure 23 – Silencing of VEGF-D signaling disrupts regular bursting behavior.

Developmental changes of bursting behavior in cultured hippocampal networks deficient in VEGF-D signaling are assessed by daily recordings. Represented are the mean values of four key parameters of bursting behavior in the second week of culturing: burst duration (A), burst frequency (B), interburst interval (C) and spike frequency in bursts (D). Representative traces of three electrodes of a recording on DIV 13 are shown for a recording from a shVEGF-D-infected and a control culture. Perpendicular lines represent the detection of spikes on the respective electrode. Lines are color-coded to visualize spike density (E). Network activity of cultures was recorded twice on DIV 13: before and two hours after bicuculline treatment (50 µM). Numbers in the legend reveal corresponding sample sizes (number of MEAs / number of independent cultures). * $p<0.05$; ** $p<0.01$; *** $p<0.001$.

5.3.5 Bath application of exogenous VEGF-D as a tool to retrieve spontaneous activity in hippocampal cultures deficient in shVEGF-D signaling

VEGF-D was initially described in the mouse as *c-fos*-induced growth factor (FIGF) and it belongs to the VEGF family of growth factors (Orlandini et al., 1996; Joukov et al., 1996; Achen et al., 1998). It is extracellularly secreted since it comprises a N-terminal peptide for the Golgi apparatus-mediated secretory pathway and, once secreted, binds specifically to VEGFR-3 (Achen et al., 1998; Baldwin et al., 2001). VEGFR-3 is a receptor tyrosine kinase (RTK) expressed in the rodent hippocampus and might therefore be crucial in the neuronal VEGF-D signaling pathway.

Given VEGF-D an impact in the development of the electric properties of cultured hippocampal networks, I wished to directly test whether bath application of exogenous VEGF-D can rescue the impairments on neuronal network in shVEGF-D-infected cultures. Exogenous VEGF-D is a biogenic compound which gets degraded by proteases in the extracellular space. Since less is known about its physical properties such as half-life and dissociation constant with VEGFR-3, 100 ng/ml VEGF-D were used. This is in accordance with other reports (Marconcini el al., 1999). That bath application of exogenous VEGF-D in the order of 100 ng/ml might reconstitute the effects of silcencing VEGF-D signaling on neuronal network activity is supported by studies on neuronal morphology. Here, in shVEGF-D transfected neurons reduction in dendritic arborization on DIV 13 is retrieved by about 50 % when adding 100 ng/ml exogenous VEGF-D on DIV 10.

This part of the study, reporting about the ability of exogenous VEGF-D to rescue developmental implications on neuronal network activity in hippocampal cultures deficient in VEGF-D signaling, includes data of the following groups (number of MEAs / number of independent preparations): shVEGF-D: 17/12; shVEGF-D + exogVEGF-D on DIV 6: 11/8; shVEGF-D + exogVEGF-D on DIV 10: 11/9; uninf.contr.: 17/12; uninf.contr. + exogVEGF-D on DIV 6: 8/7; uninf.contr. + exogVEGF-D on DIV 10: 12/8. Experiments were done similar to 5.2.2 and 5.3.2. Two time points were chosen for adding exogenous VEGF-D: On DIV 6 when VEGF-D

has probably not yet an impact on neuronal network dynamics and, second, on DIV 10 when the first effects on network activity have already emerged.

To assure that bath application of exogenous VEGF-D itself does not affect basal synaptic transmission, spontaneous network activity recorded on DIV 7 was analyzed. Bath application of exogenous VEGF-D had no effect on spontaneous network activity, neither in shVEGF-D infected- nor in control cultures (0.95 Hz ± 0.12 for shVEGF-D, 1.00 Hz ± 0.16 for shVEGF-D + exogVEGF-D on DIV 6, 1.02 Hz ± 0.10 for uninf.contr., and 1.10 Hz ± 0.18 for uninf.contr. + exogVEGF-D on DIV 6) (Figure 24 A). Statistical distribution was similar for all groups too (Figure 24 B). 'Number of electrodes showing activity' did also not show a significant difference between groups (33.0 ± 2.6 for shVEGF-D, 30.4 ± 3.8 for shVEGF-D + exogVEGF-D on DIV 6, 33.9 ± 3.4 for uninf.contr., and 32.1 ± 2.7 for uninf.contr. + exogVEGF-D on DIV 6) (Figure 24 C). Statistical distribution was similar for all groups (Figure 24 D). Plotting 'number of active electrodes showing activity' against 'absolute spike frequency' is also similar for all groups which support the finding that spontaneous network activity was not affected by supplementing medium with recombinant VEGF-D until DIV 7 (Figure 24 E). Additionally, in all groups distribution of activity within the electrodes showing activity is similar (Figure 24 F).

Additionally, bursting behavior of the four different groups was analyzed to show that bath application of exogenous VEGF-D on DIV 6 has no acute effects on synchronized firing activity. The same key parameters as in 5.2.2 and 5.3.2 were chosen to simplify comparability. Each of the four depicted parameters as well as the other analyzed parameter (data not shown) did not show significant differences between the groups. However, bath application of 100 ng/ml exogenous VEGF-D slightly increased burst duration on DIV 7 (

Figure 25 A). Furthermore spike frequency in bursts was slightly decreased in shVEGF-D infected cultures treated with exogenous VEGF-D (

Figure 25 D).

Taken together, no significant differences in one of the analyzed parameters of both spontaneous and synchronized activity were found in the mean values of the recordings from DIV 7. These results substantiate the findings of 5.3.2 that it is unlikely that VEGF-D signaling is of importance for spontaneous activity in the first week of network development.

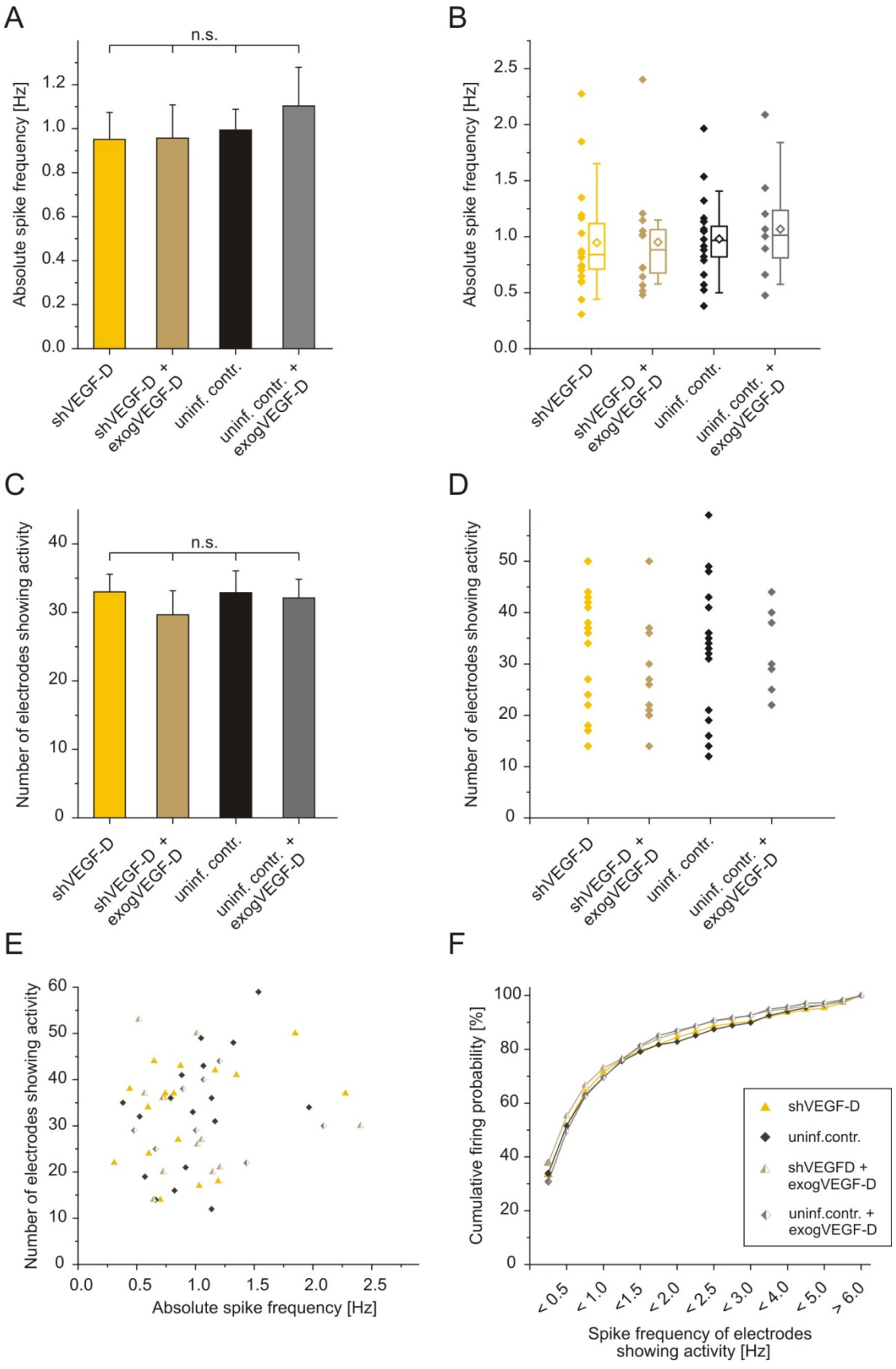
A
n.s.
Absolute spike frequency [Hz]
0.0
0.2
0.4
0.6
0.8
1.0
1.2
shVEGF-D
shVEGF-D + exogVEGF-D
uninf. contr.
uninf. contr. + exogVEGF-D
B
Absolute spike frequency [Hz]
0.0
0.5
1.0
1.5
2.0
2.5
shVEGF-D
shVEGF-D + exogVEGF-D
uninf. contr.
uninf. contr. + exogVEGF-D
C
n.s.
Number of electrodes showing activity
0
10
20
30
40
shVEGF-D
shVEGF-D + exogVEGF-D
uninf. contr.
uninf. contr. + exogVEGF-D
D
Number of electrodes showing activity
0
10
20
30
40
50
shVEGF-D
shVEGF-D + exogVEGF-D
uninf. contr.
uninf. contr. + exogVEGF-D
E
Number of electrodes showing activity
0
10
20
30
40
50
60
0.0
0.5
1.0
1.5
2.0
2.5
Absolute spike frequency [Hz]
F
Cumulative firing probability [%]
0
20
40
60
80
100
shVEGF-D
uninf.contr.
shVEGFD + exogVEGF-D
uninf.contr. + exogVEGF-D
< 0.5
< 1.0
< 1.5
< 2.0
< 2.5
< 3.0
< 4.0
< 5.0
> 6.0
Spike frequency of electrodes showing activity [Hz]

Figure 24 – Hippocampal cultures treated with exogenous VEGF-D: Assessment of spontaneous network activity of recordings on DIV 7.

Mean values of network activity for the four indicated different groups recorded three days after infection and one day after adding exogenous VEGF-D (100 ng/ml) (A). Mean activity of individual recordings from all groups are plotted as single data points. Additionally, the respective box plot analyses (including quartiles, median and mean) are shown (B). Mean values of the 'number of electrodes showing activity' for the four different groups recorded 24 hours after adding exogenous VEGF-D (C). Mean values of the 'number of electrodes showing activity' of individual recordings are plotted as single data points (D). Calculation of individual values for each recording was confined on electrodes with an activity of higher than 0.01 Hz (A+C). Number of electrodes showing activity of every individual recording is plotted against the respective mean value of the spike frequency (E). For each group, electrodes above threshold (0.01 Hz) of all recordings are pooled and firing probability is plotted in bins (F). n.s. – not significant.

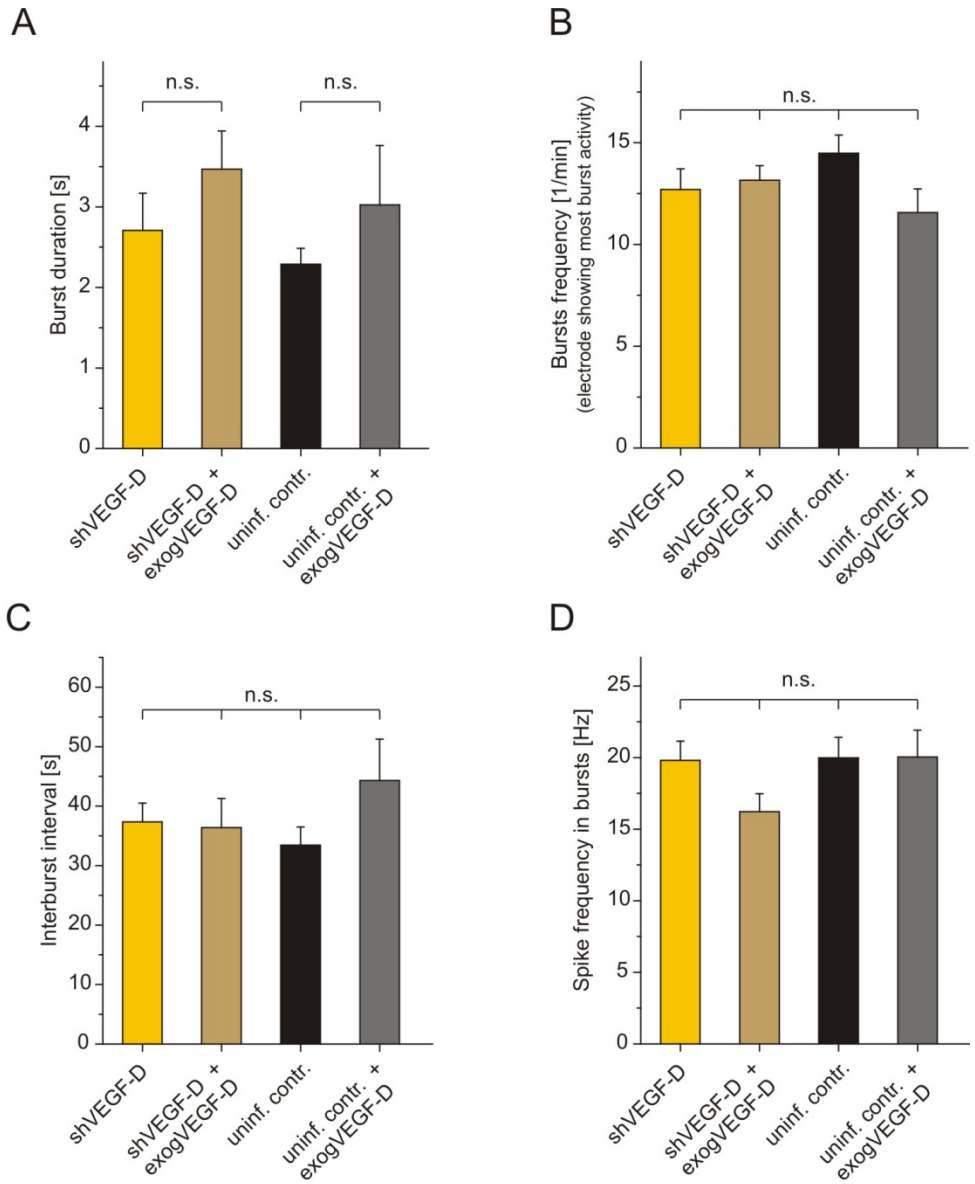

Figure 25 – Hippocampal cultures treated with exogenous VEGF-D: Assessment of bursting behavior of recordings on DIV 7.

Mean values of burst duration (A), burst frequency (B), interburst intervals (C), and spike frequency in bursts (D) of recordings of hippocampal cultures treated with and without exogenous VEGF-D (100 ng/ml) are depicted as exemplary parameters to characterize bursting behavior. n.s. – not significant.

5.3.6 Bath application of exogenous VEGF-D partly rescues spontaneous activity in hippocampal cultures deficient in shVEGF-D signaling

Next, it was investigated whether bath application of exogenous VEGF-D in the order of 100 ng/ml is able to retrieve neuronal network activity in shVEGF-D infected cultures. When half medium was changed (DIV 9, DIV 12) fresh medium contained exogenous VEGF-D for the substituted volume. During the second week of culturing developmental changes in spike frequency and number of electrodes showing activity were assessed by daily recordings. Mean values were analyzed as relative values compared to DIV 7. Thereby it turned out that bath application of exogenous VEGF-D on DIV 6 but not on DIV 10, was able to partly rescue neuronal network activity on both levels, on spontaneous firing frequency and on the number of electrodes showing activity (Figure 26 A+B). Upregulation in spontaneous activity by VEGF-D bath application was about 3-fold and number of electrodes showing activity was increased about 2-fold compared to untreated shVEGF-D infected cultures (spontaneous activity on DIV 13: shVEGF-D: 9.1 % ± 3.0, shVEGF-D + exogVEGF-D on DIV 6: 30.9 % ± 7.4; number of electrodes showing activity on DIV 13: shVEGF-D: 28.0 % ± 5.9, shVEGF-D + exogVEGF-D on DIV 6: 49.4 % ± 7.8). However, under bicuculline no further rescue could be detected. Control cultures treated in the same way did not show an upregulation in network activity rather a slight down-regulation when VEGF-D was added on DIV 10 (Figure 26 A). These results confirm the potential of exogenous VEGF-D to rescue silenced VEGF-D expression as it was shown on neuronal morphology (unpublished observations). The positive effect on firing frequency by adding exogenous VEGF-D on DIV 6 to cultures deficient in VEGF-D signaling was also demonstrated by the cumulative firing probability on DIV 13. Here, shVEGF-D infected cultures treated with VEGF-D on DIV 10 showed a slight rescue on DIV 13 too. Again, under bicuculline treatment each group whether or not treated with exogenous VEGF-D had shown similar results (Figure 27).

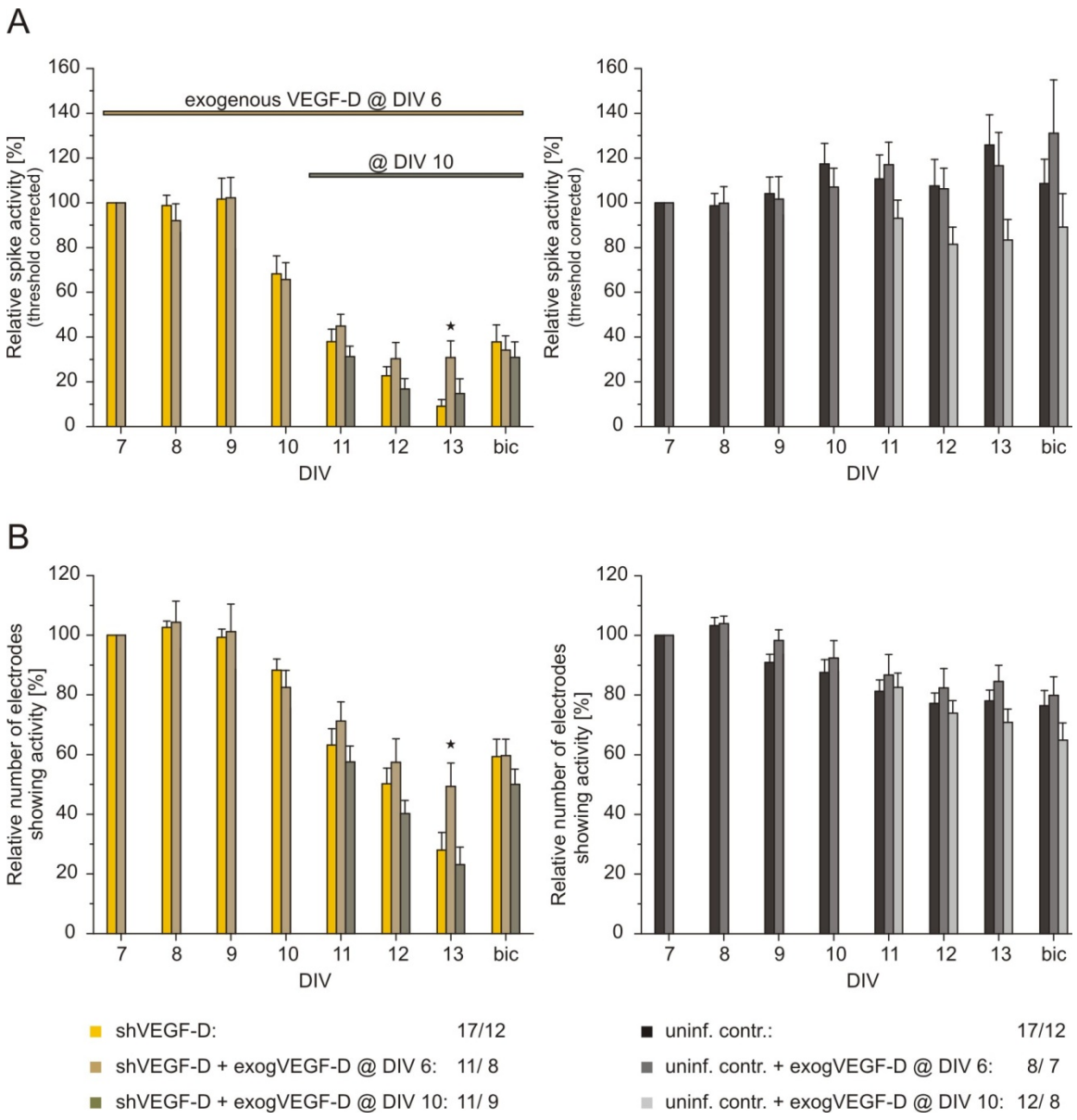

Figure 26 – Spontaneous activity in shVEGF-D-infected cultures is partly rescued by bath application of exogenous VEGF-D on DIV 6.

Developmental changes of spontaneous network activity in cultured hippocampal networks deficient in VEGF-D signaling are assessed by daily recordings. For clearness shVEGF-D infected and control groups are separated. Relative values of spontaneous firing frequency are depicted for each group on every day taking account of the time point of adding exogenous VEGF-D (A). Relative values of the number of electrodes showing activity are illustrated alike spontaneous firing frequency (B). Network activity of cultures was recorded twice on DIV 13: before and two hours after bicuculline treatment (50 µM). Numbers in the legend reveal corresponding sample sizes (number of MEAs / number of independent cultures). * $p<0.05$

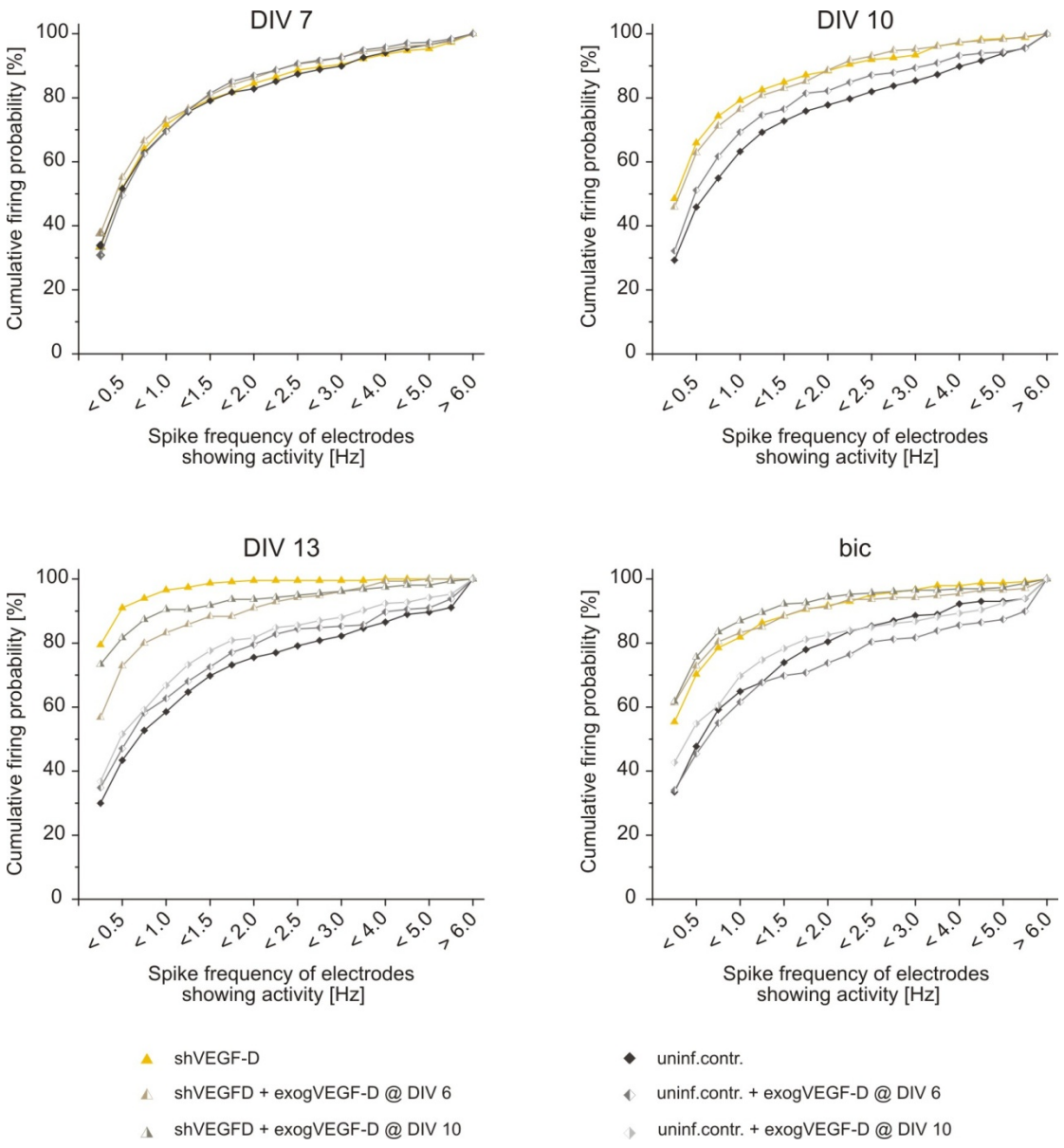

Figure 27 – Hippocampal cultures infected with shVEGF-D and treated with exogenous VEGF-D reveal a rescue in cumulative firing probability.

Charts show the cumulative firing probability of each group on the depicted day *in vitro*. For each group, electrodes of all recordings showing an activity above threshold (0.01 Hz) are pooled and firing probability is plotted in bins. Traces for 'exogVEGF-D @ DIV 10' are present for DIV 13 and bic only.

Besides spontaneous activity, bursting behavior was analyzed in cultures treated with exogenous VEGF-D too. There, I focused only on cultures being handled with exogenous VEGF-D from DIV 6 on since bath application on DIV 10 did not show significant effects on spontaneous activity. Likewise to spontaneous spike activity (Figure 26 A) key parameters of bursting behavior which were altered in shVEGF-D infected cultures were slightly brought back

towards the control groups. Cultures treated with 100 ng/ml VEGF-D upon DIV 6 and deficient in VEGF-D signaling revealed shorter bursts (apart from DIV 13), a slightly higher mean values in burst frequency and shorter interburst intervals while spike frequency in bursts was not changed (Figure 28). This indicates that the shVEGF-D caused impairments on neuronal network activity were either slightly rescued or delayed by bath application of VEGF-D. Bath application of exogenous VEGF-D had no effects on bursting behavior in uninfected cultures (Figure 28).

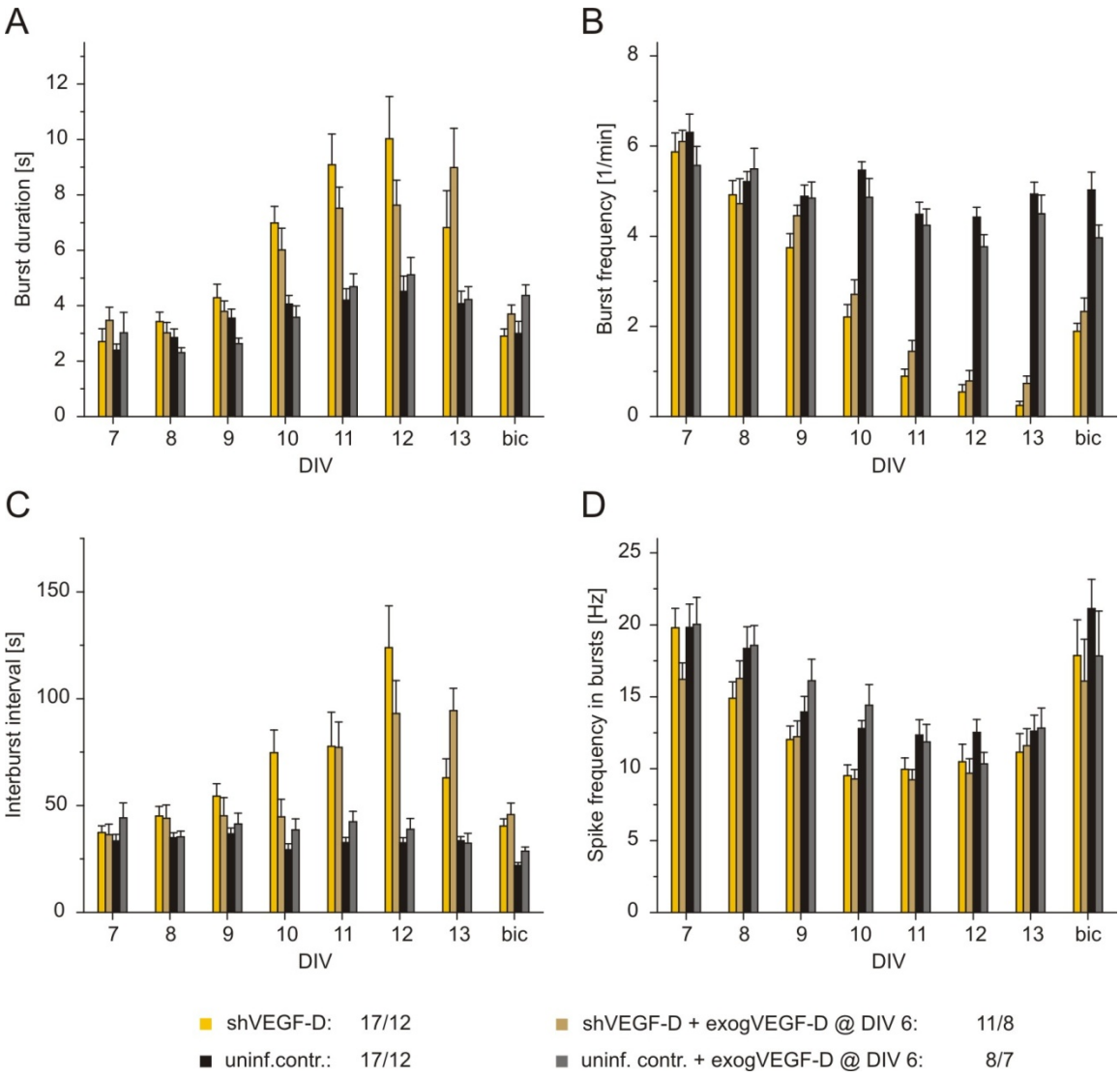

Figure 28 – Recombinant VEGF-D partly rescues shVEGF-D-mediated disorders in bursting behavior.

Possible rescue of bursting behavior in cultured hippocampal networks deficient in VEGF-D signaling by bath application of exogenous VEGF-D is assessed by daily recordings. Represented are the mean values of four key parameters of bursting behavior in the second week of culturing: burst duration (A), burst frequency (B), interburst interval (C) and spike frequency in bursts (D). Network activity of cultures was recorded twice on DIV 13: before and two hours after bicuculline treatment (50 µM). Numbers in the legend reveal corresponding sample sizes (number of MEAs / number of independent cultures).

5.4 LTP IN ACUTE SLICE PREPARATIONS

5.4.1 LTP in Schaffer collateral – CA1 synapses lasts 4 hours and longer

Acute hippocampal slices were positioned on the electrode field of MEAs having planar electrodes of 30 µm diameter and a 200 µm distance to each other (Figure 29). Spontaneous spike activity could be recorded along the whole CA3 – CA1 pyramidal cell layer as well as in the DG at a wide range of frequencies (data not shown). To evoke electrical activity, monopolar stimulation of Schaffer collateral fibers was done through MEA electrodes located in *stratum radiatum*. Negative fEPSPs could be recorded along the apical dendrites in the entire *stratum radiatum* and in *stratum lacunosum moleculare* on both sides of the stimulation electrode. In some slices population spikes in the pyramidal cell layer could be detected. However, in *stratum oriens*, only the positive reflections of the synaptic activation could be seen. To exclude slices that showed unspecific rundown of synaptic transmission after LTP induction a second, independent pathway was stimulated and served as an internal control. IO curves were acquired to assess total connectivity in the slice and to determine an appropriate stimulation strengths. IO curves of both Schaffer collaterals and perforant path fibers were comparable (Figure 30 A). For technical reasons, the highest stimulation strength applied was 3 V although synaptic responses had not yet reached a plateau level. Nevertheless, stimulation strength for test pulses was set to about 30 % of the maximal synaptic response.

Baseline recordings for up to 50 minutes were performed to assess the stability of evoked synaptic responses. Slopes of the baseline EPSP responses were used to normalize data of different recordings. Four trains of high-frequency stimulation induced robust L-LTP which lasted four hours and longer (relative EPSP slopes four hours after LTP-induction: potentiated pathway 140.0 % ± 7.4; control pathway 92.8 % ± 8.1; n = 9) (Figure 30 B). Exemplary traces of evoked synaptic responses at different timepoints during a recording are shown in Figure 30 C. To investigate whether induction of LTP by stimulation through MEA electrodes is NMDA receptor-dependent slices were perfused with the NMDA receptor antagonists AP5 (50 µM) and MK801 (10 µM) starting 25 minutes before LTP induction. As expected (Collingridge et al., 1983), NMDA receptor antagonists blocked the induction of LTP (Figure 30 D). EPSP slopes of synapses that received HFS were slightly scaled-down for a short time immediately after HFS. Additionally, the mRNA translation-dependency of L-LTP was investigated by perfusing slices with anisomycin (25 µM). When applied during LTP induction the maintenance phase of LTP was blocked whereas LTP induction and the early phase of LTP remained unaffected (relative EPSP slopes four hours after LTP-induction: potentiated pathway 98.8 % ± %; control pathway 87.6 % ± 5.3; n = 4) (Figure 30 E) (Frey et al., 1988). Exemplary traces of evoked synaptic responses at different time points during a recording are shown in Figure 30 F. Hence, MEA recordings on acute hippocampal slices depict a suitable technique to study especially the late phase of LTP.

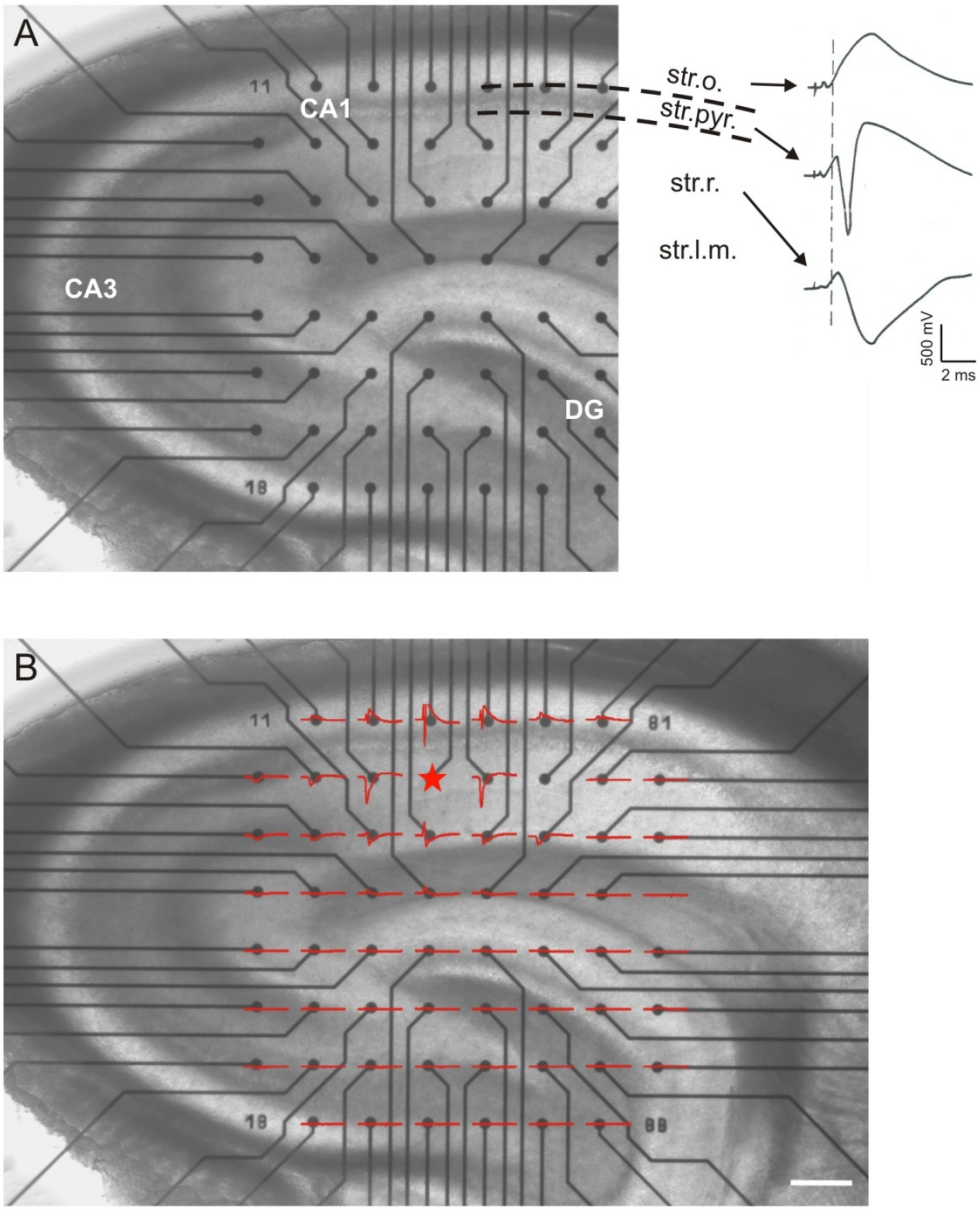

Figure 29 – An acute hippocampal slice positioned on a MEA.

An acute hippocampal slice from a p37 rat is positioned on a MEA. Different regions of the hippocampus are indicated as well as the different layers of region CA1 and expected EPSP slopes in CA1 upon Schaffer collateral stimulation (A). Shown in overlay (red traces) are signals recorded on all 60 electrodes in response to stimulation (100 µs, 1.0 V) by electrode 42 (asteric) (B). Scale bar: 200 µm. CA – cornu ammonis; DG – dentate gyrus; Str.o. – *stratum oriens*; str.pyr. – *stratum pyramidale*; str.r. – *stratum radiatum*; str.l.m. – *stratum lacunosum moleculare.*

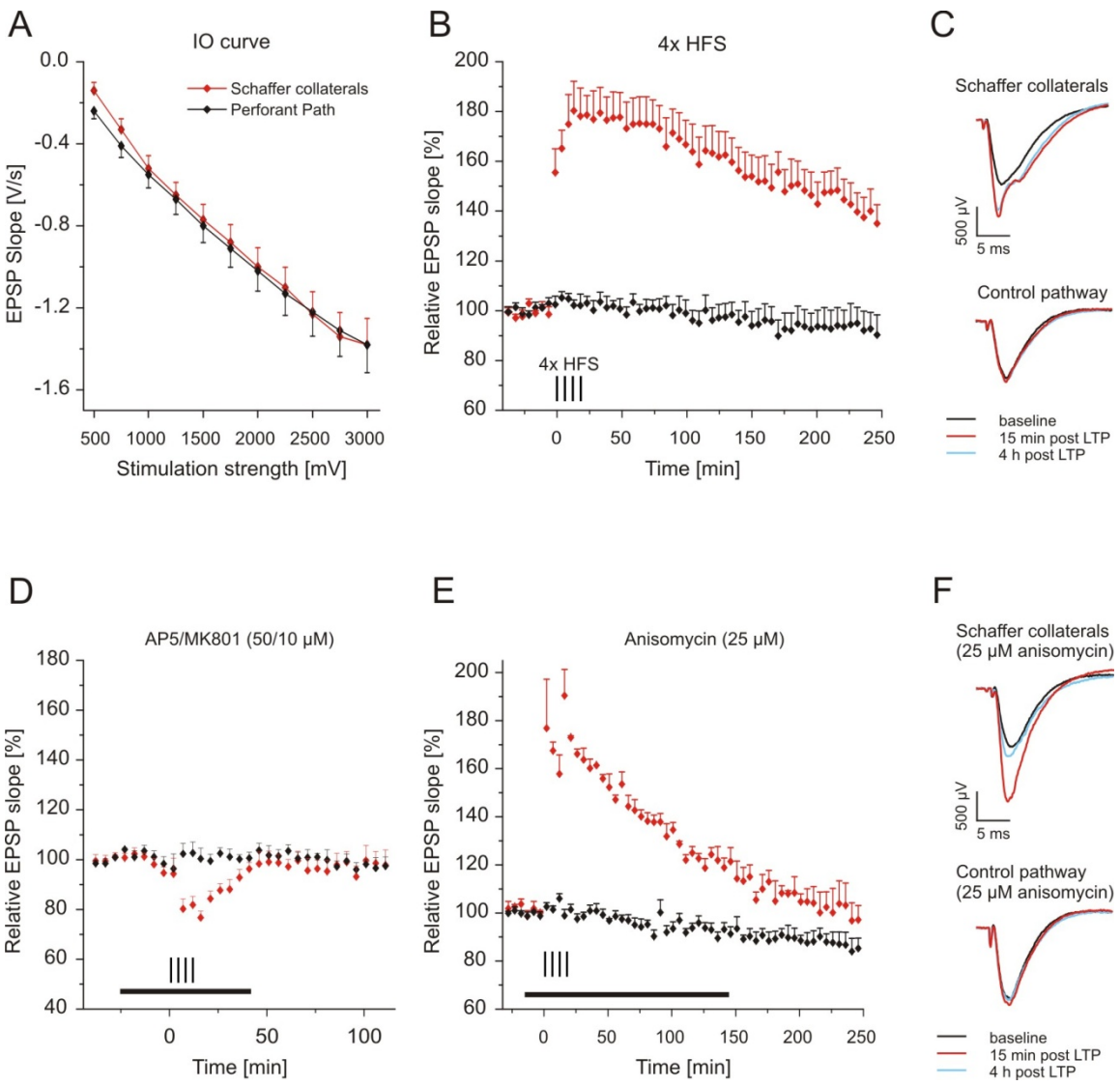

Figure 30 – Repeated high-frequency stimulation induces L-LTP in acute slice preparations.

IO curves show average EPSP slopes with increasing stimulation strength in acute hippocampal slices (A). Relative EPSP slopes are increased at Schaffer collateral – CA1 synapses after four trains of HFS stimulation, whereas perforant path – CA1 synapses (control pathway) do not alter their strength (B). Exemplary traces recorded during baseline, 15 minutes and 4 hours after four trains of 100 Hz stimuli (C). Perfusion with the NMDA receptor antagoinsts AP5 (50 µM) and MK801 (10 µM) during HFS blocks LTP induction (D) whereas perfusion with the mRNA translation blocker anisomycin (25 µM) blocks long-lasting LTP but not LTP induction (E). Exemplary traces recorded during baseline, 15 minutes and 4 hours after four trains of 100 Hz stimuli (F) (compare to (C)). Horizontal bars represent time when drugs were applied (D, E). HFS – High-frequency stimulation.

5.4.2 Acute slice preparations of genetically modified rats

A future prospect of LTP recordings using MEAs is the dissection of signaling pathways involved in the transcription-dependent late phase of LTP. Since it is known that the expression of

long-term LTP is gene transcription-sensitive more sophisticated questions concerning this issue arise (Frey et al., 1996; Nguyen and Kandel, 1997; Barco et al., 2005). For instance, the particular role of nuclear calcium signaling in the maintenance phase of LTP is to date unclear. Exploration of this question requires advanced techniques on par with the molecular biology techniques available for the fast and efficient screening for the genes that are upregulated upon LTP induction and that are essential for L-LTP expression. The ability to generate genetically modified rats by virus-mediated gene transfer may elegantly and quickly facilitate the answering of these questions (Cetin et al., 2006). To investigate whether rAAV-mediated gene transfer into the rat hippocampus is a suitable technique to answer questions related to nuclear calcium signaling and LTP, viruses expressing a nuclearly localized YFP were injected into the ventral hippocampi of 21 day old rats. Two weeks later, YFP expressing cells were prominent in the CA1 pyramidal layer (most often also in CA3 and DG) throughout the hippocampus, especially in those slices appropriate for LTP recordings (Figure 31).These data suggest that genetically modified rats may indeed be appropriate for functional LTP studies using MEAs.

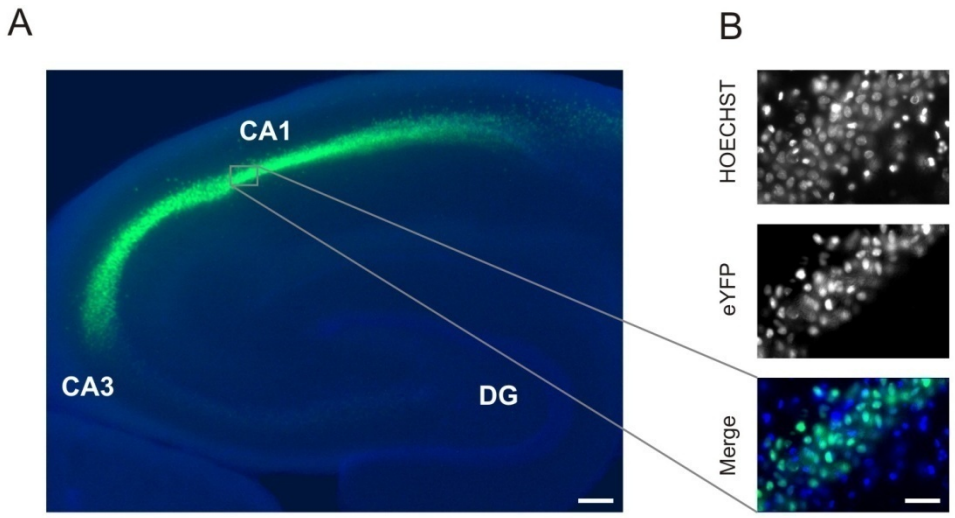

Figure 31 – Hippocampal slice of a p36 rat expressing a nuclear localized GFP.

rAAV-eYFP-NLS were stereotaxically injected into the hippocampus two weeks prior to preparing 300 µm thick horizontal slices. CA1 and CA3 pyramidal cell layer show a large fraction of infected cells (A). Confocal images showing a nuclear staining (Hoechst), eYFP fluorescence or merged image, respectively (B). Scale bars: A: 200 µm; B: 50 µm. CA – cornu ammonis; DG – dentate gyrus

To investigate further whether acute slices from genetically modified rats can be used for functional experiments involving calcium imaging, animals expressing the genetically encoded nuclearly localized calcium probe GCaMP2.0-NLS were generated. Evoked synaptic responses of genetically modified rats expressing GCaMP2.0-NLS were slightly increased in comparison to those recorded from uninfected animals (Figure 32 B; compare to Figure 30 A). HFS induced

robust calcium signals in the nuclei of infected CA1 cells (Figure 32 A). Analysis of confocal images (data not shown) and calcium responses to stimulation in *stratum oriens* (background) (Figure 32 D) showed that GCaMP2.0-NLS was almost exclusively nuclearly localized. These results demonstrate that stereotaxically guided viral gene transfer into the hippocampus may be used in combination with MEA recordings to investigate the calcium signaling pathways involved in late phase of LTP.

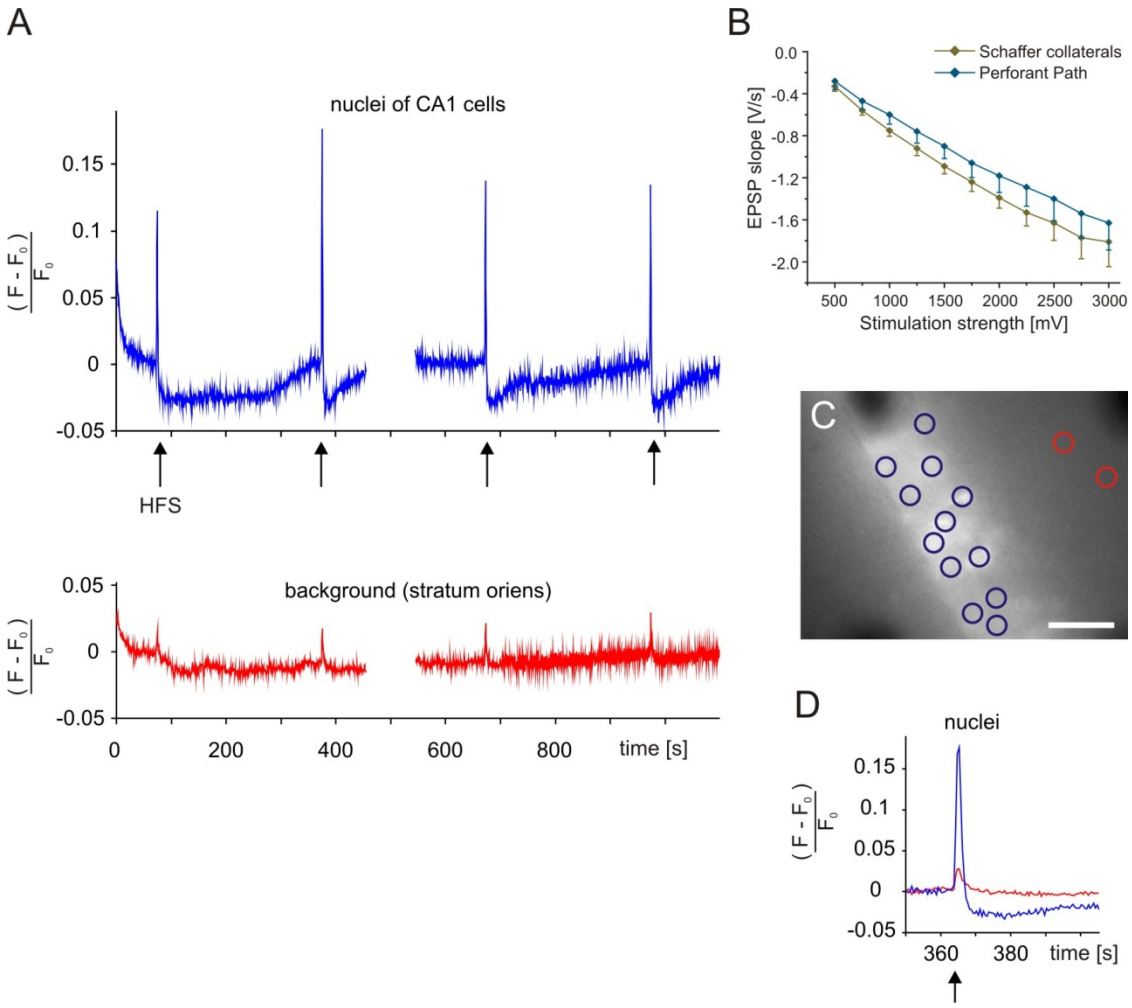

Figure 32 – Imaging nuclear calcium signals from CA1 pyramidal cells during HFS.

Acute slices of a 34 day old, genetically modified rat expressing the nuclear calcium indicator GCaMP2.0-NLS were used to image calcium signals in nuclei of CA1 cells (blue trace) and *stratum oriens* (red trace) in response to HFS of Schaffer collateral fibers. A hippocampal slice was positioned on a thin-ITO-MEA and imaged at 2 Hz (A). IO curves show average EPSP slopes with increasing stimulation in acute hippocampal slices (B). Example of an acute hippocampal slice positioned on a thin-ITO-MEA expressing GCaMP2.0-NLS in CA1 pyramidal cell layer (C). Temporal enlargement of the second calcium response shown in A (D). Scale bar: 50 µm.

6 DISCUSSION

If the brain were so simple that we could understand it,
we would be so simple we couldn't.

Emerson M. Pugh

In this study Micro-Electrode-Arrays were used to analyze calcium signaling pathways involved in neuronal plasticity. It was investigated whether nuclear calcium signals are involved in neuronal network activity of primary hippocampal cultures and whether this is regulated by the temporal expression profile of the nuclear calcium-regulated gene *vegf-d*. The results indicate that VEGF-D massively affects neuronal network behavior, an effect that was partly rescued by supplementing medium with recombinant VEGF-D. In a second study long-lasting LTP recordings from acute slice preparations on MEAs were established. Additionally, it was shown that acute slices from genetically modified rats can be used to functionally study signaling pathways involved in the late phase of LTP.

6.1 MICRO-ELECTRODE-ARRAY RECORDINGS OF CULTURED HIPPOCAMPAL NETWORKS

6.1.1 Reusing MEAs for multiple cycles slightly decreases signal detection

Similar to what has been described for primary hippocampal neurons (Fletcher and Banker, 1989) it was found that neuronal cultures become resynchronized after dissociation. In dissociated cultures, the original cellular architecture is lost during the dissociation and neurons re-wire with random connections. The goal of this study was to investigate whether the inactivation of different gene transcription pathways alters network activity pattern during the second week of development. Neuronal networks grown on MEAs were recorded first on DIV 7 to acquire a baseline since network activity is not yet dependent on activity induced changes in gene-expression at that time-point (Valor et al., 2007). Then cultures were recorded daily and changes of intrinsic properties of network activity such as spontaneous activity and synchronized firing were analyzed during different developmental stages. This is in contrast to many other studies in which neuronal network activity is analyzed after electrical stimulation or

pharmacological manipulation (Wagenaar et al., 2006; Arnold et al., 2005). On DIV 7 network activity was composed of both spontaneous and synchronized activity, the two major activity patterns that are shared by many different developing neuronal systems *in vitro* (O'Donovan and Chub, 1997; O'Donovan, 1999; Arnold et al., 2005) and *in vivo* (Buzsaki and Draguhn, 2004; Mazzoni et al., 2007; Garcia-Perez et al., 2007).

To quantify changes in recorded activity during development requires a special approach applicable both to the sequences of action potentials (spontaneous activity) and to the sequences of bursts (synchronized activity). Since MEAs were reused for multiple cycles it was first investigated how detection of neuronal activity changes after multiple culturing cycles. Although average means of 'spontaneous activity' and 'number of electrodes showing activity' revealed slight decreases with increasing reuse cycles (Figure 12), MEAs were used up to seven times since inter-culture variability was far larger than differences in average mean values after multiple measurements (Figure 13). Due to these large variations in 'spontaneous activity' and 'number of electrodes showing activity' data was normalized to DIV 7 recordings. A minimal threshold was implemented for both network properties since normalizing data allocates every unit (in this study: units equal electrodes) the same weight and thus carries the risk of scaling negligible differences of units that reveal a few spikes only. In contrast, properties of synchronized activity patterns such as burst duration and burst frequency were comparable between cultures. These parameters were analyzed by software implemented plugins for pattern recognition and did not need to be normalized to the recording of DIV 7.

Having demonstrated that MEA recordings can be used to assess spontaneous activity independently from the reuse cycle of MEAs, prerequisites were fulfilled to study the development of neural network behavior.

6.1.2 Inhibition of nuclear calcium signaling

Self-assembled *in vitro* neuronal networks are widely used as an experimental model system for studying the basic mechanisms governing neuronal network activity; their collective dynamic modes, information processing, and learning capabilities (Marom and Shahaf, 2002; Segev et al., 2004; Baruchi and Ben-Jacob, 2007 – aus Fuchspaper).

To investigate the role of nuclear calcium signaling in basal network plasticity, the nuclear calcium inhibitor peptide, CaMBP4, was fused at the N-terminus of the fluorescent protein mCherry to facilitate visualization und localization of the over-expressed recombinant proteins (Figure 14). CaMBP4-mC has already been characterized (e.g. by Q-PCR and by immunoblot analysis) by our group (Lau et al., 2009) and was therefore not confirmed again. Furthermore, it was recently shown that inhibition of nuclear calcium signaling by CaMBP4 affects gene transcription of a specific subset of genes (Zhang et al., 2009). Infection rates of all viruses tested

in this study were about 70 % of viable neurons. Furthermore, none of the constructs increased neuronal mortality in comparison to uninfected controls. These findings and the fact that hippocampal neurons transfected with CaMBP4 reveal massively reduced dendritic complexity and loss in spine density (unpublished observation by D. Mauceri, Heidelberg) were the ground to study the role of nuclear calcium on network activity. Neuronal network activity was recorded first on DIV 7 for all groups in an order which has been documented in previous studies (Figure 15 + Figure 16) (Wagenaar et al., 2006). However, the network activity of cultures of neurons from the same brain region of two different species can also massively differ (Arnold et al., 2005). The finding that neuronal network activity of CaMBP4-mC-infected cultures was not altered three days after infection can have two different reasons. Either protein levels of CaMBP4 are not yet high enough to successively interfere with nuclear calcium-mediated gene transcription (mCherry fluorescence is not detectable yet) or maturation of synaptic efficacy and network activity are not dependent on nuclear calcium signaling at that stage of development. Several reports have shown that synapse maturation and neuronal network activity develop independently of a specific genetic program during the first week of culture (Valor et al., 2007; Mazzoni et al., 2007). To address whether the protein level of CaMBP4-mC is high enough to interfere with nuclear calcium signaling, Q-PCR and immunoblot anylsis at different developmental stages can be done. To increase protein levels in DIV 7 cultures can also be earlier infected (e.g. on DIV 1).

Given the fact that on DIV 7 CaMPB4-mC-infected cultures behave similar to controls allowed me to assess whether nuclear calcium signaling is important for neuronal network behavior during the second week of development at the level of spontaneous and synchronized activity. Interestingly, independent of the level of CaMBP4-mC expression, the average mean of spontaneous network activity and synchronized activity hardly changes during the second week in culture (Figure 17Figure 18). None of the analyzed properties of bursting behavior (see 3.4.2) significantly changed during the second week of culture. This is the first study that reports about the development of network firing in hippocampal cultures by daily recordings. Furthermore, network behavior appears to be stable in the third week of culturing, too, although this was investigated for a few cultures, only (H.E. Freitag, personal observation). Bicuculline treatment for two hours at the end of the experiments was performed to activate all excitatory inputs and to induce recurrent synchronized action potential bursting (Figure 18 D) (Arnold et al., 2005). Average mean frequency was not altered by bicuculline, a phenomenon that points to possible homeostatic mechanisms of these cultured networks (Miller, 1996; LeMasson et al., 1993).

Focusing on CaMBP4-mC-infected cultures, among all analyzed parameters of both spontaneous and synchronized network activity only one significantly changed during the second week of development. Mean burst duration increased approximately two fold between DIV 10 and DIV 13 (Figure 18). However, only one or two bursts per 5 minutes recording increased their duration to 30 – 40 s, sometimes up to 60 s within a single recording. All other bursts were fairly

similar to bursts of the control groups. This also suggests that a recording duration of five minutes is not long enough to exactly determine length, frequency and periodicity of the “long” bursts. If these “long” bursts are similar to superbursts requires further investigation (Wagenaar et al., 2006). Interestingly, the remaining burst pattern (Figure 18 C) as well as overall activity (Figure 17 A) of CaMBP4-mC-infected cultures remained fairly stable. The latter might be attributed to either to homeostatic network properties or that CREB-mediated gene-expression is necessary to keep a highly regular and periodic bursting behavior upon DIV 10. Hence, this study hints to the direction that the development and maybe also the maintenance of neuronal network activity is regulated by CREB-mediated gene transcription in a temporally-controlled manner.

Taken together, in hippocampal networks nuclear calcium signaling is not only of importance for dendritic morphology but also to maintain regular network activity. Why the fairly massive effects on dendritic arborization and on spine density reveal only rather small effects on neuronal network activity cannot be explained by this study. Homeostatic mechanisms or the intrinsic properties of hippocampal neurons might be involved (Turrigiano and Nelson, 2004). However since basal nuclear calcium signaling is involved in keeping neuronal networks firing regularly I asked the question if this is mediated by a defined gene whose expression level is regulated by nuclear calcium. With the recent study of Zhang et al., 2009 one gene was of particular interest since its RNA interference-mediated knock-down showed similar effects on dendritic morphology: vascular endothelial growth factor D (*vegf-d*).

6.1.3 Knock-down of VEGF-D expression in primary hippocampal cultures

Given nuclear calcium signaling and CREB-mediated gene transcription’s role in the maintenance of regular network activity, a single or subset of these genes might specifically regulate network development and maturation, either directly e.g. by function at the synapse level or indirectly e.g. by controlling neuronal morphology. Whole genome transcriptional profiling revealed several candidate genes that`s expression is regulated by nuclear calcium (Zhang et al., 2009). I became interested in VEGF-D, also termed as FIGF, because RNA interference-mediated knock-down of VEGF-D shapes the morphological phenotype of CA1 pyramidal neurons *in vitro* and *in vivo* similar to those expressing CaMBP4. Furthermore, supplementing medium with mature recombinant VEGF-D fully rescues CaMBP4 induced impairments on dendritic arborization (unpublished observations by D. Mauceri, Heidelberg). Since both down-regulation of *vegf-d* expression by CaMBP4 as well as knock-down of VEGF-D expression by RNA interference, was confirmed by Q-PCR experiments. To investigate whether VEGF-D expression is of vital importance for neuronal network behavior during the second week of development, hippocampal cultures plated on MEAs were infected with viruses expressing either shVEGF-D or a control virus.

Q-PCR studies of hippocampal cultures infected with shVEGF-D show a dramatic decrease in *vegf-d* mRNA levels to about 10 % on DIV 10. In contrast, cultures infected with CaMBP4-mC still reveal *vegf-d* mRNA levels of about 75 % (unpublished observations by D. Mauceri, Heidelberg). Although over-expression of CaMBP4-mC does not impair neuronal survival I first investigated whether the complete and specific knock-down of VEGF-D affects neuronal mortality. Similar to CaMBP4-mC infected cultures the complete knock-down of VEGF-D does not interfere with neuronal survival (Figure 19). A possible effect on neuronal network activity by knock-down of VEGF-D was investigated by daily recordings on MEAs. Again, cultures were recorded first on DIV 7 to assess basal activity levels. No significant effects between groups could be detected three days after infection (Figure 20). Although it cannot be excluded that the *vegf-d* mRNA level is not yet fully down-regulated, network behavior of hippocampal cultures appears to be independent of VEGF-D signaling at that stage of development. It might also be possible that VEGF-D knockdown does not exhibit an effect on network activity at that time. It is a future project to exactly answer the question at which time-point during *in vitro* development VEGF-D signaling becomes crucial for network plasticity in hippocampal cultures. To investigate this, *vegf-d* mRNA levels of shVEGF-D-infected cultures and a control group should be compared by Q-PCR experiments on earlier time-points such as DIV 6, DIV 7 and DIV 8. Furthermore, it would be possible to infect cultures on DIV 1 to prolong the time window between infection and recording. Hippocampal cultures of conditional VEGF-D knock-out mice would answer this issue too.

Due to the fact that on DIV 7 shVEGF-D infected cultures do not behave differently from control data that was normalized to minimize inter-culture variation. Astonishingly, knock-down of VEGF-D expression massively affects neuronal network behavior on both, spontaneous and synchronized activity levels during the second week of development. If experiments are carried out as described in this work, impairments of neuronal network activity in shVEGF-D-infected cultures have a precise onset on DIV 10. Within four days of development (DIV 10 – DIV 13) shVEGF-D infected cultures completely loose their stable, periodic activity. This is different from results obtained from CaMBP4-mC infected cultures although both groups show a few similarities. For example, in both CaMBP4-mC and shVEGF-D groups the first significant difference to the control groups can be detected on DIV 10 (Figure 22Figure 23). This strongly argues that VEGF-D might be a key mediator of the effects on neuronal network activity reported above about CaMBP4-mC. Furthermore shVEGF-D infected cultures reveal similar effects on burst duration including the occurrence of “long” bursts (Figure 23). However, knock-down of VEGF-D expression showed much stronger effects on network behavior than CaMBP4-mediated down-regulation of VEGF-D. Among these, down-regulation of spike frequency and burst frequency are the most robust (Figure 22 + Figure 23).

Recorded data of shVEGF-D-infected cultures was very carefully analyzed since loss of more than 90 % of its activity can easily lead to misinterpretations. For example, on DIV 13 several shVEGF-D infected cultures did not show any activity during a 5 minutes recording. It is not possible to answer whether these cultures do not fire action potentials anymore or whether in these cultures the interburst intervals exceed a 5 minutes. Furthermore, burst behavior of shVEGF-D-infected cultures recorded on DIV 13 can be very diverse itself. Some cultures still reveal prolonged bursts with a few shorter ones, while recordings from a different culture reveal only one or two short bursts. Since these observations have not been prominent in recordings on DIV 12 it might well be that shVEGF-D-infected cultures change their bursting behavior around DIV 13 another time. However, spike frequency in bursts was not different between groups. Whether this is due to the fraction of uninfected neurons in shVEGF-D-infected cultures cannot be answered by extracellular recordings (Figure 23 D). Furthermore, shVEGF-D-infected cultures did not show any increase in cell mortality up to DIV 20. Thus, delayed onset of cell death cannot explain the effects on neuronal network activity (data not shown). The effects of the knock-down of VEGF-D on neuronal network activity are indeed interesting in the view of neuronal viability. It is well-accepted that neuronal activity is a trigger for neuronal survival and, moreover, tonic exposure of TTX kills neurons (Zhang et al., 2009). It has been proven by Q-PCR that the shVEGF-D virus specifically down-regulates VEGF-D mRNA levels but not the structurally closely related VEGF-C (unpublished observations by D. Mauceri, Heidelberg).

Taken together, in hippocampal networks developmentally-controlled expression of VEGF-D is not only of vital importance for dendritic morphology of hippocampal neurons but also to maintain neuronal network behavior and maybe even for electrical activity of these neurons . In this work I used extracellular recordings to analyze effects of VEGF-D on neuronal network behavior. More profound studies as to why VEGF-D-deficient neurons loosetheir electrical properties can easily be answered by single cell recordings. The results of this part of this work can be controversially compared with those from CaMBP4-mC infected cultures. On the one hand, knock-down of VEGF-D has more severe effects on network activity than down-regulation of VEGF-D by CaMBP4-mC. On the other hand, dendritic morphology of neurons transfected with CaMBP4 is as impaired as neurons transfected with shVEGF-D. This argues that the CaMBP4-mediated down-regulation of VEGF-D expression to about 75 % of control groups is sufficient to fully block the effect on dendritic arborization. It is known that VEGF-D is involved in angiogenesis and lymphathogenesis (Jeltsch et al., 1997; Stacker et al., 2001) and neuronal morphology of hippocampal CA1 pyramidal cells *in vivo* (unpublished observations by D. Mauceri, Heidelberg). However, this is the first study investigating the effects of VEGF-D on electrical properties of hippocampal networks.

6.1.4 Recombinant VEGF-D partly rescues shVEGF-D-mediated impairments of neuronal network activity

To further confirm that the impairments in neuronal network activity (see 5.3) are mediated by the specific knock-down of VEGF-D I tried to restore the VEGF-D signaling pathway, by supplementing the medium with mature recombinant VEGF-D. To test whether VEGF-D functions as a tonic signal to keep neuronal network activity stable or whether VEGF-D can also restore the impairments on network dynamics, I supplemented VEGF-D at two different time-points: starting on DIV 6 and DIV 10, respectively. Uninfected cultures were equally treated with recombinant VEGF-D and did not show any significant effect on network behavior throughout the experiments. However, supplementing medium with 100 ng/ml recombinant VEGF-D on DIV 6 partly rescued both spontaneous and synchronized activity (Figure 26Figure 28). Although these differences are fairly small and appear to be present on DIV 12 and DIV 13 only, they are statistical significant. However, the extent of the rescue on neuronal network behavior is not as high as on the morphological phenotype. Since proteolytic cleavage continuously degrades VEGF-D in the medium, I also treated cultures with higher concentrations of recombinant VEGF-D. However, also adding VEGF-D daily (50 ng/µl) did not further rescued neuronal network activity (personal observations, H.E. Freitag). Interestingly, supplementing medium with VEGF-D on DIV 10 did not show an effect on network firing activity. Since I have shown that VEGF-D signaling is important for the maintenance of neuronal network activity, this raises the question whether network behavior is mediated by extracellular VEGF-D (and probably VEGFR-3 function) what is shown for neuronal morphology. I want to investigate that issue in the future by infecting neuronal cultures with a construct which expresses a genetically modified VEGF-D: it will exhibit two unique properties: its mRNA is resistant against shVEGF-D and the protein is exclusively intracellular localized. It is shown that VEGF-D is developmentally upregulated in hippocampal tissue but not in cortical tissue. Whether VEGF-D signaling is also important for neuronal network of cortical cultures is a goal of a future study, too. Single cell recordings by patch-clamp techniques will also help to elucidate the interactions between VEGF-D and neuronal network activity.

Taken together, I have shown that the impairment of neuronal network behavior in shVEGF-D-infected cultures is partly rescued by supplementing medium with recombinant VEGF-D. That supports the finding that recombinant VEGF-D partly restore the morphological phenotype induced by knock-down of endogenous VEGF-D-induced, too. However, MEA recordings only revealed a small rescue on neuronal network activity. Whether the VEGF-D signaling pathways and relative signaling cascades which shape neuronal morphology and maintain neuronal network activity are equal is object of a future study.

6.2 LATE PHASE LTP RECORDINGS IN ACUTE HIPPOCAMPAL SLICES

6.2.1 LTP from acute slices on MEAs lasts four hours and longer

A second goal of my thesis was developing a technique that allows investigating the physiological relevance of nuclear calcium signaling in late phase LTP. Acute hippocampal slices are closer to the *in vivo* situation than neuronal networks and stable long-term extracellular recordings via MEAs provide a relatively easy means to investigate the late phase of LTP. The signals recorded from rat hippocampal slices with planar extracellular electrodes showed a similar shape and laminar distribution as in other studies with planar arrays (Oka et al., 1999; Shimono et al., 2002). However, with an average slope of -1.3 to -1.4 V/s the size of the evoked signals was considerably larger and in the same range that has been reported for recordings with three dimensional electrodes (Kopanitsa et al., 2006; Heuschkel et al., 2002). The IO curves acquired at the beginning of each experiment did not always show a plateau at the highest stimulation strength that was used (3 V), meaning that the maximal signal was not always reached (Figure 30 A). I did not use stronger stimuli as not to exceed the safe charge injection limit of the electrodes.

In parallel to long term recordings of evoked signals, the spontaneous activity of the slices in the CA1 and CA3/DG area was monitored. Activity mainly consisted of spikes along the cell layer (unpublished observations, F. Hofmann and H.E. Freitag, Heidelberg), whereby the variability in signal frequencies was rather high. It has to be kept in mind that the amount of spontaneous activity recorded with MEAs depends not only on the quality of the slice and the quality of contact between electrodes and tissue. It has been shown that MEA electrodes can pick up spikes only up to a distance of 100 µm (Egert et al., 2002), so the amount of recorded spontaneous activity also depends on the relative position of cell layer and recording electrodes.

To study especially the late phase of LTP acute slices had to be recorded for at least four hours after induction of LTP. Low quality slices that revealed a decreasing signal on the control pathway were maybe damaged during the preparation procedures and had to be excluded from further analysis. However, this happened to about 25 % of the slices only. After four repeated tetanic stimuli synaptic strength in potentiated Schaffer collateral – CA1 synapses was robustly increased (Figure 30 B) while induction of LTP was prevented by blocking NMDA receptors with AP5 and MK801 (Figure 30 C) (Morris et al., 1986). Moreover, perfusing slices with the translational blocker anisomycin during the time of tetanic stimulation results only in a decreasing LTP, although LTP induction was not impaired (Figure 30 D) (Frey et al., 1996; Nguyen and Kandel, 1997).

To investigate the gene expression-dependent late phase of LTP, transcriptional blockers such as actinomycin D should reveal only a transient potentiation of synaptic strength with a decline four hours after tetanic stimulation. However, so far I have not been able to record a

transcription-sensitive late-phase of LTP. This can be due to recovery conditions after preparations (Capron et al., 2006). It might also be possible that the onset of the transcription-dependent late phase is not yet started four hours after tetanic stimulation. It is also reported that under certain conditions L-LTP of acute slice can be independent of transcription (Huang and Kandel, 2005). It is also conceivable that an increase in spontaneous activity during the preparation procedure or the recovery period leads to increased calcium signaling that may activate signaling pathways sufficient to trigger the transcription-dependent maintenance phase of LTP (Hardingham et al., 2001a; Hardingham et al., 2001b).

6.2.2 Functional studies from acute slices of genetically modified rats

I further wanted to study the importance of nuclear calcium signaling in the late phase of LTP. Since acute slices are usually not accessible to standard transfection and infection techniques I used virus-mediated gene transfer to generate genetically modified rats (Cetin et al., 2006). After an expression period of two weeks several slices per hemisphere showed a large fraction of infected cells in the CA1 pyramidal cell layer (Figure 31) which are usable for LTP recordings as well as single cell recordings by the patch-clamp technique and calcium imaging experiments (unpublished observations, C.P. Bengtson and H.E. Freitag).

Nuclear calcium has emerged as an important regulator of activity-induced genomic responses required for long-term memory. Since increases in nuclear calcium concentrations cannot be investigated with small molecule indicators the genetically encoded nuclear localized calcium indicator GCaMP2.0-NLS was used to visualize and characterize nuclear calcium transients. First tests on MEA revealed that acute slices expressing the calcium indicator GCaMP2.0-NLS tend to have slightly larger evoked signals than native slices although this is not significant (Figure 30 A + Figure 32 B). I show here that the nuclear calcium concentration greatly increases in amplitude after applying a typical L-LTP stimulation protocol. However the combination of a MEA-based electrophysiology platform and imaging setup on an inverse microscope gave limited possibilities to investigate the role of nuclear calcium signaling in the late phase of LTP in detail. In contrast, calcium imaging in single slices at an upright microscope revealed much larger nuclear calcium signals and was easier to manipulate (unpublished observations by C.P. Bengtson, Heidelberg).

However, acute slices of genetically modified animals can be used to investigate the intracellular signaling pathways involved in the late phase of LTP. Since I known from my studies on hippocampal cultures that the nuclear calcium signaling pathway and the expression of VEGF-D are of vital importance during network development it would be of high interest to investigate whether these signaling pathways are crucial for the expression of the maintenance phase of LTP too.

Conclusions:

With this thesis I have shown that Micro-Electrode-Arrays are an excellent tool to investigate calcium signaling pathways involved in neuronal network plasticity and late phase long-term potentiation. I combined MEA recordings and virus-mediated gene transfer with different systems of neuronal networks to establish two novel techniques that are easy to handle. I have show in this thesis that both nuclear calcium signaling as well as expression of *vegf-d* are important for regular network activity patterns in dissociated hippocampal cultures. Moreover, I have demonstrated that LTP recordings from acute hippocampal slices on MEAs can be used to study the maintenance phase of LTP. In future experiments I will record from acute slices of genetically modified rats to investigate how nuclear calcium signaling pathways and its relative genes are involved in the late phase of LTP.

LIST OF ABBREVIATIONS

ACSF	Artificial cerebrospinal fluid
AKAPs	A-kinase anchoring proteins
AMPA	α-Amino-3-hydroxyl-5-methyl-4-isoxazolepropionic acid
AP5	a NMDA receptor antagonist
AraC	Cytosine β-D-arabinofuranoside
ATP	Adenosine triphosphate
BDNF	Brain derived neurotrophic factor
Bic	Bicuculline
BSA	Bovine serum albumin
CA	Cornu ammonis
CaM	Calmodulin
CaMBP4	Calmodulin-binding protein 4
CaMK	Calcium/calmodulin-dependent kinase
cAMP	Cyclic adenosine monophosphate
CBP	CREB binding protein
cDNA	complementary DNA
c-fos	a proto-oncogene
ClCR	Calcium-induced calcium release
CNS	Central nervous system
CRE	cAMP response element
CREB	cAMP response element binding protein
DNA	Deoxyribonucleic acid
DG	Dentate Gyrus
DIV	Day *in vitro*
EC	Entorhinal cortex
E-LTP	Early LTP
EPSP	Excitatory postsynaptic potential
ER	Endoplasmic reticulum
ERK	Extracellular signal-regulated kinase
eYFP	Enhanced yellow fluorescent protein
fEPSP	field EPSP
FIGF	c-Fos induced growth factor
GABA	γ-Amino butyric acid
GCaMP	a Recombinant calcium indicator
GFP	Green fluorescent protein
GOI	Gene of interest
GSK3	Glycogen synthase kinase 3
HEK293	Human embryonic kidney 293 cells
HFS	High-frequency stimulation

IEG	Immediate early gene
IL	Interleukin
InsP3	Inositol triphosphate
IO	Input/output
kbp	Kilo-base pairs
KN-62	a CaMK inhibitor
L-LTP	Late phase LTP
LTP	Long-term potentiation
MAP	Mitogen-activated protein
MAPK	MAP kinase
MEA	Micro-Electrode-Array
MK801	a NMDA receptor antagonist
mRNA	Messenger ribonucleic acid
n.s.	not significant
NFAT	Nuclear factor of activated T-cells
NLS	Nuclear localization sequence
NMDA	N-methyl-D-aspartic acid
NRP	Neuropilins
PBS	Phosphate buffered saline
PCR	Polymerase chain reaction
PI3-K	Phosphoinositide 3-kinase
PKA/C	Protein kinase A/C
PlGF	Placental growth factor
PNS	Peripheral nervous system
PSD	Postsynaptic density
rAAV	Recombinant adeno-associated virus
RNA	Ribonucleic acid
RNAi	RNA interference
ROI	Region of interest
RSK2	Ribosomal S6 protein kinase
RT	Room temperature
sh	Short hairpin
scr	Scramble
SRE	Serum response element
TNF-α	Tumor necrosis factor – α
TTX	Tetrodotoxin
VEGF	Vascular endothelial growth factor
VEGFR	VEGF receptor
VGCC	Voltage-gated calcium channel
VP16	Virus protein 16
WPRE	Woodstock postregulatory response element

7 REFERENCES

Achen, M. G., Jeltsch, M., Kukk, E., Mäkinen, T., Vitali, A., Wilks, A. F., Alitalo, K., Stacker, S. A. "Vascular endothelial growth factor D (VEGF-D) is a ligand for the tyrosine kinases VEGF receptor 2 (Flk1) and VEGF receptor 3 (Flt4)." Proc Natl Acad Sci U S A. ***95***, 1998: 548-553.

Achen, M. G., Stacker, S. A. "The vascular endothelial growth factor family; proteins which guide the development of the vasculature." Int J Exp Pathol. **79**, 1998: 255-265.

Adams, J. P., Sweatt, J. D. "Molecular psychology: roles for the ERK MAP kinase cascade in memory." Annu Rev Pharmacol Toxicol. **42**, 2002: 135-163.

Ahmed, M. S., Siegelbaum, S. A. "Recruitment of N-Type Ca2+ Channels during LTP Enhances Low Release Efficacy of Hippocampal CA1 Perforant Path Synapses." Neuron **63**, 2009: 372-385.

Akhtar, A., Gasser, S. M. "The nuclear envelope and transcriptional control." Nat Rev Genet. **8**, 2007: 507-517.

Alarcon, J. M., Barco, A., Kandel, E. R. "Capture of the late phase of long-term potentiation within and across the apical and basilar dendritic compartments of CA1 pyramidal neurons: synaptic tagging is compartment restricted." J Neurosci. **26**, 2006: 256-264.

Alarcon, J. M., Hodgman, R., Theis, M., Huang, Y. S., Kandel, E. R., Richter, J. D. "Selective modulation of some forms of schaffer collateral-CA1 synaptic plasticity in mice with a disruption of the CPEB-1 gene." Learn Mem. **11**, 2004: 381-327.

Allbritton, N. L., Meyer, T., Stryer, L. "Range of messenger action of calcium ion and inositol 1,4,5-trisphosphate." Science **258**, 1992: 1812-1815.

Andersen, P., Bliss, T. V., Skrede, K. K. "Unit analysis of hippocampal population spikes." Exp Brain Res **13**, 1971: 208-221.

Andersen, P., Sundberg, S. H., Sveen, O. "Specific long-lastingpotentiation of synaptic transmission in hippocampal slices." Nature **266**, 1977: 736-737.

Anderson, K. A., Ribar, T. J., Illario, M., Means, A. R. "Defective survival and activation of thymocytes in transgenic mice expressing a catalytically inactive form of Ca2+/calmodulin-dependent protein kinase IV." Mol Endocrinol. **11**, 1997: 725-737.

Antonova, I., Arancio, O., Trillat, A. C., Wang, H. G., Zablow, L., Udo, H., Kandel, E. R., Hawkins, R. D. "Rapid increase in clusters of presynaptic proteins at onset of long-lasting potentiation." Science **294**, 2001: 1547-1550.

Arias, J., Alberts, A. S., Brindle, P., Claret, F. X., Smeal, T., Karin, M., Feramisco, J., Montminy. M. "Activation of cAMP and mitogen responsive genes relies on a common nuclear factor." Nature **370**, 1994: 226-229.

Arnold, F. J., Hofmann, F., Bengtson, C. P., Wittmann, M., Vanhoutte, P., Bading, H. "Microelectrode array recordings of cultured hippocampal networks reveal a simple model for transcription and protein synthesis-dependent plasticity." J Physiol. **564**, 2005: 3-19.

Arthur, J. S., Fong, A. L., Dwyer, J. M., Davare, M., Reese, E., Obrietan, K., Impey, S. "Mitogen- and stress-activated protein kinase 1 mediates cAMP response element-binding protein phosphorylation and activation by neurotrophins." J Neurosci. **24**, 2004: 4324-4332.

Avantaggiato, V., Orlandini, M., Acampora, D., Oliviero, S., Simeone, A. "Embryonic expression pattern of the murine figf gene, a growth factor belonging to platelet-derived growth factor/vascular endothelial growth factor family." Mech Dev. **73**, 1998: 221-224.

Bading, H. "Transcription-dependent neuronal plasticity: the nuclear calcium hypothesis." Eur J Biochem. **267**, 2000: 5280-5283.

Bading, H., Ginty, D. D., Greenberg, M. E. "Regulation of gene expression in hippocampal neurons by distinct calcium signaling pathways." Science **260**, 1993: 181-186.

Bading, H., Greenberg, M. E. "Stimulation of protein tyrosine phosphorylation by NMDA receptor activation." Science **253**, 1991: 912-914.

Bading, H., Segal, M. M., Sucher, N. J., Dudek, H., Lipton, S. A., Greenberg, M. E. "N-methyl-D-aspartate receptors are critical for mediating the effects of glutamate on intracellular calcium concentration and immediate early gene expression in cultured hippocampal neurons." Neuroscience **64**, 1995: 653-664.

Baird, G. S., Zacharias, D. A., Tsien R. Y. "Circular permutation and receptor insertion within green fluorescent proteins." Proc Natl Acad Sci USA. **96**, 1999: 11241-11246.

Baldwin, M. E., Catimel, B., Nice, E. C., Roufail, S., Hall, N. E., Stenvers, K. L., Karkkainen, M. J., Alitalo, K., Stacker, S. A., Achen, M. G. "The specificity of receptor binding by vascular endothelial growth factor-d is different in mouse and man." J Biol Chem. **276**, 2001: 19166-19171.

Balschun, D., Wolfer, D. P., Gass, P., Mantamadiotis, T., Welzl, H., Schütz, G., Frey, J. U., Lipp, H. P. "Does cAMP response element-binding protein have a pivotal role in hippocampal synaptic plasticity and hippocampus-dependent memory?" J Neurosci. **23**, 2003: 6304-6314.

Barco, A., Alarcon, J. M., Kandel, E. R. "Expression of constitutively active CREB protein facilitates the late phase of long-term potentiation by enhancing synaptic capture." Cell **108**, 2002: 689-703.

Barco, A., Patterson, S., Alarcon, J. M., Gromova, P., Mata-Roig, M., Morozov, A., Kandel, E. R. "Gene expression profiling of facilitated L-LTP in VP16-CREB mice reveals that BDNF is critical for the maintenance of LTP and its synaptic capture." Neuron **48**, 2005: 123-137.

Baruchi, I., Ben-Jacob, E. "Towards neuro-memory-chip: imprinting multiple memories in cultured neural networks." Phys Rev E Stat Nonlin Soft Matter Phys. **75**, 2007: e050901.

Baugham, R. W., Huettner, J. E., Jones, K. A., Khan, A. A. "Cell culture of neocortical and basal forebrain from postnatal rats." Culturing Nerve Cells, 1991: 227-250.

Berridge, M. J. "Inositol triphosphat and calcium signaling." Nature **361**, 1993: 315-325.

Berridge, M. J., Lipp, P., Bootman, M. D. "The versatility and universality of calcium signaling." Nat Rev Mol Cell Biol **1**, 2000: 11-21.

Bito, H., Deisseroth, K., Tsien, R. W. "CREB phosphorylation and dephosphorylation: a Ca(2+)- and stimulus duration-dependent switch for hippocampal gene expression." Cell **87**, 1996: 1203-1214.

Blendy, J. A., Maldonado, R. "Genetic analysis of drug addiction: the role of cAMP response element binding protein." J Mol Med. **76**, 1998: 104-110.

Blenis, J. "Signal transduction via the MAP kinases: proceed at your own RSK." Proc Natl Acad Sci USA. **90**, 1993: 5898-5892.

Bliss, T. V., Collingridge, G. L. "A synaptic model of memory: long-term potentiation in the hippocampus." Nature **361**, 1993: 31-39.

Bliss, T. V., Lomo, T. "Long-lasting potentiation of synaptic transmission in the dentate area of the anaesthetized rabbit following stimulation of the perforant path." J. Physiol. **232**, 1973: 331-56.

Bloodgood, B. L., Sabatini, B. L. "Calcium signaling in dendritic spines." Curr Opin Neurobiol **17**, 2007: 345-351.

Brewer, G. J., Boehler, M. D., Ide, A. N., Wheeler, B. C. "Chronic electrical stimulation of cultured hippocampal networks increases spontaneous spike rates." J Neurosci Methods. **8**, 2009: ePub.

Brewer, G. J., Boehler, M. D., Pearson, R. A., DeMaris, A. A., Ide, A. N., Wheeler, B. C. "Neuron network activity scales exponentially with synapse density." J Neural Eng. **6**, 2009: 014001.

Brockington, A., Lewis, C., Wharton, S., Shaw, P. J. "Vascular endothelial growth factor and the nervous system." Neuropathol Appl Neurobiol. **30**, 2004: 427-446.

Buzsáki, G., Draguhn, A. "Neuronal oscillations in cortical networks." Science **304**, 2004: 1926-1929.

Cajal, S. R. "The structure of Ammon`s Horn." Thomas Springfield, *MA*, 1968.

Capron, B., Sindic, C., Godaux, E., Ris, L. "The characteristics of LTP induced in hippocampal slices are dependent on slice-recovery conditions." Learn Mem. **13**, 2006: 271-277.

Carafoli, E., Penniston, J. T. "The calcium signal." *Sci Am 253*, 1985: 70-78.

Carmeliet, P., Ferreira, V., Breier, G., Pollefeyt, S., Kieckens, L., Gertsenstein, M., Fahrig, M., Vandenhoeck, A., Harpal, K., Eberhardt, C., Declercq, C., Pawling, J., Moons, L., Collen, D., Risau, W., Nagy, A. "Abnormal blood vessel development and lethality in embryos lacking a single VEGF allele." Nature **380** , 1996: 435-439.

Cetin, A., Komai, S., Eliava, M, Seeburg, P. H., Osten, P. "Stereotaxic gene delivery in the rodent brain." Nat Protoc **1**, 2006: 3166-3173.

Chakravarti, D., LaMorte, V. J., Nelson, M. C., Nakajima, T., Schulman, I. G., Juguilon, H., Montminy, M., Evans, R. M. "Role of CBP/P300 in nuclear receptor signalling." Nature **383**, 1996: 99-103.

Chawla, S., Hardingham, G. E., Quinn, D. R., Bading H. "CBP: a signal-regulated transcriptional coactivator controlled by nuclear calcium and CaM kinase IV." Science **281**, 1998: 1505-1509.

Chrivia, J. C., Kwok, R. P., Lamb, N., Hagiwara, M., Montminy, M. R., Goodman, R. H. "Phosphorylated CREB binds specifically to the nuclear protein CBP." Nature **365**, 1993: 855-859.

Clapham, D. E. "Calcium signaling." Cell **80**, 1995: 259-268.

Collingridge, G. L., Kehl, S. J., McLennan, H. "The antagonism of amino acid-induced excitations of rat hippocampal CA1 neurones in vitro." J Physiol. **334**, 1983: 19-31.

Comb, M., Birnberg, N. C., Seasholtz, A., Herbert, E., Goodman, H. M. "A cyclic AMP- and phorbol ester-inducible DNA element." Nature **323**, 1986: 353-356.

Cruzalegui, F. H., Bading, H. "Calcium-regulated protein kinase cascades and their transcription factor targets." Cell Mol Life Sci **57**, 2000: 402-410.

Dash, P. K., Hochner, B., Kandel, E. R. "Injection of the cAMP-responsive element into the nucleus of Aplysia sensory neurons blocks long-term facilitation." Nature **345**, 1990: 718-721.

Deisseroth, K., Heist, E. K., Tsien, R. W. "Translocation of calmodulin to the nucleus supports CREB phosphorylation in hippocampal neurons." Nature **392**, 1998: 198-202.

Deisseroth, K., Mermelstein, P. G., Xia, H., Tsien, R. W. "Signaling from synapse to nucleus: the logic behind the mechanism." Curr Opin Neurobiol **13**, 2003: 354-365.

DiSalvo, J., Bayne, M. L., Conn, G., Kwok, P. W., Trivedi, P. G., Soderman, D. D., Palisi, T. M., Sullivan, K. A., Thomas, K. A. "Purification and characterization of a naturally occurring vascular endothelial growth factor.placenta growth factor heterodimer." J Biol Chem. **270**, 1995: 7717-7723.

Dolmetsch, R. E., Pajvani, U., Fife, K., Spotts, J. M., Greenberg, M.E. "Signaling to the nucleus by an L-type calcium channel-calmodulin complex through the MAP kinase pathway." Science **294**, 2001: 333-339.

Douglas, R. M., Goddard, G. V. "Long-term potentiation of the perforant path-granule cell synapse in the rat hippocampus." Brain Res. **86**, 1975: 205-215.

Dudek, S. M., Fields, R. D. "Somatic action potentials are sufficient for late-phase LTP-related cell signaling." Proc Natl Acad Sci U S A. **99**, 2002: 3962-3967.

Dumont, D. J., Jussila, L., Taipale, J., Lymboussaki, A., Mustonen, T., Pajusola, K., Breitman, M., Alitalo, K. "Cardiovascular failure in mouse embryos deficient in VEGF receptor-3." Science **282**, 1998: 946-949.

Dvorak, H. F., Brown, L. F., Detmar, M., Dvorak, A. M. "Vascular permeability factor/vascular endothelial growth factor, microvascular hyperpermeability, and angiogenesis." Am J Pathol. **146**, 1995: 1029-1039.

Eder, A., Bading, H. "Calcium signals can freely cross the nuclear envelope in hippocampal neurons: somatic calcium increases generate nuclear calcium transients." BMC Neuroscience **8**, 2007: 57-67.

Egert, U., Heck, D., Aertsen, A. "Two-dimensional monitoring of spiking networks in acute brain slices." Exp Brain Res. **142**, 2002: 268-274.

Egert, U., Schlosshauer, B., Fennrich, S., Nisch, W., Fejtl, M., Knott, T., Müller, T., Hämmerle, H. "A novel organotypic long-term culture of the rat hippocampus on substrate-integrated multielectrode arrays." Brain Res Brain Res Protoc. **2**, 1998: 229-242.

Eichenbaum, H. "A cortical-hippocampal system for declarative memory." Nat. Rev. Neurosci. **1,** 2000: 41-50.

Emptage, N. "Calcium on the up: supralinear calcium signaling in central neurons." Neuron **24**, 1999: 495-497.

Emptage, N., Bliss, T. V., Fine, A. "Single synaptic events evoke NMDA receptor-mediated release of calcium from internal stores in hippocampal dendritic spines." Neuron **22**, 1999: 115-124.

Engert, F., Bonhoeffer, T. "Dendritic spine changes associated with hippocampal long-term synaptic plasticity." Nature **399**, 1999: 66-70.

Enholm, B., Paavonen, K., Ristimäki, A., Kumar, V., Gunji, Y., Klefstrom, J., Kivinen, L., Laiho, M., Olofsson, B., Joukov, V., Eriksson, U., Alitalo, K. "Comparison of VEGF, VEGF-B, VEGF-C and Ang-1 mRNA regulation by serum, growth factors, oncoproteins and hypoxia." Oncogene **14**, 1997: 2475-2483.

Enoki, R., Hu, Y. L., Hamilton, D., Fine, A.,. "Expression of long-term plasticity at individual synapses in hippocampus is graded, bidirectional, and mainly presynaptic: optical quantal analysis." Neuron **62**, 2009: 242-253.

Ferrara, N., Carver-Moore, K., Chen, H., Dowd, M., Lu, L., O'Shea, K. S., Powell-Braxton, L., Hillan, K. J., Moore, M. W. "Heterozygous embryonic lethality induced by targeted inactivation of the VEGF gene." Nature **380**, 1996: 439-442.

Ferrara, N., Davis-Smyth, T. "The biology of vascular endothelial growth factor." Endocr Rev. **18**, 1997: 4-25.

Ferrara, N., Gerber, H. P., LeCouter, J. "The biology of VEGF and its receptors." Nat Med. **9**, 2003: 669-676.

Fletcher, T. L., Banker, G. A. "The establishment of polarity by hippocampal neurons: the relationship between the stage of a cell's development in situ and its subsequent development in culture." Dev Biol. **136**, 1989: 446-454.

Folkman, J., Shing, Y.. "Angiogenesis." J Biol Chem. **267**, 1992: 10931-10934.

Forstreuter, F., Lucius, R., Mentlein, R. "Vascular endothelial growth factor induces chemotaxis and proliferation of microglial cells." J Neuroimmunol. **132**, 2002: 93-98.

Frey, U., Frey, S., Schollmeier, F., Krug, M. "Influence of actinomycin D, a RNA synthesis inhibitor, on long-term potentiation in rat hippocampal neurons in vivo and in vitro." J Physiol. **490**, 1996: 703-711.

Frey, U., Krug, M., Reymann, K. G., Matthies, H. "Anisomycin, an inhibitor of protein synthesis, blocks late phases of LTP phenomena in the hippocampal CA1 region in vitro." Brain Res. **452**, 1988: 57-65.

Frey, U., Morris, R. G. "Synaptic tagging and long-term potentiation." Nature **385**, 1997: 533-536.

Frey, U., Morris, R. G. "Synaptic tagging: implications for late maintenance of hippocampal long-term potentiation." Trends Neurosci. **21**, 1998: 181-188.

Garcia-Perez, E., Mazzoni, A., Torre, V. "Spontaneous electrical activity and behavior in the leech hirudo medicinalis." Front Integr Neurosci. **1**, 2007.

Gau, D., Lemberger, T., von Gall, C., Kretz, O., Le Minh, N., Gass, P., Schmid, W., Schibler, U., Korf, H. W., Schütz, G. "Phosphorylation of CREB Ser142 regulates light-induced phase shifts of the circadian clock." Neuron **34**, 2002: 245-253.

Ghosh, A., Greenberg, M. E. "Calcium signaling in neurons: molecular mechanisms and cellular consequences." Science **268**, 1995: 239-247.

Greenberg, D. A., Jin, K. "From angiogenesis to neuropathology." Nature **438**, 2005: 954-959.

Gross, G. W., Rhoades, B. K., Azzazy, H. M., Wu, M. C. "The use of neuronal networks on multielectrode arrays as biosensors." Biosens Bioelectron. **10**, 1995: 553-567.

Hagenston, A. M., Fitzpatrick, J. S., Yeckel, M. F. "MGluR-mediated calcium waves that invade the soma regulate firing in layer V medial prefrontal cortical pyramidal neurons." Cereb Cortex. **18**, 2007: 407-423.

Hämmerle, H., Egert, U., Mohr, A., Nisch, W. "Extracellular recording in neuronal networks with substrate integrated microelectrode arrays." Biosens Bioelectron. **9**, 1994: 961-966.

Hardingham, G. E., Arnold, F. J., Bading, H. "Nuclear calcium signaling controls CREB-mediated gene expression triggered by synaptic activity." Nat Neurosci. **4**, 2001b: 261-267.

Hardingham, G. E., Arnold, F. J., Bading, H. "A calcium microdomain near NMDA receptors: on switch for ERK-dependent synapse-to-nucleus communication." Nat Neurosci. **4**, 2001a: 261-267.

Hardingham, G. E., Bading, H. "Nuclear calcium: a key regulator of gene expression." Biometals **11**, 1998: 345-358.

Hardingham, G. E., Bading, H. "The Yin and Yang of NMDA receptor signalling." Trends Neurosci. **26**, 2003: 81-89.

Hardingham, G. E., Chawla, S., Cruzalegui, F. H., Bading, H. "Control of recruitment and transcription-activating function of CBP determines gene regulation by NMDA receptors and L-type calcium channels." Neuron **22**, 1999: 789-798.

Hardingham, G. E., Chawla, S., Johnson, C. M., Bading, H. "Distinct functions of nuclear and cytoplasmic calcium in the control of gene expression." Nature **385**, 1997: 260-265.

Hardingham, G. E., Fukunaga, Y., Bading, H. "Extrasynaptic NMDARs oppose synaptic NMDARs by triggering CREB shut-off and cell death pathways." Nat Neurosci. **5**, 2002: 405-414.

Hebb, D. O. "The organization of behavior: A neurophysiological theory." Wiley, New Yok, 1949.

Heuschkel, M. O., Fejtl, M., Raggenbass. M., Bertrand, D., Renaud, P. "A three-dimensional multi-electrode array for multi-site stimulation and recording in acute brain slices." J Neurosci Methods **114**, 2002: 135-148.

Ho, N., Liauw, J. A., Blaeser, F., Wei, F., Hanissian, S., Muglia, L. M., Wozniak, D. F., Nardi, A., Arvin, K. L., Holtzman, D. M., Linden, D. J., Zhuo, M., Muglia, L. J., Chatila, T. A. "Impaired synaptic plasticity and cAMP response element-binding protein activation in Ca2+/calmodulin-dependent protein kinase type IV/Gr-deficient mice." J Neurosci. **20**, 2000: 6459-6472.

Hofmann, F., Bading, H. "Long term recordings with microelectrode arrays: studies of transcription-dependent neuronal plasticity and axonal regeneration." J Physiol Paris. **99**, 2006: 125-132.

Hong, M., Ross, W. N. "Priming of intracellular calcium stores in rat CA1 pyramidal neurons." J Physiol. **584**, 2007: 75-87.

Hook, S. S., Means, A. R. "Ca(2+)/CaM-dependent kinases: from activation to function." Annu Rev Pharmacol Toxicol. **41**, 2001: 471-505.

Huang, Y. Y., Kandel, E. R. "Theta frequency stimulation induces a local form of late phase LTP in the CA1 region of the hippocampus." Learn Mem. **12**, 2005: 587-593.

Huang, Y. Y., Zakharenko, S. S., Schoch, S., Kaeser, P. S., Janz, R., Südhof, T. C., Siegelbaum, S. A., Kandel, E. R. "Genetic evidence for a protein-kinase-A-mediated presynaptic component in NMDA-receptor-dependent forms of long-term synaptic potentiation." Proc Natl Acad Sci U S A. **102**, 2005: 9365-9370.

Hunter, T., Karin, M. "The regulation of transcription by phosphorylation." Cell **70**, 1992: 375-387.

Ikonomidou, C., Bosch, F., Miksa, M., Bittigau, P., Vöckler, J., Dikranian, K., Tenkova, T. I., Stefovska, V., Turski, L., Olney, J. W. "Blockade of NMDA receptors and apoptotic neurodegeneration in the developing brain." Science **283**, 1999: 70-74.

Impey, S., Fong, A. L., Wang, Y., Cardinaux, J. R., Fass, D. M., Obrietan, K., Wayman, G. A., Storm, D. R., Soderling, T. R., Goodman, R. H. "Phosphorylation of CBP mediates

transcriptional activation by neural activity and CaM kinase IV." Neuron **34**, 2002: 235-244.

Impey, S., Goodman, R. H. "CREB signaling--timing is everything." Science STKE , 2001: PE1.

Impey, S., Mark, M., Villacres, E. C., Poser, S., Chavkin, C., Storm, D. R. "Induction of CRE-mediated gene expression by stimuli that generate long-lasting LTP in area CA1 of the hippocampus." Neuron **16**, 1996: 973-982.

Impey, S., Obrietan, K., Storm, D. R. "Making new connections: role of ERK/MAP kinase signaling in neuronal plasticity." Neuron **23**, 1999: 11-14.

Janknecht, R., Nordheim, A. "Regulation of the c-fos promoter by the ternary complex factor Sap-1a and its coactivator CBP." Oncogene **12**, 1996: 1961-1969.

Jeltsch, M., Kaipainen, A., Joukov, V., Meng, X., Lakso, M., Rauvala, H., Swartz, M., Fukumura, D., Jain, R. K., Alitalo, K. "Hyperplasia of lymphatic vessels in VEGF-C transgenic mice." Science **276**, 1997: 1423-1425.

Jenny, B., Harrison, J. A., Baetens, D., Tille, J. C., Burkhardt, K., Mottaz, H., Kiss, J. Z., Dietrich, P. Y., De Tribolet, N., Pizzolato, G. P., Pepper, M. S. "Expression and localization of VEGF-C and VEGFR-3 in glioblastomas and haemangioblastomas." J Pathol. **209**, 2006: 34-43.

Jimbo, Y., Kasai, N., Torimitsu, K., Tateno, T., Robinson, H. P. "A system for MEA-based multisite stimulation." IEEE Trans Biomed Eng. **50**, 2003: 241-248.

Jin, K., Zhu, Y., Sun, Y., Mao, X. O., Xie, L., Greenberg, D. A. "Vascular endothelial growth factor (VEGF) stimulates neurogenesis in vitro and in vivo." Proc Natl Acad Sci U S A. **99**, 2002: 11946-11950.

Johnson, C. M., Hill, C. S., Chawla, S., Treisman, R., Bading, H. "Calcium controls gene expression via three distinct pathways that can function independently of the Ras/mitogen-activated protein kinases (ERKs) signaling cascade." J Neurosci. **17**, 1997: 6189-6202.

Joukov, V., Pajusola, K., Kaipainen, A., Chilov, D., Lahtinen, I., Kukk, E., Saksela, O., Kalkkinen, N., Alitalo, K. "A novel vascular endothelial growth factor, VEGF-C, is a ligand for the Flt4 (VEGFR-3) and KDR (VEGFR-2) receptor tyrosine kinases." EMBO J. **15**, 1996: 290-298.

Kaang BK, Kandel ER, Grant SG. "Activation of cAMP-responsive genes by stimuli that produce long-term facilitation in Aplysia sensory neurons." Neuron **10**, 1993: 427-435.

Kaipainen, A., Korhonen, J., Mustonen, T., van Hinsbergh, V. W., Fang, G. H., Dumont, D., Breitman, M., Alitalo, K. "Expression of the fms-like tyrosine kinase 4 gene becomes restricted to lymphatic endothelium during development." Proc Natl Acad Sci U S A. **92**, 1995: 3566-3570.

Kandel, E. R. "The molecular biology of memory storage: a dialogue between genes and synapses." Science **294**, 2001: 1030-1038.

Kang, H., Schuman, E. M. "A requirement for local protein synthesis in neurotrophin-induced hippocampal synaptic plasticity." Science **273**, 1996: 1402-1406.

Kang, H., Sun, L. D., Atkins, C. M., Soderling, T. R., Wilson, M. A., Tonegawa, S. "An important role of neural activity-dependent CaMKIV signaling in the consolidation of long-term memory." Cell **106**, 2001: 771-783.

Kaplan, M. P., Abel, T. "Genetic approaches to the study of synaptic plasticity and memory storage." CNS Spectr. **8**, 2003: 597-610.

Kelleher, R. J. 3rd, Govindarajan, A., Jung, H. Y., Kang, H., Tonegawa, S. "Translational control by MAPK signaling in long-term synaptic plasticity and memory." Cell **116**, 2004: 467-479.

Kerchner, G. A., Nicoll, R. A. "Silent synapses and the emergence of a postsynaptic mechanism for LTP." Nat Rev Neurosci **11**, 2008: 813-825.

Klugmann, M., Symes, C. W., Leichtlein, C. B., Klaussner, B. K., Dunning, J., Fong, D., Young, D., During, M. J. "AAV-mediated hippocampal expression of short and long Homer 1 proteins differentially affect cognition and seizure activity in adult rats." Mol Cell Neurosci **28**, 2005: 347-360.

Kopanitsa MV, Afinowi NO, Grant SG. "Recording long-term potentiation of synaptic transmission by three-dimensional multi-electrode arrays." BMC Neurosci. **7**, 2006: 61.

Kukk, E., Lymboussaki, A., Taira, S., Kaipainen, A., Jeltsch, M., Joukov, V., Alitalo, K. "VEGF-C receptor binding and pattern of expression with VEGFR-3 suggests a role in lymphatic vascular development." Development **122**, 1996: 3829-3837.

Kwok, R. P., Lundblad, J. R., Chrivia, J. C., Richards, J. P., Bächinger, H. P., Brennan, R. G., Roberts, S. G., Green, M. R., Goodman, R. H. "Nuclear protein CBP is a coactivator for the transcription factor CREB." Nature **370**, 1994: 223-226.

Lamprecht, R., LeDoux, J. "Structural plasticity and memory." Nat Rev Neurosci **1**, 2004: 45-54.

Lau, D., Bading, H. "Synaptic activity-mediated suppression of p53 and induction of nuclear calcium-regulated neuroprotective genes promote survival through inhibition of mitochondrial permeability transition." J Neurosci **29**, 2009: 4420-4429.

Le Bras, B., Barallobre, M. J., Homman-Ludiye, J., Ny, A., Wyns, S., Tammela, T., Haiko, P., Karkkainen, M. J., Yuan, L., Muriel, M. P., Chatzopoulou, E., Bréant, C., Zalc, B., Carmeliet, P., Alitalo, K., Eichmann, A., Thomas, J. L. "VEGF-C is a trophic factor for neural progenitors in the vertebrate embryonic brain." Nat Neurosci. **9**, 2006: 340-348.

Lee, B., Butcher, G. Q., Hoyt, K. R., Impey, S., Obrietan, K. "Activity-dependent neuroprotection and cAMP response element-binding protein (CREB): kinase coupling, stimulus intensity, and temporal regulation of CREB phosphorylation at serine 133." J Neurosci. **25**, 2005: 1137-1148.

Lee, J., Gray, A., Yuan, J., Luoh, S. M., Avraham, H., Wood, W. I. "Vascular endothelial growth factor-related protein: a ligand and specific activator of the tyrosine kinase receptor Flt4." Proc Natl Acad Sci U S A. **93**, 1992: 1988-1992.

LeMasson, G., Marder, E., Abbott, L. F. "Activity-dependent regulation of conductances in model neurons." Science **259**, 1993: 1915-1917.

Limbäck-Stokin, K., Korzus, E., Nagaoka-Yasuda, R., Mayford, M. "Nuclear calcium/calmodulin regulates memory consolidation." J Neurosci. **24**, 2004: 10858-10867.

Lisman, J. E. "The Pre/Post LTP Debate." Neuron **63**, 2009: 281-284.

Lonze, B. E., Ginty, D. D. "Function and regulation of CREB family transcription factors in the nervous system." Neuron **35**, 2002: 605-623.

Lu, B. "BDNF and activity-dependent synaptic modulation." Learn Mem. **10**, 2003: 86-98.

Lynch, G. S., Dunwiddie, T., Gribkoff, V. "Heterosynaptic depression: a postsynaptic correlate of long-term potentiation." Nature **266**, 1977: 737-739.

Lynch, G., Larson, J., Kelso, S., Barrionuevo, G., Schottler, F. "Intracellular injections of EGTA block induction of hippocampal long-term potentiation." Nature **305**, 1983: 719-721.

Lynch, M. A. "Long-term potentiation and memory." Physiol Rev. **84**, 2004: 87-136.

MacDermott, A. B., Mayer, M. L., Westbrook, G. L., Smith, S. J., Barker, J. L. "NMDA-receptor activation increases cytoplasmic calcium concentration in cultured spinal cord neurones." Nature **321**, 1986: 519-522.

Magee, J. C., Johnston, D. "A synaptically controlled, associative signal for Hebbian plasticity in hippocampal neurons." Science **275**, 1997: 209-213.

Maglione, D., Guerriero, V., Viglietto, G., Delli-Bovi, P., Persico, M. G. "Isolation of a human placenta cDNA coding for a protein related to the vascular permeability factor." Proc Natl Acad Sci U S A. **88**, 1991: 9267-9271.

Malenka, R. C., Kauer, J. A., Zucker, R. S., Nicoll, R. A. "Postsynaptic calcium is sufficient for potentiation of hippocampal synaptic transmission." Science **242**, 1988: 81-84.

Marconcini, L., Marchio, S., Morbidelli, L., Cartocci, E., Albini, A., Ziche, M., Bussolino, F., Oliviero, S. "c-fos-induced growth factor/vascular endothelial growth factor D induces angiogenesis in vivo and in vitro." Proc Natl Acad Sci U S A. **96**, 1999: 9671-9676.

Marom, S., Shahaf, G. "Development, learning and memory in large random networks of cortical neurons: lessons beyond anatomy." Q Rev Biophys. **35**, 2002: 63-87.

Martin, K. C., Kosik, K. S. "Synaptic tagging -- who's it?" *Nat Rev Neurosci. 3*, 2002: 813-820.

Martin, S. J., Grimwood, P. D., Morris, R. G. "Synaptic plasticity and memory: an evaluation of the hypothesis." Annu Rev Neurosci. **23**, 2000: 649-711.

Matthews, R. P., Guthrie, C. R., Wailes, L. M., Zhao, X., Means, A. R., McKnight, G. S. "Calcium/calmodulin-dependent protein kinase types II and IV differentially regulate CREB-dependent gene expression." Mol Cell Biol. **14**, 1994: 6107-6116.

Mazzoni, A., Broccard, F. D., Garcia-Perez, E., Bonifazi, P., Ruaro, M. E., Torre, V. "On the dynamics of the spontaneous activity in neuronal networks." PLoS One **2**, 2007: e439.

McDonald, N. Q., Hendrickson, W. A. "A structural superfamily of growth factors containing a cystine knot motif." Cell **73**, 1993: 421-424.

McNaughton, B. L., Douglas, R. M., Goddard, G. V. "Synaptic enhancement in fascia dentata: cooperativity among coactive afferents." Brain Res. **157**, 1978: 277-293.

Mermelstein, P. G., Deisseroth, K., Dasgupta, N., Isaksen, A. L., Tsien, R. W. "Calmodulin p riming: nuclear translocation of a calmodulin complex and the memory of prior neuronal activity." Proc Natl Acad Sci USA **98**, 2001: 4132-4133.

Meyer, M., Clauss, M., Lepple-Wienhues, A., Waltenberger, J., Augustin, H. G., Ziche, M., Lanz, C., Büttner, M., Rziha, H. J., Dehio, C. "A novel vascular endothelial growth factor encoded by Orf virus, VEGF-E, mediates angiogenesis via signalling through VEGFR-2 (KDR) but not VEGFR-1 (Flt-1) receptor tyrosine kinases." EMBO J. **18**, 1999: 363-374.

Miller, K. D. "Synaptic economics: competition and cooperation in synaptic plasticity." Neuron **17**, 1996: 371-374.

Minta, A., Tsien, R. Y. "Fluorescent indicators for cytosolic sodium." J Biol Chem. **264**, 1989: 19449-19457.

Miyamoto, E. "Molecular mechanism of neuronal plasticity: induction and maintenance of long-term potentiation in the hippocampus." J Pharmacol Sci. **100**, 2006: 433-442.

Miyawaki, A., Llopis, J., Heim, R., McCaffery, J. M., Adams, J. A., Ikura, M., Tsien, R. Y. "Fluorescent indicators for Ca2+ based on green fluorescent proteins and calmodulin." Nature **388**, 1997: 882-887.

Morris, R. G., Anderson, E., Lynch, G. S., Baudry, M. "Selective impairment of learning and blockade of long-term potentiation by an N-methyl-D-aspartate receptor antagonist, AP5." Nature **319**, 1986: 774-776.

Morris, R. G., Garrud, P., Rawlins, J. N., O'Keefe, J. "Place navigation impaired in rats with hippocampal lesions." Nature **297**, 1982: 681-683.

Nagai, T., Sawano, A., Park, E. S., Miyawaki, A. "Circularly permuted green fluorescent proteins engineered to sense Ca2+." Proc Natl Acad Sci USA. **98**, 2001: 3197-3202.

Nakamura, T., Barbara, J. G., Nakamura, K., Ross, W. N. "Synergistic release of Ca2+ from IP3-sensitive stores evoked by synaptic activation of mGluRs paired with backpropagating action potentials." Neuron **24**, 1999: 727-737.

Nakanishi, K., Kukita, F. "Functional synapses in synchronized bursting of neocortical neurons in culture." Brain Res. **795**, 1998: 137-146.

Nayak, A., Zastrow, D. J., Lickteig, R., Zahniser, N. R., Browning, M. D. "Maintenance of late-phase LTP is accompanied by PKA-dependent increase in AMPA receptor synthesis." Nature ***394***, 1998: 680-683.

Nguyen, P. V., Kandel, E. R. "Brief theta-burst stimulation induces a transcription-dependent late phase of LTP requiring cAMP in area CA1 of the mouse hippocampus." Learn Mem. **4**, 1997: 230-243.

Nguyen, P. V., Woo, N. H. "Regulation of hippocampal synaptic plasticity by cyclic AMP-dependent protein kinases." Prog Neurobiol. **71**, 2003: 401-437.

Nicoll, R. A., Malenka, R. C. "Expression mechanisms underlying NMDA receptor-dependent long-term potentiation." Ann N Y Acad Sci **868**, 1999: 515-525.

Nicosia, R. F. "What is the role of vascular endothelial growth factor-related molecules in tumor angiogenesis?" Am J Pathol. **53**, 1998: 11-16.

O'Donovan, M. J. "The origin of spontaneous activity in developing networks of the vertebrate nervous system." Curr Opin Neurobiol. **9**, 1999: 904-104.

O'Donovan, M. J., Chub, N. "Population behavior and self-organization in the genesis of s pontaneous rhythmic activity by developing spinal networks." Semin Cell Dev Biol. 8, 1997: 21-28.

Ogryzko, V. V., Schiltz, R. L., Russanova, V., Howard, B. H., Nakatani, Y. "The transcriptional coactivators p300 and CBP are histone acetyltransferases." Cell **87**, 1996: 953-939.

Oka, H., Shimono, K., Ogawa, R., Sugihara, H., Taketani, M. "A new planar multielectrode array for extracellular recording: application to hippocampal acute slice." J Neurosci Methods. **93**, 1999: 61-67.

Olofsson, B., Pajusola, K., Kaipainen, A., von Euler, G., Joukov, V., Saksela, O., Orpana, A., Pettersson, R. F., Alitalo, K., Eriksson, U. "Vascular endothelial growth factor B, a novel growth factor for endothelial cells." Proc Natl Acad Sci U S A. **93**, 1996: 2576-2581.

Orlandini, M., Marconcini, L., Ferruzzi, R., Oliviero, S. "Identification of a c-fos-induced gene that is related to the platelet-derived growth factor/vascular endothelial growth factor family." Proc Natl Acad Sci U S A. **93**, 1996: 11675-11680.

Papadia, S., Stevenson, P., Hardingham, N. R., Bading, H., Hardingham, G. E. "Nuclear Ca2+ and the cAMP response element-binding protein family mediate a late phase of activity-dependent neuroprotection." J Neurosci. **25**, 2005: 4279-4287.

Parker, D., Ferreri, K., Nakajima, T., LaMorte, V. J., Evans, R., Koerber, S. C., Hoeger, C., Montminy, M. R. "Phosphorylation of CREB at Ser-133 induces complex formation with CREB-binding protein via a direct mechanism." Mol Cell Biol. **16**, 1996: 694-703.

Parrish, J. Z., Emoto, K., Kim, M. D., Jan, Y. N. "Mechanisms that regulate establishment, maintenance, and remodeling of dendritic fields." Annu Rev Neurosci **30**, 2007: 399-423.

Potter, S. M. "Distributed processing in cultured neuronal networks." Prog Brain Res. **130**, 2001: 49-62.

Potter, S. M., DeMarse, T. B. "a new approach to neural cell culture for long-term studies." J Neurosci Methods **110**, 2001: 17-24.

Ptashne, M., Gann, A. "Transcriptional activation by recruitment." Nature **386**, 1997: 569-577.

Rao, A., Luo, C., Hogan, P. G. "Transcription factors of the NFAT family: regulation and function." Annu Rev Immunol. **15**, 1997: 707-747.

Redmond, L., Kashani, A. H., Ghosh, A. "Calcium regulation of dendritic growth via CaM kinase I V and CREB-mediated transcription." Neuron **34**, 2002: 999-1010.

Rhoads, A. R., Friedberg, F. "Sequence motifs for calmodulin recognition." Faseb J. **11**, 1997: 331-340.

Risau, W. "Differentiation of endothelium." FASEB J. **9**, 1995: 926-933.

Risau, W. "Mechanisms of angiogenesis." Nature **386**, 1997: 671-674.

Roeder, R. G. "The role of general initiation factors in transcription by RNA polymerase II." Trends Biochem Sci. **21**, 1996: 327-335.

Romoser, V. A., Hinkle, P. M., Persechini, A. "Detection in living cells of Ca2+-dependent changes in the fluorescence emission of an indicator composed of two green fluorescent protein variants linked by a calmodulin-binding sequence. A new class of fluorescent indicators." J Biol Chem. **272**, 1997: 13270-13274.

Schulman, H. "The multifunctional Ca2+/calmodulin-dependent protein kinases." Curr Opin Cell Biol. **5**, 1993: 247-253.

Segev, R., Baruchi, I., Hulata, E., Ben-Jacob, E. "Hidden neuronal correlations in cultured networks." Phys Rev Lett. **92**, 2004: e118102.

Senger, D. R., Galli, S. J., Dvorak, A. M., Perruzzi, C. A., Harvey, V. S., Dvorak, H. F. "Tumor cells secrete a vascular permeability." Science **219**, 1983: 983-985.

Serrano P, Yao Y, Sacktor TC. "Persistent phosphorylation by protein kinase Mzeta maintains late-phase long-term potentiation." J Neurosci. **25**, 2005: 1979-1984.

Sheng, M., Dougan, S. T., McFadden, G., Greenberg, M. E. "Calcium and growth factor pathways of c-fos transcriptional activation require distinct upstream regulatory sequences." Mol Cell Biol. **8**, 1988: 2787-2796.

Sheng, M., Greenberg, M. E. "The regulation and function of c-fos and other immediate early genes in the nervous system." Neuron **4**, 1990: 477/485.

Sheng, M., McFadden, G., Greenberg, M. E. "Membrane depolarization and calcium induce c-fos transcription via phosphorylation of transcription factor CREB." Neuron **4**, 1990: 571-582.

Sheng, M., Thompson, M. A., Greenberg, M. E. "CREB: a Ca(2+)-regulated transcription factor phosphorylated by calmodulin-dependent kinases." Science **25**, 1991: 427-430.

Shimono, K., Kubota, D., Brucher, F., Taketani, M., Lynch, G. "Asymmetrical distribution of the Schaffer projections within the apical dendrites of hippocampal field CA1." Brain Res. **950**, 2002: 279-287.

Shin, Y. J., Choi, J. S., Lee, J. Y., Choi, J. Y., Cha, J. H., Chun, M. H., Lee, M. Y. "Differential regulation of vascular endothelial growth factor-C and its receptor in the rat hippocampus following transient forebrain ischemia." Acta Neuropathol. **116**, 2008: 517-527.

Shu, X., Shaner, N. C., Yarbrough, C. A., Tsien, R. Y., Remington, S. J. "Novel chromophores and buried charges control color in mFruits." Biochemistry **45**, 2006: 9639-9647.

Shuai, J. W., Jung, P. "Optimal ion channel clustering for intracellular calcium signaling." Proc Natl Acad Sci U S A. **100**, 2003: 506-510.

Silva, A. J., Kogan, J. H., Frankland, P. W., Kida, S. "CREB and memory." Annu Rev Neurosci. **21**, 1998: 127-148.

Soderling, T. R. "The Ca-calmodulin-dependent protein kinase cascade." Trends Biochem Sci **24**, 1999: 232-236.

Soker, S., Takashima, S., Miao, H. Q., Neufeld, G., Klagsbrun, M. "Neuropilin-1 is expressed by endothelial and tumor cells as an isoform-specific receptor for vascular endothelial growth factor." Cell ***92***, 1998: 735-745.

Stacker, S. A., Caesar, C., Baldwin, M. E., Thornton, G. E., Williams, R. A., Prevo, R., Jackson, D. G., Nishikawa, S., Kubo, H., Achen, M. G. "VEGF-D promotes the metastatic spread of tumor cells via the lymphatics." Nat Med. **7**, 2001: 186-191.

Stacker, S. A., Stenvers, K., Caesar, C., Vitali, A., Domagala, T., Nice, E., Roufail, S., Simpson, R. J., Moritz, R., Karpanen, T., Alitalo, K., Achen, M. G. "Biosynthesis of vascular endothelial growth factor-D involves proteolytic processing which generates non-covalent homodimers." J Biol Chem. **274**, 1999: 32127-32136.

Stett, A., Barth, W., Weiss, S., Haemmerle, H., Zrenner, E. "Electrical multisite stimulation of the isolated chicken retina." Vision Res. **40**, 2000: 1785-1795.

Stett, A., Egert, U., Guenther, E., Hofmann, F., Meyer, T., Nisch, W., Haemmerle, H. "Biological application of microelectrode arrays in drug discovery and basic research." Anal Bioanal Chem. ***377***, 2003: 486-495.

Steward, O., Worley, P. F. "Selective targeting of newly synthesized Arc mRNA to active synapses requires NMDA receptor activation." Neuron **30**, 2001: 227-240.

Stoppini, L., Buchs, P. A., Muller, D. "A simple method for organotypic cultures of nervous tissue." J Neurosci Methods **37**, 1991: 173-182.

Sun, P., Enslen, H., Myung, P. S., Maurer, R. A. "Differential activation of CREB by Ca2+/calmodulin-dependent protein kinases type II and type IV involves phosphorylation of a site that negatively regulates activity." Genes Dev. **8**, 1994: 2527-2539.

Suto, K., Yamazaki, Y., Morita, T., Mizuno, H. "Crystal structures of novel vascular endothelial growth factors (VEGF) from snake venoms: insight into selective VEGF binding to kinase insert domain-containing receptor but not to fms-like tyrosine kinase-1." J Biol Chem. **280**, 2005: 2126-2131.

Swope, D. L., Mueller, C. L., Chrivia, J. C. "CREB-binding protein activates transcription through multiple domains." J Biol Chem. **271**, 1996: 28138-28145.

Taddei, A., Van Houwe, G., Hediger, F., Kalck, V., Cubizolles, F., Schober, H., Gasser, S. M. "Nuclear pore association confers optimal expression levels for an inducible yeast gene." Nature **441**, 2006: 774-778.

Takahashi H, Shibuya M. "The vascular endothelial growth factor (VEGF)/VEGF receptor system and its role under physiological and pathological conditions." Clin Sci (Lond). **109**, 2005: 227-241.

Taubenfeld, S. M., Wiig, K. A., Bear, M. F., Alberini, C. M. "A molecular correlate of memory and amnesia in the hippocampus." Nat Neurosci. **2**, 1999: 309-310.

Thomas, C. A. Jr., Springer, P. A., Loeb, G. E., Berwald-Netter, Y., Okun, L. M. "A miniature microelectrode array to monitor the bioelectric activity of cultured cells." Exp Cell Res., 1972: 61-66.

Treisman, R. "Identification and purification of a polypeptide that binds to the c-fos serum response element." EMBO **6**, 1987: 2711-2717.

Tsokas, P., Ma, T., Iyengar, R., Landau, E. M., Blitzer, R. D. "Mitogen-activated protein kinase upregulates the dendritic translation machinery in long-term potentiation by controlling the mammalian target of rapamycin pathway." J Neurosci **27**, 2007: 5885-5894.

Tully, T., Preat, T., Boynton, S. C., Del Vecchio, M. "Genetic dissection of consolidated memory in Drosophila." Cell **79**, 1994: 35-47.

Turrigiano, G. G., Nelson, S. B. "Homeostatic plasticity in the developing nervous system." Nat Rev Neurosci. **5**, 2004: 97-107.

Valor, L. M., Charlesworth, P., Humphreys, L., Anderson, C. N., Grant, S. G. "Network activity-independent coordinated gene expression program for synapse assembly." Proc Natl Acad Sci U S A. **104**, 2007: 4658-4663.

Van Den Pol, A. N., Obrietan, K., Belousov, A. "Glutamate hyperexcitability and seizure-like activity throughout the brain and spinal cord upon relief from chronic glutamate receptor blockade in culture." Neuroscience **74**, 1996: 653-674.

van Pelt, J., Wolters, P. S., Corner, M. A., Rutten, W. L., Ramakers, G. J. "Long-term characterization of firing dynamics of spontaneous bursts in cultured neural networks." IEEE Trans Biomed Eng. **51**, 2004: 2051-2062.

Wagenaar, D. A., Madhavan, R., Pine, J., Potter, S. M. "Controlling bursting in cortical cultures with closed-loop multi-electrode stimulation." J Neurosci. **25**, 2005: 680-688.

Wagenaar, D. A., Pine, J., Potter, S. M. "An extremely rich repertoire of bursting patterns during the development of cortical cultures." BMC Neurosci. **7**, 2006: 11-28.

Walton, M. R., Dragunow, I. "Is CREB a key to neuronal survival?" Trends Neurosci. **23**, 2000: 109-115.

Wang, J., Campos, B., Jamieson, G. A., Kaetzel, M. A., Dedman, J. R. "Functional elimination of calmodulin within the nucleus by targeted expression of an inhibitor peptide." J Biol Chem **270**, 1995: 30245-30248.

Watanabe, S., Hong, M., Lasser-Ross, N., Ross, W. N. "Modulation of calcium wave propagation in the dendrites and to the soma of rat hippocampal pyramidal neurons." J Physiol. **575**, 2006: 455-468.

Weislogel, J.-M. "Visualisation of nuclear localised calcium signals using recombinant calcium indicators in in vivo model systems." PhD Thesis, 2007.

West, A. E., Griffith, E. C., Greenberg, M. E. "Regulation of transcription factors by neuronal activity." Nat Rev Neurosci **3**, 2002: 921-931.

Whitmarsh, A. J., Davis, R. "Regulation of transcription factor function by phosphorylation." Cell. Mol. Life Scci. **57**, 2000: 1172-1183.

Wiegert, J. S., Bengtson, C. P., Bading, H. "Diffusion and not active transport underlies and limits ERK1/2 synapse-to-nucleus signaling in hippocampal neurons." J Biol Chem **282**, 2007: 29621-29633.

Witmer, A. N., Dai, J., Weich, H. A., Vrensen, G. F., Schlingemann, R. O. "Expression of vascular endothelial growth factor receptors 1, 2, and 3 in quiescent endothelia." J Histochem Cytochem. **50**, 2002: 767-777.

Wu, G. Y., Deisseroth, K., Tsien, R. W. "Activity-dependent CREB phosphorylation: convergence of a fast, sensitive calmodulin kinase pathway and a slow, less sensitive mitogen-activated protein kinase pathway." Proc Natl Acad Sci U S A. **98**, 2001: 2808-2813.

Xing, J., Ginty, D. D., Greenberg, M. E. "Coupling of the RAS-MAPK pathway to gene activation by RSK2, a growth factor-regulated CREB kinase." Science **273**, 1996: 959-963.

Yamamoto, K. K., Gonzalez, G. A., Biggs, W. H. 3rd, Montminy, M. R. "Phosphorylation-induced binding and transcriptional efficacy of nuclear factor CREB." Nature **334**, 1988: 494-498.

Yin, J. C., Del Vecchio, M., Zhou, H., Tully, T. "CREB as a memory modulator: induced expression of a dCREB2 activator isoform enhances long-term memory in Drosophila." Cell **81**, 1995: 107-115.

Yin, J. C., Wallach, J. S., Del Vecchio, M., Wilder, E. L., Zhou, H., Quinn, W. G., Tully, T. "Induction of a dominant negative CREB transgene specifically blocks long-term memory in Drosophila." Cell **79**, 1994: 49-58.

Young, J. Z., Isiegas, C., Abel, T., Nguyen, P. V. "Metaplasticity of the late-phase of long-term potentiation: a critical role for protein kinase A in synaptic tagging." Eur J Neurosci. **23,** 2006: 1784-1794.

Zhang, S. J., Steijaert, M. N., Lau, D., Schütz, G., Delucinge-Vivier, C., Descombes, P., Bading, H. "Decoding NMDA receptor signaling: identification of genomic programs specifying neuronal survival and death." Neuron **53**, 2007: 549-562.

Zhang, S. J., Zou, M., Lu, L., Lau, D., Ditzel, D. A. W., Delucinge-Vivier, C., Aso, Y., Descombes, P., Bading, H. "Nuclear calcium signaling controls expression of a large gene pool: Identification of a gene program for acquired neuroprotection induced by synaptic activity." PLoS Genet **8**, 2009.